CONFORMATIONAL STUDIES OF HETEROCYCLIC COMPOUNDS

Isabel Mary Magennis

A Thesis Submitted for the Degree of PhD
at the
University of St Andrews

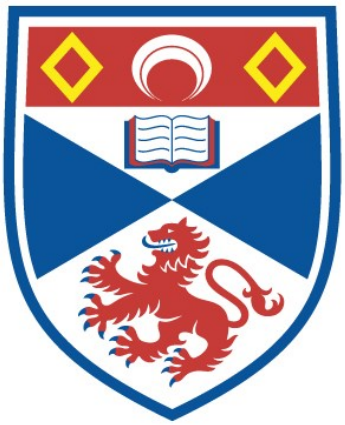

1970

CONFORMATIONAL STUDIES OF HETEROCYCLIC COMPOUNDS

A Thesis
presented for the degree of
Doctor of Philosophy
in the Faculty of Science
of the
University of St. Andrews
by

ISABEL MARY MAGENNIS M.Sc.

May 1970 United College of St. Salvator and St. Leonard

ProQuest LLC.
789 East Eisenhower Parkway
P.O. Box 1346
Ann Arbor, MI 48106 – 1346

To my Father

CERTIFICATE

I certify that ISABEL MARY MAGENNIS M.Sc. has spent eleven terms at research work under my supervision, and that she has fulfilled the conditions of Ordinance 16 (St. Andrews), so that she is qualified to submit the following thesis for the degree of Ph.D.

Lecturer in Chemistry
United College of St. Salvator
and St. Leonard
University of St. Andrews.

I declare that this thesis is my own composition, that the work of which it is a record has been carried out by myself and that it has not been submitted in any previous application for a Higher Degree.

The thesis describes the results of research carried out at the Department of Chemistry, United College of St.Salvator and St.Leonard, University of St.Andrews under the supervision of Dr. R. K. Mackie since 1st October 1967, the date of my admission as a research student.

Signed

Date

ABSTRACT

Twelve heterocyclic ring compounds have been prepared and a high resolution Nuclear Magnetic Resonance study of each carried out. In particular, solvent effects and coupling constants have been studied. Some axial and equatorial shifts of methylene protons were found to be reversed compared to the predicted situation. Observed coupling constants have been found to be slightly solvent dependent. Some interesting values of coupling constants prompted a full X-ray crystal analysis of two of the compounds. This has been done, yielding bond lengths, bond angles, configuration around the phosphorus atom and conformation of the heterocyclic ring, all in the solid state. Dihedral angles for P-O-C-H systems have been calculated and an attempt has been made to correlate observed coupling constants with dihedral angles and electronegativity of substituents.

ACKNOWLEDGEMENTS

I wish to express my thanks to the following :

Professor J. I. G. Cadogan, F.R.I.C., F.R.S. for accepting me into the Department of Chemistry of the University of St. Andrews.

Professor J. F. Allen, F.R.S. for giving me permission to use the X-ray facilities in the School of Physical Sciences.

Dr. R. K. Mackie for his patient and encouraging supervision of this work.

Dr. R. C. Killean and Dr. J. Lawrence for their kindness in guiding me with the X-ray section.

All the technicians of both the Chemistry and Physical Sciences Departments, especially Mr. A. Watson and Mr. T. McQueen.

Dr. P. Curnuck, I.C.I. Runcorn, for running the 200 mega-cycle spectra for me.

Dr. M. Jeffs, I.C.I. Runcorn, for doing the broad-line N.M.R. for me.

Mr. M. Green, Perkin-Elmer, Beaconsfield, for enabling me to make use of the Perkins-Elmer Laboratory for variable temperature work.

The University of St. Andrews for a research grant, without which this work would have been impossible.

To my husband, Michael, for his great encouragement and interest whilst this thesis was being written.

CONTENTS

TABLES

FIGURES

INTRODUCTION

The idea of "Conformational Analysis" was born relatively recently[1] and is understood to be that branch of science which is concerned with the detailed spatial structure of the molecule. The molecular "Conformations" have been defined by Klyne[2] as denoting the different arrangements in space of the atoms in a single classical organic structure (configuration); the arrangements being produced by rotation or twisting (but not breaking) of bonds. However the origin of conformational analysis can be traced back to the late 19th Century when Van't Hoff[3] and LeBel began[4] their research into mirror image isomerism. Together their theories incorporated two basic hypotheses, both of which were confirmed later:- [20] the tetrahedral theory and the principle of free rotation.

Baeyer[5], in his Strain Theory extended the original work and tried to show the dependence of ring formation on the number of ring components. He used the regular tetrahedron (lowest energy) for his atomic model, but assumed a planar structure for cyclic aliphatic compounds. Since some molecules of this type can only be formed with distortion of the tetrahedral angle, energy must expended and this expenditure Baeyer called angle - strain. Sachse[6] wanted strain free rings and so had to make his model of cyclohexane non-planar. In fact it could be constructed strain - free in two forms.

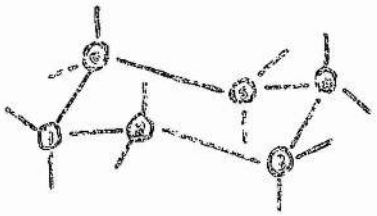

I

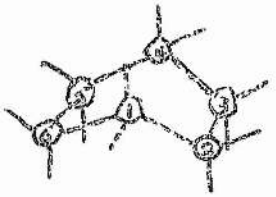

II

I being called "chair" or "rigid" form where free rotation is prevented and II being called "boat" or "flexible" form which is not completely rigid. If the principle of free rotation as used for acyclic compounds is taken into account then two cyclohexanes and two monosubstituted cyclohexanes should exist. However this type of isomerism had never been observed in the case of cyclohexane and so Sachse's postulate of a spatial structure was ignored for a long time. Meanwhile cyclohexane and all other rings were still regarded as planar. In 1918 Mohr[8] demonstrated with a model that the two forms of the cyclohexane were interchangeable without requiring a great amount of Activation Energy. The interchanging arises, Mohr claimed, from the flipping over of two carbon atoms. Experimental confirmation[9] for the Sachse - Mohr Theory was soon obtained. In the flipping over process a very small distortion of the tetrahedral angles occurs and to a certain extent free rotation is still possible along some bonds. Heteroatoms will alter tetrahedral angles but in general similar

strain and isomeric conditions will exist in heterocyclic compounds.[21]

What makes conformation analysis possible is the fact that certain chemical and physical properties of organic compounds are related to preferred conformations. The methods used can be divided into two main groups :- physical methods and chemical methods. We shall be interested in the present study with the former. These comprise, electron diffraction,[10] x-ray diffraction,[11] determination of dipole moments,[12] ultra-violet and infra-red spectroscopy,[13] Raman-spectroscopy,[14] microwave spectroscopy,[15] the Kerr effect,[16] measurement of optical rotary dispersion,[17] just recently Ultrasonic Relaxation,[22] and finally Nuclear Magnetic Resonance.[18,19]

The two methods used to study the conformational analysis of the compounds under review here have been x-ray crystallography and Nuclear Magnetic Resonance (N.M.R). These are both discussed in detail in later chapters.

CHAPTER I

NUCLEAR MAGNETIC RESONANCE PHENOMENA

Solvent Effects[1,2]

Two factors determine the shielding constant and hence the chemical shift of a nucleus in a specific molecule, the electronic distribution within the molecule and the nature of the surrounding medium. Thus the observed shielding constant can be represented by

$$\sigma = \sigma_{medium} + \sigma_{mol}$$

Buckingham, Schaefer and Schneider,[3] however, have studied medium effects and suggest that σ_{medium} itself has five sources :

$$\sigma_{med} = \sigma_b + \sigma_a + \sigma_W + \sigma_E + \sigma_H$$

σ_b is proportional to the bulk diamagnetic susceptibility of the medium. When measurements are made with the sample in a cylindrical tube, as in the present measurements, $\sigma_b = (2/3)\pi\chi_v$ where χ_v is the volume susceptibility of the medium ; σ_a arises from the non-zero averaging of the anisotropy in the diamagnetic susceptibility of the solvent molecules; for a disc-shaped solvent like benzene this is important and is given by :

$$\sigma_a = -2m(\chi_{11} + \chi_1) / 3R^3$$

where R is the distance between the nucleus in the solute molecule and the centre of the solvent molecule and m is the number of solute molecules lying within this distance R. For benzene $(\chi_{11} - \chi_1) = -9 \times 10^{-29}$. σ_W arises from the weak Van der Waal's forces between solute and solvent molecules.[3,4] Two effects contribute to σ_W :

(a) an expansion of the electronic environment of the

solute nuclei originating in a distortion, due to solvent, of the solute from its equilibrium electronic configuration, and

(b) a time varying distortion of the electronic environment of solute molecules arising from non-equilibrium configuration of solvent molecules.

Effect (a) is independent of temperature but (b) should increase. Both lead to a negative σ_W. σ_E is due to the effect of an electric field on the shielding constant.[5] If an Onsager model is used to calculate the reaction field arising from polar groups, then σ_E is proportional to $(\epsilon - 1)(\epsilon + 1)$, ϵ being the dielectric constant of the medium. Finally, σ_H which is usually the largest term, is the result of specific solvent-solute interactions, such as hydrogen bonding. Buckingham and co-workers have tested their equation[3] for both polar and non-polar solutes in a variety of liquid solvents. Specific solvent-solute interactions will now be discussed.

Aromatic Solvents

Aromatic compounds have weak complexing properties ; nevertheless, benzene and others often produce large changes in the chemical shifts of polarisable solutes. These can be explained as due to the large diamagnetic anisotropy associated with the existing induced ring currents in aromatics. A preferred solute-solvent orientation will result if a weak complex is formed and the result would be a shift in the resonance position relative to that of the non-complexed solute. Whether the shift is too high or low field will depend on the nature of the complex. Schneider and Reeves[5] have shown that the hydrogen resonance signal of chloroform moves by 1.5 p.p.m. to high fields on going from pure chloroform to a 5 per cent. solution of chloroform in benzene. This shift is explained as due to a preferred orientation of the complex which is shown below :

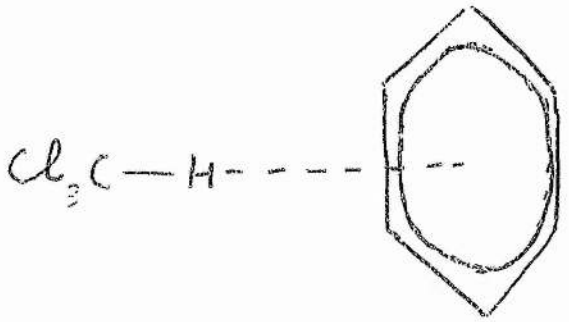

Thus, the hydrogen nucleus experiences an applied field which is reduced in magnitude by the induced field which arises from diamagnetic ring currents in the benzene molecule. It has been shown[1] that molecules which have hydrogen atoms with some degree of charge polarisation, experience a similar effect.

Schaefer and Schneider[6] have found that in unsaturated heterocyclics the shielding of ring protons depends very much on solvent effects. They compared chemical shifts measured in solvents such as benzene and acetone, where specific solvent-solute interactions would be expected, with those in hexane solution, a relatively inert solvent. They found that acetone deshielded the α-hydrogen nuclei in pyrrole, thiophene and furan, whereas benzene increased shielding. Moreover, in benzene solution the hydrogen nuclei nearest to the electronegative atom was affected to a greater extent.

In the equation given previously for the shielding constant

$$\sigma = \sigma_{med} + \sigma_{mol}$$

σ_{mol} is the value for the 'isolated molecule', ideally a gaseous sample at low pressures. For solids the 'isolated molecule' can be approximated to by using a dilute solution of the compound in an inert solvent. In the present study an attempt has been made to study the

effect of benzene, as a solvent, on the dioxaphosphorinanes under observation. The compounds have therefore been examined in $CDCl_3$ and C_6D_6.

Analysis of Nuclear Magnetic Resonance Spectra[1,2,7]

In general, a resonance of a given nucleus will be split into $(n + 1)$ lines by n magnetically equivalent nuclei with spin number $I = \frac{1}{2}$ provided $J \ll \delta$ where J is the coupling constant between the interacting nuclei and δ their chemical shift difference. If, however, J is not $\ll \delta$, or more than one non-equivalent nucleus is involved and $\delta < 10J$, the situation is more complex. To obtain values of chemical shifts and coupling constants, the spectra must be given a full quantum mechanical analysis. This analysis requires the following stages :

1. Obtaining the basic product spin wave functions for the particular system being analysed.

2. Working out the expression for the Hamiltonian operator. This is given by[8]

$$\mathcal{H} = + \sum_i \nu_i I_{zi} + \sum\sum_{i<j} J_{ij} I_i I_j \qquad (1)$$

where ν_i is the linear frequency for the i th nucleus and is

$$= \frac{W_i}{2\pi} = \frac{\gamma_i H_i}{2\pi} \qquad (2)$$

W_i being the resonance frequency in angular units, γ_i the magnetogyric ratio of the i th nucleus and H_i the resonance field for the i th nucleus. H_i is given by $H_o (1 - \sigma_i)$ where H_o is the applied magnetic field and σ_i is the screening coefficient for the i th nucleus. In equation (1) $\mathbb{I}_i$ is the spin-angular momentum operator with components (I_{xi}, I_{yi}, I_{zi}) and J_{ij} is the coupling constant between nuclei i and j, in Hertz.

3. The energy levels and wave functions are then found by

solving the time independent Schrödinger equation[9] :

$$H\psi = E\psi \tag{3}$$

To do this the wave function ψ is taken to be a linear combination of an eigen function ϕ_n. In this case the wave functions making up the Hamiltonian matrix are linear combinations of product spin functions which are simultaneous eigenfunctions of I_z and $\mathbb{I}_i^2$.

4. Having found the energy levels of the system, selection rules for transitions between the levels of ψ_k and ψ_l are applied :

(a) $\Delta m = -1$

(b) $\Delta \mathbb{I}_i^2 = 0$

(c) ψ_k and ψ_l must belong to the same irreducible representation.

Allowed transitions give rise to the resonance lines observed in the spectra.

5. Finally, transition intensities are calculated. These intensities are proportional to $|(\psi_k|\mathbb{I}^-|\psi_l)|^2$ where ψ_k and ψ_l are eigenfunctions of the Hamiltonian and $\mathbb{I}^-$ is a "lowering" operator and $= I_x - iI_y$.

In the compounds under study the spin-spin system was usually AA'BB'CDX. This could be decoupled to give an AA'BB'X system and where ring coupling is small, this approximates to an ABX case. The detailed analysis of the ABX case is discussed below.

ABX System

The ABX system consists of three non-equivalent magnetic nuclei, two of which have $J_{AB} \sim (\nu_A - \nu_B)$ and a third nucleus X which has a chemical shift difference from the other two which is large compared with the coupling constants J_{AX} or J_{BX}. In the present case X represents the phosphorus nucleus. For this system three resonance frequencies and three coupling constants are needed to describe it completely. This can be seen from the diagram below :

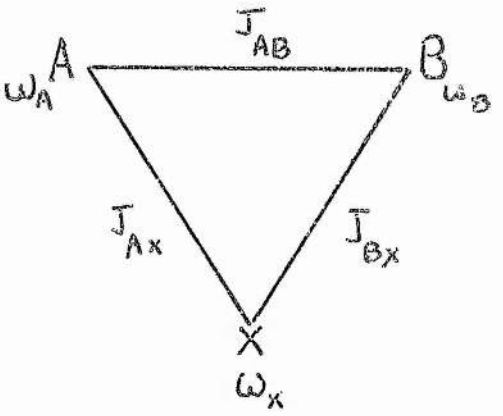

The basic product functions are from ϕ_1 to ϕ_8 consecutively $\alpha\alpha\alpha$, $\alpha\alpha\beta$, $\alpha\beta\alpha$, $\beta\alpha\alpha$, $\alpha\beta\beta$, $\beta\alpha\beta$, $\beta\beta\alpha$ and $\beta\beta\beta$. Since the system has no symmetry properties, these functions are themselves used as a basis for the formation of the wave functions. The Hamiltonian operator for the system using equation (1) above is :

$$\begin{aligned}\mathcal{H} = (&W_A I_{A_Z} + W_B I_{B_Z} + W_X I_{X_Z} + J_{AB} I_{AZ} I_{BZ} + J_{AX} I_{A_Z} I_{X_Z} \\ &+ J_{BX} I_{B_Z} I_{X_Z} + \tfrac{1}{2} J_{AB} [I_A^+ I_B^- + I_A^- I_B^+] + \tfrac{1}{2} J_{AX} [I_A^+ I_X^- + I_A^- I_X^+] \\ &+ \tfrac{1}{2} J_{BX} [I_B^+ I_X^- + I_B^- I_X^+]) \end{aligned} \qquad (4)$$

where I^+ and I^- are the "raising" and "lowering" operators of the spin angular momentum and are given by :

$$I^+ = I_x + iI_y$$
$$I^- = I_x - iI_y$$

The stationary state energy levels and wave functions (four non-mixing basic product functions and four mixed functions) obtained from solving equation (3) are given in Table 1.1.

TABLE 1.1.

	Wave functions	Energy levels
ψ_1	ϕ_1	$\frac{1}{2}(\nu_A+\nu_B+\nu_X)+\frac{1}{4}(J_{AB}+J_{AX}+J_{BX})$
ψ_2	ϕ_2	$\frac{1}{2}(\nu_A+\nu_B-\nu_X)+\frac{1}{4}(J_{AB}-J_{AX}-J_{BX})$
ψ_3	$(\cos\theta_+)\phi_3+(\sin\theta_+)\phi_4$	$\frac{1}{2}\nu_x-\frac{1}{4}J_{AB}+D_+$
ψ_4	$-(\sin\phi_+)\phi_3+(\cos\phi_+)\phi_4$	$\frac{1}{2}\nu_x-\frac{1}{4}J_{AB}-D_+$
ψ_5	$(\cos\theta_-)\phi_5+(\sin\theta_-)\phi_6$	$-\frac{1}{2}\nu_x-\frac{1}{4}J_{AB}+D_-$
ψ_6	$-(\sin\theta_-)\phi_5+(\cos\theta_-)\phi_6$	$-\frac{1}{2}\nu_x-\frac{1}{4}J_{AB}-D_-$
ψ_7	ϕ_7	$\frac{1}{2}(-\nu_A-\nu_B+\nu_X)+\frac{1}{4}(J_{AB}-J_{AX}-J_{BX}$
ψ_8	ϕ_8	$\frac{1}{2}(-\nu_A-\nu_B-\nu_X)+\frac{1}{4}(J_{AB}+J_{AX}+J_{BX}$

D_+, D_- and the angles θ_+ and θ_- (lying between 0 and π) are defined by the following equations :

$$\begin{aligned} D_+\cos 2\theta_+ &= \tfrac{1}{2}(\nu_A-\nu_B)+\tfrac{1}{4}(J_{AX}-J_{BX}) \\ D_+\sin 2\theta_+ &= \tfrac{1}{2}J_{AB} \\ D_-\cos 2\theta_- &= \tfrac{1}{2}(\nu_A-\nu_B)-\tfrac{1}{4}(J_{AX}-J_{BX}) \\ D_-\sin 2\theta_- &= \tfrac{1}{2}J_{AB} \end{aligned} \qquad (5)$$

Thus
$$D_+ = \{[\tfrac{1}{2}(\nu_A-\nu_B)+\tfrac{1}{4}(J_{AX}-J_{BX})]^2+\tfrac{1}{4}J_{AB}^2\}^{\frac{1}{2}}$$
$$D_- = \{[\tfrac{1}{2}(\nu_A-\nu_B)-\tfrac{1}{4}(J_{AX}-J_{BX})]^2+\tfrac{1}{4}J_{AB}^2\}^{\frac{1}{2}}$$

$$\tfrac{1}{2}|J_{AX}-J_{BX}| = [(D_++\tfrac{1}{2}J_{AB})(D_+-\tfrac{1}{2}J_{AB})]^{\frac{1}{2}}-[(D_-+\tfrac{1}{2}J_{AB})(D_--\tfrac{1}{2}J_{AB})]^{\frac{1}{2}} \qquad (6)$$

$$\tfrac{1}{2}|\nu_A-\nu_B| = (D_+^2-\tfrac{1}{4}J_{AB}^2)^{\frac{1}{2}}-\tfrac{1}{4}(J_{AX}-J_{BX}) \qquad (7$$

TABLE 1.2

TABLE 8.30 TRANSITION ENERGIES AND RELATIVE INTENSITIES FOR THE ABX SYSTEM

Transition number	Transition	Origin	Energy	Relative intensity
1	$\psi_8 \rightarrow \psi_6$	B	$\frac{1}{2}(\nu_A + \nu_B) - \frac{1}{4}(2J_{AB} + J_{AX} + J_{BX}) - D_-$	$(\cos\theta_- - \sin\theta_-)^2$
2	$\psi_7 \rightarrow \psi_4$	B	$\frac{1}{2}(\nu_A + \nu_B) - \frac{1}{4}(2J_{AB} - J_{AX} - J_{BX}) - D_+$	$(\cos\theta_+ - \sin\theta_+)^2$
3	$\psi_5 \rightarrow \psi_2$	B	$\frac{1}{2}(\nu_A + \nu_B) + \frac{1}{4}(2J_{AB} - J_{AX} - J_{BX}) - D_-$	$(\cos\theta_- + \sin\theta_-)^2$
4	$\psi_3 \rightarrow \psi_1$	B	$\frac{1}{2}(\nu_A + \nu_B) + \frac{1}{4}(2J_{AB} + J_{AX} + J_{BX}) - D_+$	$(\cos\theta_+ + \sin\theta_+)^2$
5	$\psi_8 \rightarrow \psi_5$	A	$\frac{1}{2}(\nu_A + \nu_B) - \frac{1}{4}(2J_{AB} + J_{AX} + J_{BX}) + D_-$	$(\cos\theta_- + \sin\theta_-)^2$
6	$\psi_7 \rightarrow \psi_3$	A	$\frac{1}{2}(\nu_A + \nu_B) - \frac{1}{4}(2J_{AB} - J_{AX} - J_{BX}) + D_+$	$(\cos\theta_+ + \sin\theta_+)^2$
7	$\psi_6 \rightarrow \psi_2$	A	$\frac{1}{2}(\nu_A + \nu_B) + \frac{1}{4}(2J_{AB} - J_{AX} - J_{BX}) + D_-$	$(\cos\theta_- - \sin\theta_-)^2$
8	$\psi_4 \rightarrow \psi_1$	A	$\frac{1}{2}(\nu_A + \nu_B) + \frac{1}{4}(2J_{AB} + J_{AX} + J_{BX}) + D_+$	$(\cos\theta_+ - \sin\theta_+)^2$
9	$\psi_8 \rightarrow \psi_7$	X	$\nu_X - \frac{1}{2}(J_{AX} + J_{BX})$	1
10	$\psi_5 \rightarrow \psi_3$	X	$\nu_X + D_+ - D_-$	$\cos^2(\theta_+ - \theta_-)$
11	$\psi_6 \rightarrow \psi_4$	X	$\nu_X - D_+ + D_-$	$\cos^2(\theta_+ - \theta_-)$
12	$\psi_2 \rightarrow \psi_1$	X	$\nu_X + \frac{1}{2}(J_{AX} + J_{BX})$	1
13	$\psi_7 \rightarrow \psi_2$	comb.	$2\nu_0 - \nu_X$	0
14	$\psi_5 \rightarrow \psi_4$	comb.	$\nu_X - D_+ - D_-$	$\sin^2(\theta_+ - \theta_-)$
15	$\psi_6 \rightarrow \psi_3$	comb.	$\nu_X + D_+ + D_-$	$\sin^2(\theta_+ - \theta_-)$

When selection rules and transition probabilities are worked out between the eight energy levels, it is found that there are fifteen possible transitions, one of which has zero intensity and two of which have very low intensity. Transition energies and relative intensities are given in Table 1.2.

Observation of this table shows that J_{AB} can be obtained by subtracting the frequencies of any one of the following four pairs of bands :

$$J_{AB} = 3 - 1 = 4 - 2 = 7 - 5 = 8 - 6$$

$\frac{1}{2}|J_{AX} + J_{BX}|$ is the separation between mid-points of (8 7 3 4) and (1 2 5 6).

D_+ and D_- can be calculated by subtracting frequencies of the following bands :

$$2D_+ = 6 - 2 = 8 - 4$$

$$2D_- = 5 - 1 = 7 - 3$$

$|J_{AX} - J_{BX}|$ and $|\nu_A - \nu_B|$ can be obtained using equations (6) and (7) and hence J_{AX} and J_{BX} can be determined. However, it is not possible to identify D_+ from D_- and unless the signs of the coupling constants are known, more than one set of assignments can be made. Any assignment must, however, obey the same subtraction rules as the transition energies. The spectrum in fact consists of two symmetrical quartets, usually overlapping for the A and B parts and six lines for the X part, two of which are the combination lines of low intensity. Figure 1.1. shows a typical theoretical ABX spectrum.

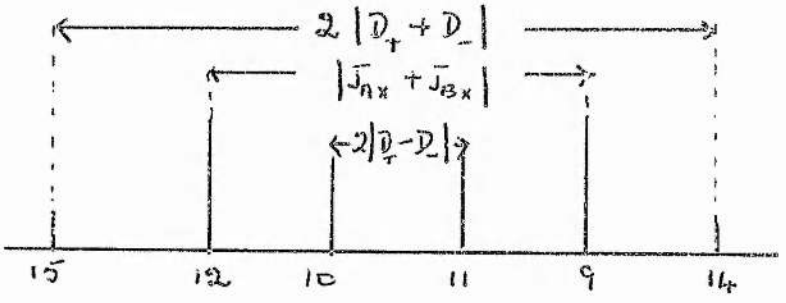

Figure 1.1.

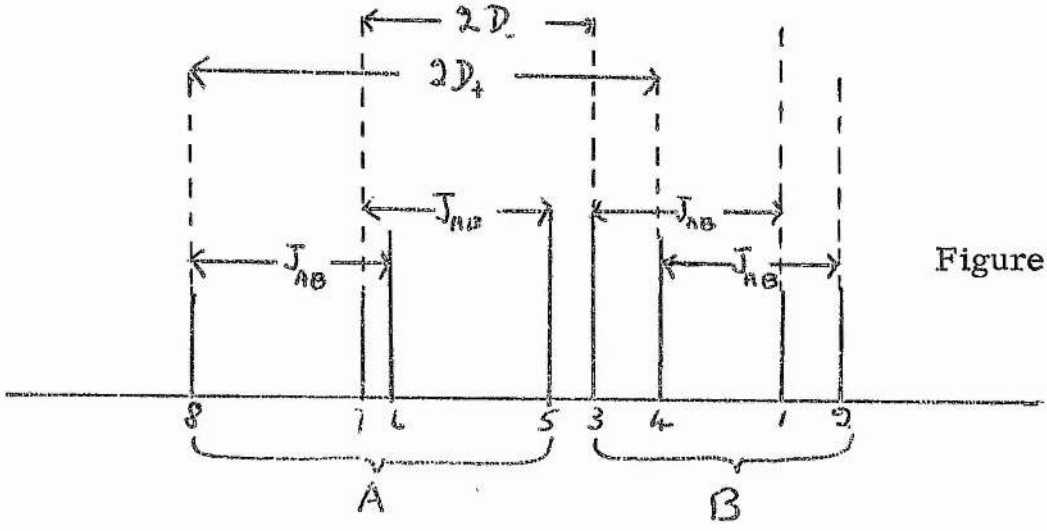

Figure 1.1.

Double Resonance[1,2,7]

An invaluable technique in N.M.R. which can be used to simplify complex spectra is double resonance.

Its aim is to remove the effect of spin-coupling by applying an audio-frequency,[12,13,14] or second radio-frequency[15] in addition to the one already used for observation. Basically, the method involves the irradiation of one group of equivalent nuclei, with a strong R.F. field close to their resonance frequency. This results in saturation and in effect, decouples the irradiated nuclei from the remaining nuclei and so the spectrum is simplified. Double resonance has other applications[2] : it may help to determine the position of a resonance line which is itself completely obscured by other resonances but which is coupled to a second proton with an observable resonance pattern ; it may be used to show that two protons are, in fact, coupled where this is not immediately obvious and finally, it helps, in some cases in determining

relative signs of coupling constants.

In 1956 Anderson[12] demonstrated for the first time that chemically non-equivalent nuclei could be decoupled. He used a two-crystal controlled radio-frequency oscillator which had a controlled frequency difference. The Varian HA 100 spectrometer was used for the final results and calculations given in Chapter 4 and, in some cases, spin decoupling was necessary to simplify the spectra. The method of spin decoupling on the HA 100 requires a knowledge of the system of operation for the internal lock. The double resonance experiments are best carved out with the spectrometer in "frequency sweep" mode. This involves modulation of the 100 mHz centreband with a manually controlled audiofrequency, ω_3, which is "locked" on a reference absorption at H_3 in the spectrum, e.g. tetramethylsilane TMS.

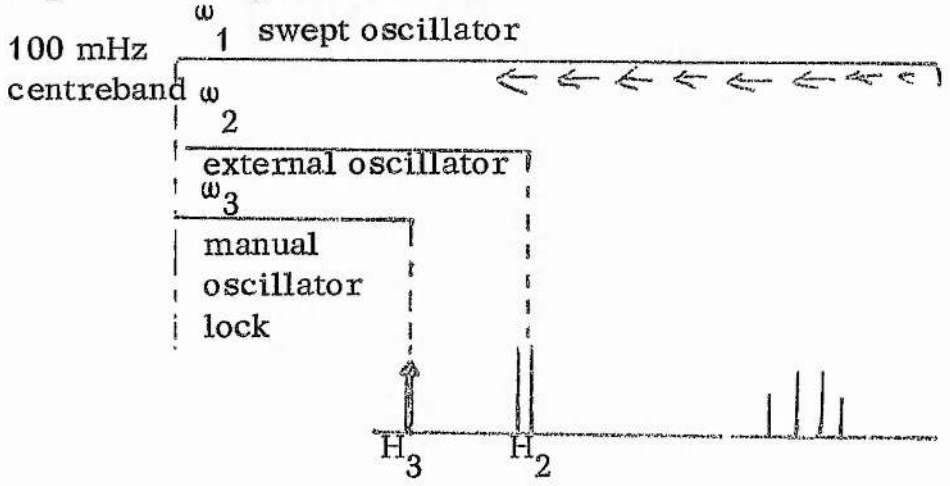

upper audio side bands

A swept oscillator ω_1, excites the resonances in the spectrum. To carry out spin decoupling a manual external oscillator, ω_2, at high amplitude is set such that the frequency ω_2 corresponds to the resonance at H_2 which is to be decoupled. The swept oscillator, ω_1, is used as the analytical channel.

Techniques and Instruments Used

Perkin Elmer R 10) Initial spectra
) Variable Temperature work
) Phosphorus P_{31} probe

Perkin Elmer R 12	)	Decoupling of one compound
Jeol 100 Megacycle	)	2, 5-diphenyl-2-oxo-1, 3, 2-dioxaphosphorinane
	)	Spectra at 31, 5°C
Varian HA 100	)	Decoupled spectra
	)	Phosphorus (P_{31}) spectra

Broad line N.M.R. of 2-phenyl-2-oxo-1, 3, 2-dioxaphosphorinane and 4, 4-dimethyl-2-phenyl-2-oxo-1, 3, 2-dioxaphosphorinane were run at I.C.I. Runcorn and four compounds were run on the 220 megacycle instrument also at Runcorn.

CHAPTER 2

HETEROCYCLIC PHENOMENA

Although heterocyclic compounds have received much attention,[1,2] only recently has the conformation of phosphorus heterocyclics aroused interest. In particular, 2,2-disubstituted-1,3,2-dioxaphosphorinanes are interesting because of the configuration around the phosphorus atom and the possibility of the phosphorinane ring having a 'chair' or 'boat' form. This latter possibility has been investigated by X-ray crystallography[3,4] and more recently by N.M.R.[5]; the former by X-ray studies,[6] dipole moments[15] and only tentatively by N.M.R.[8]

Nuclear magnetic resonance however, could be an especially valuable tool for the above conformational studies, if it could provide a quick, relatively easy and unambiguous analysis. That this is mostly the case in conformational analysis will be shown below.

The phenomenon of chemical-shift has aided the assignment of axial and equatorial substituents and that of spin-spin coupling has helped the assignment of 'boat' or 'chair' form. Configuration around the phosphorus has proved to be more difficult.

Axial-Equatorial Analysis

Numerous experiments[9,12] have shown that axial ring protons (or groups) absorb at higher field than do their equatorial counterparts. Jackmann[10] attributes this to a long range shielding effect connected with the diamagnetic anisotropy of the carbon-carbon single bonds which bear a 2-3 relationship to the absorbing protons. In the reference just quoted, Jackmann uses the McConnell equation[11] to show quantitatively that a difference in chemical shift between the axial and equatorial protons, see Fig.2.1, is to be expected. This equation was originally derived as an approximate

relation for an axially symmetrical group of electrons G and is

$$\sigma_{av.}(G) = \frac{(3\cos^2\theta - 1)(\chi_L - \chi_T)}{3r^3}$$

where r is the distance between the proton and the electrical centre of gravity of G (in the present case the mid-point of the single bond); θ is the acute angle which r makes with the symmetry axis, and σ is the shielding, ('av' indicates that this has been averaged over all orientations of the system) and χ_L, χ_T are longitudinal and transverse magnetic susceptibilities respectively. It can be seen from figure 2.1 that the bonds will have a different r & θ value for the axial proton and the equatorial proton.

The $C_1 - C_2$ and $C_1 - C_6$ bonds are symmetrically orientated with respect to the two protons at C and thus make an equal contribution to their shielding. Jackmann concludes that the H_e will be deshielded by 2:3 and 5:6 bonds and that the axial proton will be shielded. The value he calculates for σ is 0.40 p.p.m and this is in agreement with experimental values.[9,12]

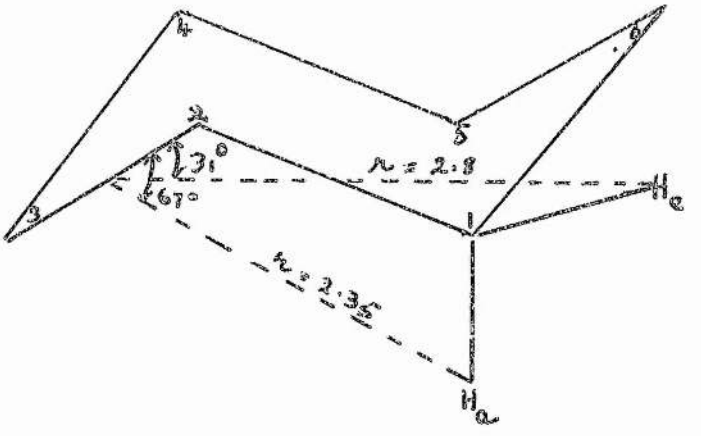

Figure 2.1

The effect of the 3:4 and 4:5 bonds is taken as negligible. When the ring system is heterocyclic an uncertainty in the location of the electrical centre of gravity of the hetero-bond arises making application of the McConnell equation difficult. However, experimental evidence[13] suggests that the carbon - oxygen single bond has a similar magnetic anisotropy to that of the carbon - carbon single bond. Thus Jackmann's theory could be applied to systems containing carbon - oxygen single bonds. No such quantitative analysis can be made when a hetero - atom such as phosphorus is introduced since the value of $(\chi_L - \chi_T)$ can not be calculated for a bond containing phosphorus. However, unless this value is positive (it is negative for C - C, C - O) then H_e will be deshielded as before and H_a shielded - the only change will be in the magnitude of the chemical shift difference.

Although Jackmann saw his analysis as nothing more than "a promising approach" and although he maintained that "a number of critical experiments are required to establish the utility of proton chemical shifts for conformational analysis of cyclic systems", no further advance has been made and it is generally accepted[14] that axial protons resonate at higher field than equatorial protons.

Ring Conformation

Attempts have been made for many years to try and relate coupling constants between two atoms with their angular relationship. If such a relation exists, then N.M.R. would provide a direct method for distinguishing 'chair' and 'boat' cyclic conformations, since dihedral angles between bonds are different for these.

In 1959 Karplus[15] postulated such a relationship for vicinal protons, i.e. H-C-C'-H' and this has been followed by many structural N.M.R. studies.[16,17,18] However, in 1963 Karplus[19] stressed that dihedral angle dependence is not the only one for vicinal protons and he outlined four main factors that contribute to the size of the coupling constant.

1. Angular Dependence

Using an unperturbed, non-ionic six-orbital fragment HCC'H to determine the contact interaction, Karplus derived an equation for vicinal proton coupling :

$$J_{HH'} = 4.2 - 0.5 \cos \phi + 4.5 \cos^2 \phi$$

This equation is a 'zero-order' approximation, "the variability of the observed coupling constants is not predicted by the simple model considered,"[15] and further refinement was seen to be necessary. A modified experimental version of Karplus' first equation has been postulated by Williamson,[20]

$$J = 10 \cos^2 \phi \qquad 0 \leq \phi \leq 90^\circ$$
$$J = 16 \cos^2 \phi \qquad 90^\circ \leq \phi \leq 180^\circ$$

However, for any such equation, agreements with experimental values are only approximate.[21] A result of the above relationship is that in ring compounds, axial-axial coupling will be greater than axial-equatorial or equatorial-equatorial interactions. Experiments have confirmed this.[21]

2. Electronegativity

Introduction of a substituent whose electronegativity differs from that of the hydrogen atom will cause perturbation. Changes in hybridisation around carbon atoms results and the coupling constants will alter. Theoretical calculations[19] and experimental observations[22] suggest that the coupling constant decreases as the electronegativity of the substituent increases.

3. Bond Angles

Vicinal coupling will also depend on θ and θ' where $\theta = <HCC'$ and $\theta' = <CC'H'$. Karplus using a fragment-model calculation predicted that if the dihedral angle is constant and θ and θ' increase, then $J_{HH'}$ will decrease.[23]

4. Bond Lengths

Finally, for constant bond angles, the vicinal coupling is expected to decrease for an increase in C - C bond length. In fact for this case, calculations yield an almost linear dependence for ethylenic systems, in agreement with experiment.[24]

Karplus' initial work has since been applied to coupling between vicinal hetero atoms, including fluorine and phosphorus couplings with protons. In 1966 Benezra and Durisson,[25] taking all four contributions into account, showed that J_{PH} in a H - C - C - P system approximated to a Karplus relation. In 1967, Tsuboi[26] and co-workers dealt with molecules showing free rotation. They deduced a relationship for proton-phosphorus spin-spin coupling :

$$10.4 = \frac{1}{3} J_t + \frac{2}{3} J_g$$

where J_t is the coupling constant between the proton and phosphorus in the trans relation and J_g that in the gauche. Applying this to a ring system

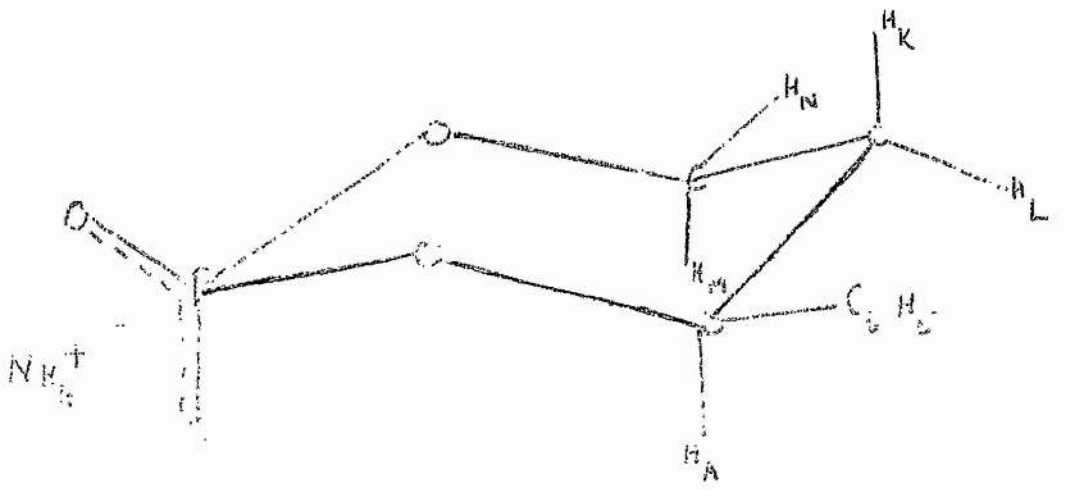

namely the ammonium salt of 1-hydroxy-4-phenyl-1,3,2-dioxaphosphorinane-2-oxide in deuterium oxide solution, they obtained for H_A

J_g	= 1.5 cps	observed
J_t	= 28.2 cps	calculated

In 1968 Hargis and Bentrude[27] studied experimental results for some 2-dioxaphosphorinanes and they found these to be in agreement with a general Karplus theory. In 1969 Kainosho and NaKamura,[28] using observed coupling constants and values of dihedral angles, estimated by photographs of a dreinding model, published the following table for the 5-membered ring of 2,7,8-trioxa-1-phosphabicyclo[3.2.1.]octane :

J_{POCH} (Hz)		ϕ^o
J_{AP}	4.4	128
J_{BP}	1.7	113
J_{CP}	9.6	163
J_{GP}	9.3	180
J_{FP}	2.5	60

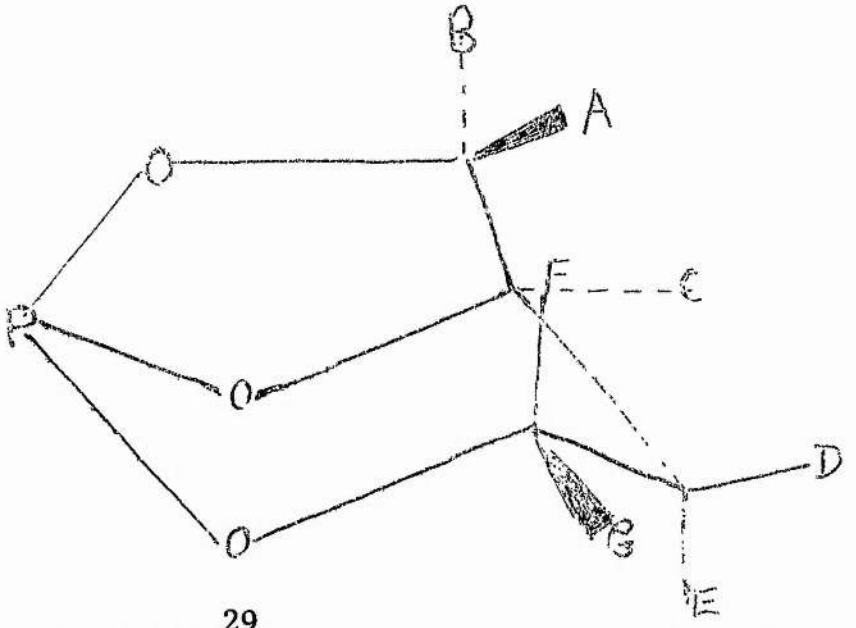

Malcolm and Hall[29] have reported angular dependencies for ring protons in 2-phenoxy-5-5-dimethyl-2-oxo-1, 3, 2-dioxaphosphorinane as shown below :

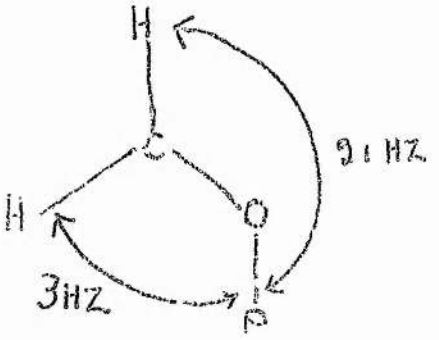

Signs of coupling constants reported show geminal coupling constants as being negative and vicinal coupling constants as being positive.

The relevance of these results to the present study will be discussed in detail in Chapter 4.

Configuration around the Phosphorus Atom

Axial and equatorial groups around the phosphorus atom can be difficult to assign using N.M.R., especially when one of the groups is a doubled bonded oxygen as in substituted 2-oxo-dioxaphosphorinanes. Recently, however, attention has focussed on these. X-ray analysis of three compounds with substituents Br, OH and OPh show that the P=O group is equatorial. On the basis of preliminary dipole moment and N.M.R. measurements, Verkade and co-workers[30] have proposed that

the methoxy group in two phosphites

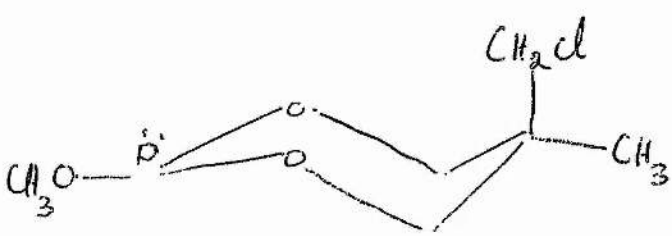

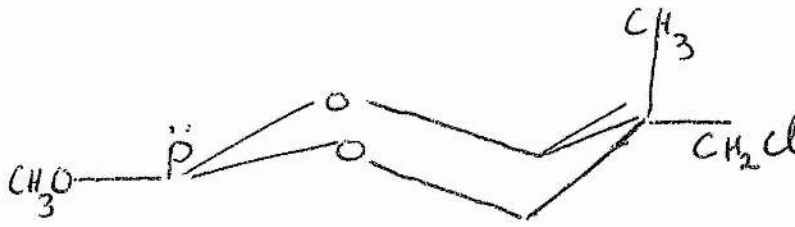

is axial. Dipole moments of seven ring compounds in benzene solution have been reported.[31] These compounds include

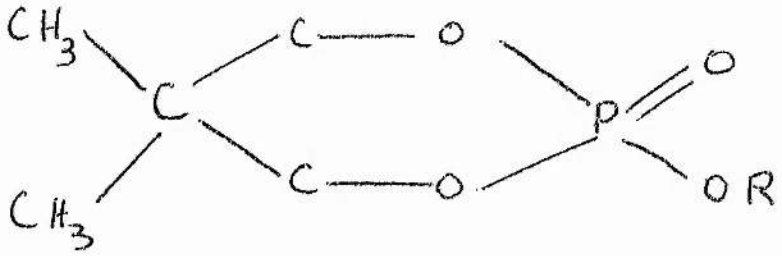

R = -n-butyl
-n-propyl

and a heterodyne-beat method was used. It was found that P=O bonds favour the equatorial position rather than axial both in solution and in solid.

CHAPTER 3

EXPERIMENTAL

ORGANIC PREPARATIONS

2-methyl-2-oxo-1,3,2-dioxaphosphorinane

26.6 gms. (0.2 moles) of methylphosphonic dichloride in 100 ml. of dry toluene was added slowly to 15.2 gms. (0.2 moles) of trimethylene glycol and 40.4 gms. (0.4 moles) of triethylamine in 300 ml. of dry toluene. The temperature of the mixture was kept between 0° and 5°C by means of an ice-bath. After addition, the mixture was heated to 100°C for one hour. Triethylamine hydrochloride, which was precipitated, was filtered off. The solvent was removed under vacuum and the remaining solution distilled under vacuum to yield a clean liquid which distilled over at 110° - 112°C at 3 mm Hg. On running the N.M.R. spectra of the product, it was found to contain a little 1,3-propane-diol. Further distillation failed to remove this. On standing the clear liquid crystallised out to give fine white crystals, m.p. 97 - 99°C (lit. m.p. 98 - 99°C). Yield 54.3%.

2-phenyl-2-oxo-1,3,2-dioxaphosphorinane

39 gms. (0.2 moles) of phenylphosphonic dichloride in 100 ml. of dry toluene was added to 15.2 gms. (0.2 moles) of trimethylene glycol and 40.4 gms. (0.4 moles) of triethylamine in 300 ml. of dry toluene. The temperature was kept between 0° and 5°C. After addition, the mixture was heated to 100°C for one hour, after which the amine salt was filtered off. The solvent was removed under vacuum and the remaining solution was distilled under reduced pressure. The phosphorinane distilled over at 158°C at 0.1 mm Hg as a clear liquid which crystallised on standing to give fine white crystals, m.p. 48°C. Analysis : Calculated : 54.55% C ; 5.56% H. Found : 54.57% C ; 5.78% H. Yield 46.4%.

For the above two preparations the dryness of the starting materials was found to be critical.

2-methyl-2-oxo- 1,3,2- dioxaphosphepane

26.6 gms (0.2 moles) of methylphosphonic dichloride in 100 ml of dry toluene was added slowly to 18.3 gm (0.2 moles) of butane - 1,4-diol and 40.4 gms (0.4 moles) of triethylamine in 300 ml of dry toluene with stirring. The temperature of the mixture was kept between 0° and 5°C. After addition the mixture was heated to 100°C for one hour. After the amine salt had been filtered off, the solvent was removed under vacuum and the remaining solution distilled under reduced pressure. The product distilled over at 141.5°C at 16.5 mm Hg. On standing the liquid crystallised to give fine white flaky crystals which were recrystallised from benzene, m.p.65 - 66°C (lit. m.p.67.5 - 69°C)[1] Yield = 42.2%

2-phenyl-2-oxo-1,3,2-dioxaphosphepane

39 gms (0.2 moles) of phenylphosphonic dichloride in 100 ml of dry toluene was added slowly to 18 gms (0.2 moles) of butane-1,4-diol and 40.4 gms (0.4 moles) of triethylamine in 300 ml of dry toluene with stirring. The temperature was kept between 0° and 5°C during addition and the mixture was then heated to 100°C for one hour. When the amine salt had been filtered off, the solvent was removed under vacuum and the remaining solution distilled under reduced pressure. The phosphepane distilled over at 125° - 7°C at 3 mm Hg. On standing it crystallised out and was recrystallised from a mixture of 60 - 80°C petroleum ether and benzene to give fine white crystals. m.p. 75 - 76°C. (lit. m.p. 76 - 77.5°C)[1] Yield = 10.7%.

2-methyl-2-oxo-1,3,2- dixoaphosphocane and 2-phenyl-2-oxo-1,3,2-dioxaphosphocane

The preparation of these compounds was not successful. Although products were obtained they could not be identified.

2,5-diphenyl-2-oxo-1,3,2-dioxaphosphorinane

This was prepared by a method similar to that mentioned above, by W. H. Gibbs, The Chemistry Department, The University, St.Andrews. m.p. 114-115°C.

2,5,5-trimethyl-2-oxo-1.3.2-dioxaphosphorinane

This preparation was similar to those given above. The quantities used were 26.6 gms. (0.2 moles) methylphosphonic dichloride, 20.8 gms. (0.2 moles) 2,2-dimethyl-propane-1,3-diol, 40.4 grms. (0.4 moles) triethylamine. After removal of the solvent under vacuum, the product crystallised out and was recrystallised from benzene to give white crystals. m.p. 116°C (lit. m.p. 119 - 121°)[2]. Yield = 73.6%

5,5-dimethyl-2-phenyl-2-oxo-1,3,2-dioxaphosphorinane

This preparation was also similar to the above, quantities used were 39 gms. (0.2 moles) phenylphosphonic dichloride, 20.8 grms. (0.2 moles) 2,2-dimethyl-propane-1,3-diol, 40.4 grms. (0.4 moles) triethylamine. Again, after removal of solvent, the product crystallised out and was recrystallised from benzene to yield white crystals. m.p. 104°C. (lit. m.p. 108.5 - 110°C)[2]. Yield = 67.1%

Trichloro-methylphosphonic dichloride

Carbon tetrachloride 53.9 gms (0.35 moles), phosphorus trichloride 34.4 gms (0.25 moles), and aluminium trichloride 33.12 gms (0.25 moles) were mixed and then shaken together and heated under reflux for one hour. The complex formed was then dissolved in methylene chloride (7 volumes) and the solution cooled to about - 20° C by the addition of solid carbon dioxide. Water (3.0 moles) was then added slowly with vigorous shaking until the milky suspension first formed coagulated. The solution was then rapidly filtered, the solvent extracted under vacuum and the product allowed to crystallise out. It was recrystallised from methylene chloride giving white crystals m.p. 156°C (lit.m.p. 156°C)[3] Yield = 80.8%.

5,5- dimethyl - 2 - trichloro methyl - 2 oxo - 1,3,2 - dioxaphosphorinane

This preparation was similar to those previously mentioned, the quantities being trichloromethylphosphonic dichloride 44.6 gms (0.2 moles), 2,2 - dimethyl propane 1,3 - diol 20.8 gms (0.2 moles) triethylamine 40.4 gms (0.4 moles).

The product crystallised out after the solvent had been removed, and was recrystallised from benzene to give white flaky crystals. m.p. 154 - 156°C (lit. m.p. 168 - 169°)[2] Yield = 58.5%.

2 - phenyl - 1,3,2 - dioxaphosphorinane

33.4 gms (0.2 moles) of dichlorophenylphosphine in 100 ml. of dry toluene was added slowly to 15.2 gms (0.2 moles) of propane 1,3 - diol and 40.4 gms (0.4 moles) of triethylamine in 300 ml of dry toluene. The whole

system was kept in an atmosphere of nitrogen and during addition of the acid chloride the temperature was kept between 0° and $5^{\circ}C$. The mixture was then heated for one hour to $100^{\circ}C$ and the amine salt filtered off. After the solvent had been removed under vacuum the remaining solution was distilled under reduced pressure and the product distilled over at $144^{\circ}C$ at 1.5 mm Hg. (lit.b.p. 137° at 0.45 mm Hg)[4]

5,5 - dimethyl - 2 - phenyl - 1,3,2 - dioxaphosphorinane

This was prepared in a similar manner to the previous compound, the starting materials being dichlorophenylphosphine 33.4 gms (0.2 moles), 2,2 - dimethylpropane - 1,3 - diol 20.8 gms (0.2 moles) and 40.4 gms (0.4 moles) of triethylamine. After the solvent had been removed the product crystallised out and was recrystallised from benzene.
m.p. 60 - $63^{\circ}C$.
(lit. m.p. 82 - $83^{\circ}C$)[4] Yield = 36.5%.

2 - phenyl - 1,3 - dioxane.

7.6 gms (0.1 moles) of dry propane 1,3 diol was shaken with 14.86 gms (0.14 moles) of benzaldehyde and hydrogen chloride gas passed through for three hours. The mixture in the flask was kept in ice during this period. Dry carbon dioxide was then passed through to expel the hydrogen chloride. Diethyl ether was added to dissolve the precipitate formed and the solution was washed with distilled water to remove final traces of hydrogen chloride. It was then dried overnight over calcium carbonate, the ether pumped off and the residue distilled under vacuum to give the product at $80^{\circ}C$ under 1.5 mm Hg as a clear liquid. On standing

this crystallised out to give white crystals. m.p. 49 - 50°C. (lit. m.p. 49.5 - 50°C).[5] Yield = 41.3%

5,5 - dimethyl - 2 - phenyl - 1,3 - dioxane

This was prepared as above. The quantities used were 2,3 - dimethyl - propane - 1,3 - diol 10.4 gms (0.1 moles) and benzaldehyde 14.86 gms (0.14 moles). The product distilled over under vacuum at 123° - 125°C at 10 mm. Hg as a clear liquid. On standing white crystals formed m.p. 35°C. (lit. m.p. 35°C).[6] Yield = 51.2%

NUCLEAR MAGNETIC RESONANCE : EXPERIMENTAL

0.4 M solutions in $CDCl_3$ and C_6D_6 (commercially produced) were used for all data collection. For the Perkin-Elmer R 10 spectrometer, 4.2 mm tubes were used and for the Varian HA 100 spectrometer and other instruments, 5.0 mm tubes. Tetramethylsilane, T.M.S., was the external reference (R 10) or internal lock signal (HA 100). ^{31}P spectra were carried out either as neat liquids or as saturated solutions in $CHCl_3$ in 8 mm tubes, using 85% H_3PO_4 as external reference.

CHAPTER 4

RESULTS AND DISCUSSION

In all, twelve compounds have been analysed to yield nuclear magnetic resonance parameters of chemical shifts and coupling constants. In two cases ambiguous results were obtained as regards ring conformation and in an attempt to clarify these, a full X-ray crystal analysis of two compounds was undertaken. It will be seen that although the X-ray analysis provided some interesting and helpful results, it has not contributed to solving the problem to the extent that it was hoped it would.

All values given in this chapter, except those for compound 6, were obtained from spectra run on the Varian HA 100 megacycle spectrometer. Data for compound 6 was obtained from the 220 megacycle machine at I.C.I., Runcorn.

Chemical Shifts

Table 4.1. gives all the chemical shifts for the twelve compounds that have been studied.

One important and interesting result is that although axial protons have been considered as resonating at higher fields than their equatorial counterparts[1] the opposite situation seems to hold, either for the 4,6 protons or 5 protons or end methyl groups, for all compounds except compound 6. The latter differs from all the others in having a phenyl group substituted at position 5 in the dioxaphosphorinane ring. Evidence for this reversal is borne out by three observations :

1. Coupling Constants

As stated in chapter 2, coupling constants between phosphorus and the axial and equatorial protons at position 4,6 will differ because the dihedral angle is different for these two protons. Numerous experiments[2,3,4,5,6] have confirmed that for a POCH system the phosphorus-equatorial coupling is greater than the phosphorus-axial coupling. However, for most of the

TABLE 4.1

CHEMICAL SHIFTS[a] FOR 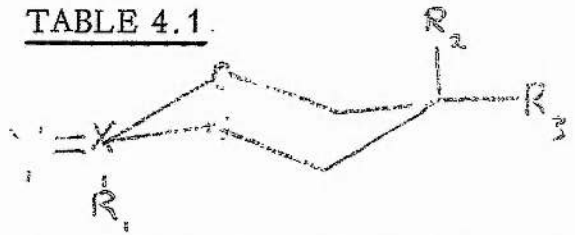

Substituents						4,6 protons		R_2		R_3	R_1	
Ref.	X	Y	R_1	R_2	R_3	ax.	eq.	ax.		eq.	C_6H_5	CH_3
1	P	O	Me	H	H	5.64 (5.90)	5.84 (6.37)	[7.70 - 8.30][d] ([8.65 - 8.84])				8.49 (8.81)
2	P	O	Me	Me	Me	5.82 (6.12)	6.20 (6.76)	8.87 (9.34)		8.95 (9.56)		8.44 (8.74)
3	P	O	Ph	H	H	5.47 (5.87)	5.82 (6.37)	[7.80 - 8.00] ([8.5 - 8.74])			[2.1 - 2.7] ([2.1 - 2.36])	
4	P	O	Ph	Me	Me	5.71 (5.94)	6.11 (6.58)	8.88 (9.26)		8.91 (9.47)	[2.0 - 2.6] ([1.94 - 2.2])	
5	P	O	CCl_3	Me	Me	5.44 (6.14)	5.70 (6.50)	8.60 (9.14)		9.03 (9.8)		
6	P	O	Ph	H	Ph	[5.28 - 5.84] (6.18)	(5.90)	~6.41 ~(7.11)			[2.10 - 2.97] ([2.2 - 3.4])	

a) all solutions are 0.4M and shifts are given in τ values, TMS Reference.

b) without brackets.

c) with round brackets.

d) square brackets indicate unresolved complex.

TABLE 4.1. (continued)

Substituents						4,6 protons		R_2	R_3	R_1		
Ref.	X	Y	R_1	R_2	R_3	ax.	eq.	ax.	eq.	C_6H_5	CH_3	others
7	P		Ph	H	H	[5.75 - 6.30] (5.97)	(6.37)	[7.90 - 8.20] ([8.10 - 8.40])		[2.4 - 2.75] ([2.25 - 2.62])		
8	P		Ph	Me	Me	6.23 (6.41)	6.47 (6.72)	8.68 (8.82)	9.42 (9.92)	[2.40 - 3.00] ([2.10 - 2.60])		-CH
9	C		Ph	H	H	6.08 (6.50)	5.78 (6.10)	7.83 (8.15)	8.62 (9.2)	([2.46 - 2.74]) ([2.28 - 2.90])		4.53 (4.66)
10	C		Ph	Me	Me	5.89 (6.21)	5.77 (5.96)	8.72 (8.83)	9.23 (>9.5)	[2.5 - 2.8] ([2.4 - 2.53])		4.64 (4.78)
7-membered rings												
11	P	O	Me			[5.52 - 6.18] (6.01)	(6.51)	[8.04 - 8.14] ([8.5 - 8.8])			8.51 (8.84)	
12	P	O	Ph			[5.60 - 6.00] (5.89)	(6.28)	[7.98 - 8.2] ([8.58 - 8.64])		[2.1 - 2.8] ([2.0 - 2.24])		

present compounds the coupling constant is greater for the proton at higher field (see Table 4.3.) and this must therefore be the equatorial proton, not the axial as expected.

2. Cross-ring or long range coupling

From some of the decoupled spectra there is evidence of cross-ring coupling (between protons at position 4 and those at position 6). For compounds 1, 3 and 12 there is more evidence for the proton resonating at lower field, and since cross-ring coupling will be greater between axial protons,[7] it seems that this confirms the assignment of the axial 4,6 protons to lower field. However, for the 7-membered ring compound 11, there is clear evidence that the lower proton is not coupled, whereas the higher proton shows broader peaks. This makes axial, equatorial assignment difficult. When, for compound 4, the end methyl groups are decoupled, there is very definite evidence that there is cros-ring coupling for both axial and equatorial 4,6 protons and so again no aid to assignment, on this ground alone, is given.

3. Broadening of methyl peak

In all cases end methyl peaks are considerably broader ($\sim$2.0 Hz) compared with the normal half-width of methyl peaks ($\sim$0.6 Hz).[8] This may be attributed to long-range phosphorus coupling or coupling with each other. Moreover, the methyl peak to lower field is slightly broader than the one at higher field. This result is in line with extensive data observed in rigid systems,[9,10] steroid series,[11,12] decalins[13,14] and dioxaphosphorinanes,[15,16] all with tertiary methyl groups attached to undistorted six-membered rings. It can be explained by the existence of a "favourable coupling path"[17] (see heavy lines in Figure 4.1) between the axial 4,6 protons and one of the protons on the axial methyl group.

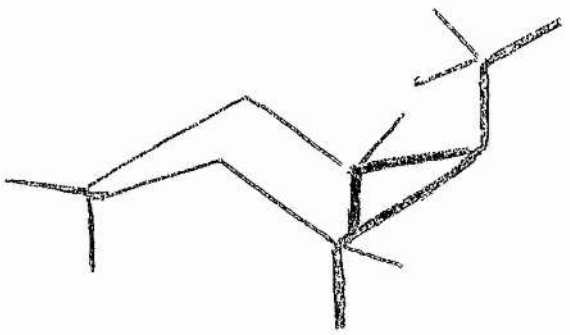

FIG. 4.1.

It does not occur when the methyl group is in an equatorial position, such as for

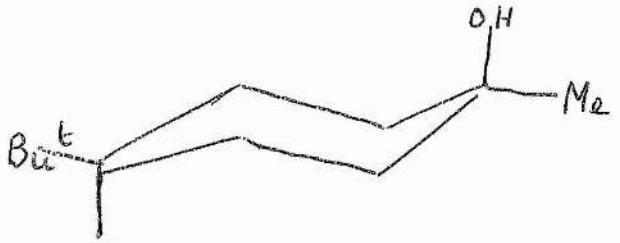

investigated by Shoppe and co-workers.[18] This means that again an axial group is resonating at lower field than its equatorial partner.

It is difficult to observe a similar effect as number 3 given above, for the end protons at position 5 in an unsubstituted ring, since their chemical shift difference is small. However, in the case of 2-phenyl-1,3-dioxane, analysis of the two end proton resonances (from very well resolved peaks, see spectra 9.2.) shows clearly that the proton at lower field has the largest vicinal coupling with the axial protons at 4,6 protons. From Figure 4.1. above, this must mean that here also, the axial proton resonates at lower field than the equatorial proton. To summarise, for dioxaphosphorinane there is an inversion of expected axial and equatorial resonances for 4,6 protons and methyl groups at position 5 on the ring; for 1,3,2-phenyl-dioxanes this holds for protons or methyl groups at position 5, but not for 4,6 protons.

DISCUSSION

As stated above, over the past six years many workers have observed anomalies in the chemical shifts of axial and equatorial ring protons or groups.

However, there is only one report of any theoretical work into the sources of these anomalies - by J. Delmau[19] and co-workers in 1967. Delmau considered what he thought were two factors that could explain why the axial methyl groups (position 5) in 5,5-dimethyl-1,3-dioxanes came at lower field than the equatorial group. Using McConnell's equation[20] he worked out what influence the anisotropy of the C-O bond had on atoms or groups at position 5. The C-O bond he considered was the O(3) - C(4)

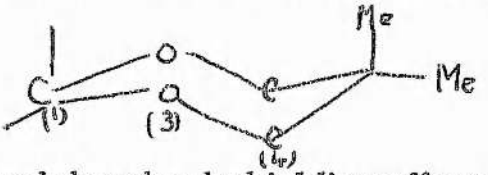

not C(1) - O(3). He found that the deshielding effect was the same for both the axial and equatorial protons - this would mean that they were magnetically equivalent which is not observed. He then adopted the work of Pople,[21] Buckingham[22] and Muscher[23] who had shown that the shielding constant of a proton originates in the surrounding electric field of the molecule, so that

$$\Delta\sigma = -k E_z - a E^2 \qquad (1)$$

where $\Delta\sigma$ is the change in shielding constant, k and a are constants, E_z is the projection of the electric field on the σ electrons of the C-H bond and E is the electric field on the σ electrons of the C-H bond and E is the electric field experienced by the proton itself. Delmau neglected the quadratic term since it involved a term r^{-6} and used the remainder of equation (1) with $k = 3.0 \times 10^{-12}$. He considered that the dipole moment of 1,3 dioxane lay normal to the plane $O_1 - C_2 - O_3$[24] and had a value of 2.15 D. The result of his calculation showed that

$$\Delta_{\sigma 5a} \approx -0.99 \text{ ppm}$$

$$\Delta_{\sigma 5e} \approx -0.51 \text{ ppm}$$

Thus, the existence of a dipole moment in the molecule introduced a chemical shift difference between the axial and equatorial protons of

$$\Delta_{5e-5a} \approx -0.48 \text{ ppm}$$

That is, the axial proton will resonate at lower field than the equatorial. He considered this to be in reasonable agreement with his observed value of ≈ -0.7ppm. - certainly it was evidence that the dipole moment of the molecule contributed to a large extent either to the shielding or deshielding of ring protons, in this case the deshielding.

The dipole moment of the substituted 2-oxo-dioxaphosphorinanes would thus explain why a similar effect on the 4, 6 protons of these compounds is observed, something McConnell's equation cannot. As regards the position 5 axial and equatorial methyl group, dipole moment theory may also explain their chemical shift difference. A calculation based on the McConnell equation

$$\frac{(3\,\mathrm{Cos}^2\theta - 1)}{r^3}\,(\chi_{\perp} - \chi_{\parallel}) \qquad \text{(see Chapter 2)}$$

is difficult since θ and r have to be calculated for each proton of each methyl group. However, a calculation for protons at position 5 with

		H_{ax}	H_{eq}
θ	$\approx$	-7^{o}	$+13$
r	$\approx$	3.6	4.2

shows that both axial and equatorial will be slightly deshielded by the X - O bond, the axial more so. However, the diamagnetic anisotropy of the P - O bond is not know, nor is the position of the electrical centre of gravity of the P - O bond. Thus, any calculation using the McConnell equation is very approximate. It would seem that a more accurate account would be given using the dipole moment equation - equation (1) above. The main problem in applying this equation to dioxaphosphorinanes, is the lack of information on dipole moments for such compounds. It seems that only six have been determined to date; among them the 2 - BH_3 adduct of 2-methoxy-5-methyl-5-chloromethyl-1, 3, 2-dioxaphosphorinane[25] and 2-phenoxy-5, 5-dimethyl-2-oxo-1, 3, 2-dioxaphosphorinane[26]. The value for these were 3.05 D and 5.71 D respectively. It would thus appear from Delmau's calculations that dioxaphosphorinanes would have a similar effect on substituents in 5, position.

General Trends

All methyl groups directly bonded to a phosphorus atom resonate at a slightly higher field than expected. A change in the substituent attached to the phosphorus from a methyl group to phenyl group does not alter the position of the 5 protons or end methyl groups, and when the substituent is a tri-chloro methyl group, only a shift of 0.2 τ is observed for the axial methyl. A change of substituent does, however, slightly alter the position of the 4, 6 protons; the axial protons are deshielded [0.17 τ (3), 0.09 τ(4)] when a phenyl group is introduced. Since the X-ray analysis in the solid state of 3 and 4 showed that the phenyl group lies equatorially with its plane perpendicular to the phosphorinane ring, this deshielding can only be explained if the phenyl ring rotates about its plane, in solution. If this is the case, a model shows that when the plane of the phenyl ring is parallel to the phosphorinane ring, the interaction will be such to deshield the axial proton. Introduction of the tri-chloro methyl group further deshields both the axial proton (by 0.27 τ) and the equatorial proton (by 0.4 τ) although the latter is unaffected by the phenyl group. The introduction of methyl groups at position 5 in the phosphorinane ring has the effect of moving the 4, 6 protons to higher field but it does not affect the methyl group attached to the phosphorus atom. Introduction of a phenyl group in the equatorial 5, position deshields the 4, 6 protons (again this seems to have free rotation) but has a greater effect on the axial proton, as expected, since equatorial-axial interactions are greater than equatorial-equatorial interactions. Removal of the double-bonded oxygen seems to cause an increase in the shielding of the 4, 6 protons. However, this may be due to a change in position of the phenyl group. There is abundant evidence[28, 29, 30] that it lies in the axial position for the pentavalent compounds but in the equatorial[31, 32] position for the trivalent compounds. X-ray crystallography work here[33] has shown that for 2-phenyl-1, 3-dioxane the phenyl ring as well as lying in the equatorial position, also lies with its plane approximately perpendicular to the dioxane

ring. Observation of chemical shifts and comparison between compounds 3 and 9, 4 and 10 and then 3 and 7, 3 and 8, show that when the phenyl changes its configuration around the phosphorus from axial to equatorial (perpendicular as stated above), in each case the 4,6 axial protons move to higher field as expected.

Another expected result is that the insertion of a phosphorus into position 2 of 1,3-dioxane has a negligible effect on any of the proton shifts. As will be seen later, it also has a negligible effect on geminal coupling constants. Relative to an 'isolated' benzene ring, the phenyl ring is pulled downfield in the dioxaphosphorinanes. That this is due mainly to the double-bonded oxygen can be seen from the chemical shift for the phenyl group when this oxygen is absent in the trivalent compounds and in the 1,3-dioxanes. Again, however, this may be due to a change in orientation of the phenyl group itself. From the values for the latter, the phosphorus would seem only to pull the phenyl group downfield by 0.1 τ.

For the seven-membered ring compounds there is a slight upfield shift of the end methylene groups and the 4,6 protons are unchanged relative to the six-membered rings.

Benzene as a Solvent

Table 4.2. gives the solvent shifts of all the compounds in deutero-benzene. These are given relative to deutero-chloroform which has been taken as an inert solvent, though this is probably not true since it may H-bond to P-O.

It can be seen that in all cases the phenyl group attached to the phosphorus or carbon atom (X) is deshielded to a slight extent, whereas substituted benzene rings are usually shielded.[34] This deshielding can be explained if the solvent molecule lies parallel to the benzene ring of the solute molecule. That the deshielding is very small could be explained by the large phosphorus and oxygen atoms preventing near approach of the solvent.

TABLE 4.2.

Solvent Shifts in Deutero-Benzene[a,b]

for

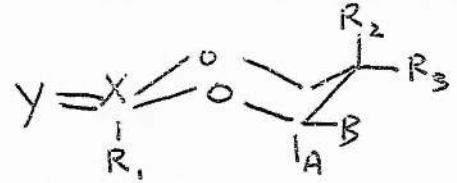

Ref.	Substituents					4, 6 protons		R_2		R_3	R_1		
	X	Y	R_1	R_2	R_3	ax.	eq.	ax.		eq.	C_6H_5[d]	CH_3	H
1	P	O	Me	H	H	+34	+53		+95[c]			+32	
2	P	O	Me	Me	Me	+30	+56	+47		+61		+30	
3	P	O	Ph	H	H	+40	+55		+70		0		
4	P	O	Ph	Me	Me	+23	+47	+38		+54	- 6		
5	P	O	CCl_3	Me	Me	+70	+84	+54		+77			
6	P	O	Ph	H	Ph	+38	+42	+50			+10		
7	P		Ph	H	H	+ 5	+20		+30		-15		
8	P		Ph	Me	Me	+18	+25	+14		+50	-30		
9	C		Ph	H	H	+41	+32	+45		+70	-18		+13
10	C		Ph	Me	Me	+19	+32	+11		+27	-10		- 2
	7 membered rings												
11	P	O	Me			+34	+62		+46			+34	
12	P	O	Ph			+18	+43		+60		-10		

a) all shifts are in Hz
b) shifts to higher field are positive
c) when only one value is given this is because chemical shift difference of 2 protons could not be calculated.
d) this is measured from lower field end of complex.

The increased shielding of the protons in the heterocyclic ring would seem to indicate a weak association[35] between these protons and the benzene solvent molecules, such that the latter's plane is lying perpendicular to the protons. With the solvent molecules in this position the diamagnetic ring current opposes the applied field. In all cases end methylene protons experience a greater shielding than the 4,6 protons. Even the methyl groups at position 5 in the ring experience as much shielding as the 4,6 protons. Since with these methyl groups the equatorial methyl is more shielded, a preferred orientation of the solvent molecule would seem to be one where a solvent molecule lies "at the side" of the heterocyclic ring as in Fig.4.2. The equatorial protons of the 4,6 protons also experience greater shielding than their axial neighbours in all cases. This could be another indication that the solvent molecule lies at the side of the ring as shown in Fig.4,2.

FIGURE 4.2

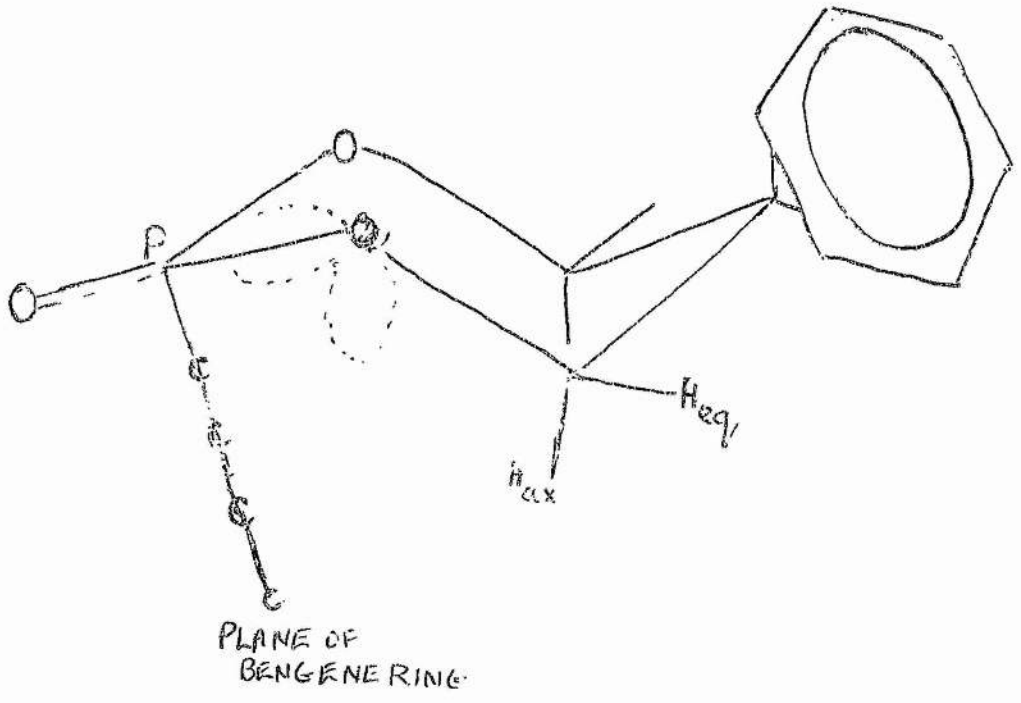

Moreover, in this position the benzene ring will avoid the p orbitals of the oxygen atoms. Anderson[36] has shown that benzene and 1,3-dioxanes interact to give very weak 1 : 1 complexes. He has also found, as in the present study, that positions 4, 5 and 6 are shielded, the 5 position particularly so. Having found also that the 2-axial position is only slightly affected, he suggests that the location of the benzene molecule can be as shown below

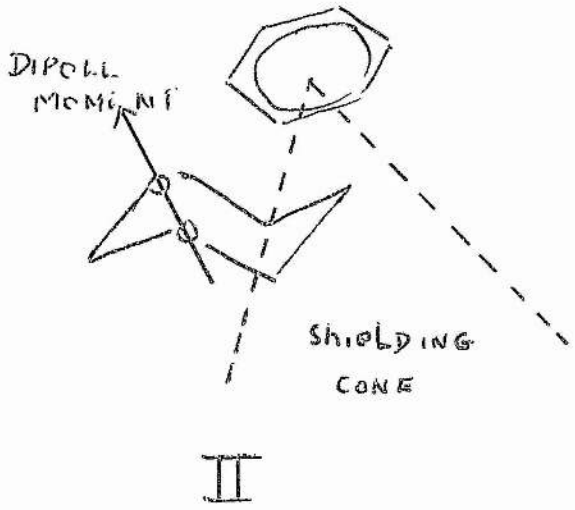

II

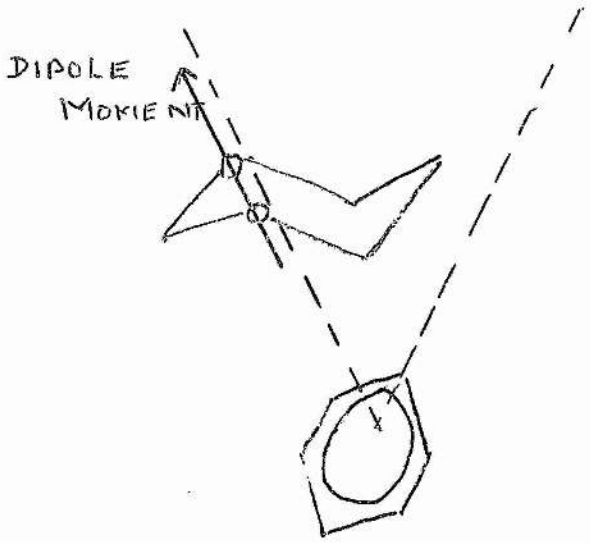

I

If the interaction with benzene is of a dipole-induced dipole type, then the nucleophilic benzene molecule will probably prefer I. However, Anderson found that when a methyl group was substituted in position 5, all the protons in 4, 5 and 6 were less shielded than before; he suggests II for this case. In this case, the axial methyl group tips the end of the benzene molecule away from the dioxane ring so that the protons at positions 4, 5 and 6 are nearer the edge of the shielding cone. In the present study such an effect of an axial methyl is found only for compounds 7 and 8 and 9 and 10, and in the latter, only the axial 4, 6 protons are affected. Certainly Anderson's theory is very plausible and a shielding cone emanating from

the benzene molecule would explain why end methylenes and methyl groups experience as great, or greater shielding, as the 4,6 protons. It is reasonable to assume that Anderson's theory will apply to phosphorinane rings also. The theory does not, however, explain why the tri-chloromethyl group (attached to the phosphorus atom) greatly enhances the shielding of the 4,6 protons and a "complexing theory" may be needed to explain this.

The seven-membered rings also show "complexing" between their ring protons and benzene as expected. Finally, the protons of the methyl group attached to the phosphorus are shielded like other non-aromatic protons.

Spin-Spin Coupling

Calculated values for spin-spin coupling constants are given in Table 4.3. For all compounds except 7, spectra obtained from the Varian HA 100 spectrometer were used for calculations. Coupling constants for compounds 2, 4, 5, 8 and 10 were calculated from the expanded spectra and for compounds 1, 3, 7, 9, 10, 11 and 12, expanded decoupled spectra were used. For compound 7, the expanded 220 megacycle spectrometer spectrum was used.

A full ABX analysis was applied for all compounds except 9 and 10. For the former case the resonances of the equatorial and axial protons at position 5 (ABCD system) could be analysed directly and the results checked with the 4,6 protons pattern. For compound 10, the 4,6 protons are an AB system and this could be analysed also.

An ABX analysis can be subject to many ambiguities;[37] in general it is impossible to determine the sign of J_{AB} and the relative signs of J_{AX} and J_{BX} can be obtained only when J_{AB}/δ_{AB} is small. (δ_{AB} is the chemical shift difference between A and B protons). An additional ambiguity arose with the compounds under study since the X (phosphorus) spectra could not be checked. Either the phosphorus spectra was too complex, or as for compounds 1, 2 and 5, it could not be calibrated accurately enough. However, some of the ambiguity could be removed by studying the intensity of the peaks making up the ABX system and sufficient evidence[38,39,40]

TABLE 4.3.

Coupling Constants[a] for 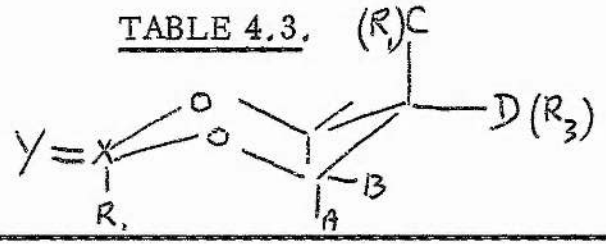 in $CDCl_3$ and C_6D_6[b]

Ref.	Substituents									long range				
	X	Y	R_1	R_2(C)	R_3(D)	J_{AX}	J_{BX}	J_{P-R_1}	J_{AB}	J_{POCCH}	J_{AC}	J_{AD}	J_{BC}	J_{BD}
1	P	O	Me	H	H	11.4 (10.0)	9.9 (11.9)	17 (17)	10.7 (10.9)					
2	P	O	Me	Me	Me	7.9 (9.0)	16.2 (15.0)	17 (17)	11 (11)					
3	P	O	Ph	H	H	11.3 (8.2)	11.3 (11.1)		11.3 (11.1)	(~2)	~5 (~7)	~5 (~5)	~5 (~5)	5 (~4)
4	P	O	Ph	Me	Me	10.6 (8.1)	12.9 (15.1)		11.3 (10.0)					
5	P	O	CCl_3	Me	Me	3.6 (3.9)	15.1 (15.6)		10.5 (10.2)					
6	P	O	Ph	H	Ph	(8.5)	(15.0)		(11)		(8.5)		(4)	

a) all values are given in Hz.
b) in round brackets

TABLE 4.3. (continued)

Ref.	X	Y	Substituents R_1	R_2(C)	R_3(D)	J_{AX}	J_{BX}	J_{P-R_1}	J_{AB}	J_{AC}	J_{AD}	J_{BC}	J_{BD}	J_{CD}
7	P		Ph	H	H	(17.9)	(19.1)		(10)					
8	P		Ph	Me	Me	3.5 (3.0)	8.5 (9.5)		10.5 (10.2)					
9	C		Ph	H	H				(11)	(11)	(1.6)	(1.4)	(5)	(13.7)
10	C		Ph	Me	Me				10.5 (10.5)					
		7 membered rings												
11	P	O		Me		(14.8)	(13.2)	18 (18)	(11.25)					
12	P	O		Ph		(14.5)	(14.0)		(11.0)	~3		~2		

for positive J_{BX} and J_{AX} enabled some sets of results to be rejected.

$J_{POC'H}$ Coupling

As mentioned in chapter 2, the parameters affecting[41] J are

(1) dihedral angle

(2) bond length

(3) bond angle and

(4) electronegativity of neighbouring groups.

In the compounds under study (2) and (3) are assumed to remain practically constant and thus the contribution from (1) and (4) can be studied. Since from compound to compound the dihedral angular relation between the phosphorus atom and the axial and equatorial 4,6 protons remains relatively unaltered, the effect of substituent groups at the phosphorus atom and position 5 could be evaluated.

In all cases for six-membered rings except the $CDCl_3$ solution of compound 1, it would seem that the phosphorus coupling with the equatorial 4,6 protons J_{BX} is greater than that with the axial 4,6 protons J_{AX}. This is in accordance with a general Karplus prediction for vicinal couplings (see chapter 2) and arises because of the dihedral angle (Ø) difference between the phosphorus atom and the equatorial and axial protons.

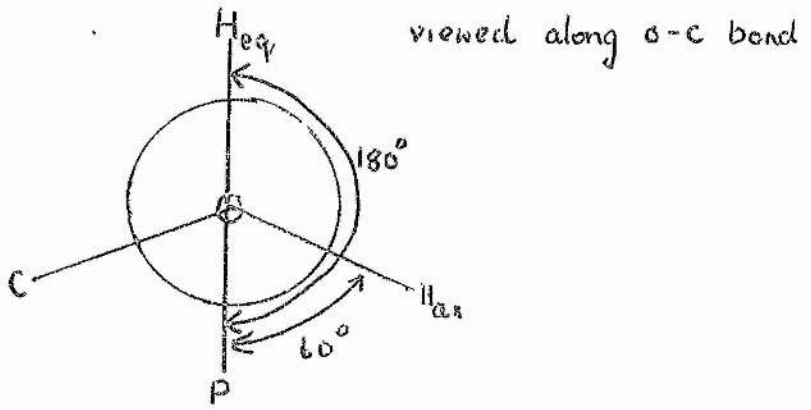

However, the difference between the equatorial and axial protons is nowhere as great as that reported for other compounds. For example, Kainosho et al[42] report for

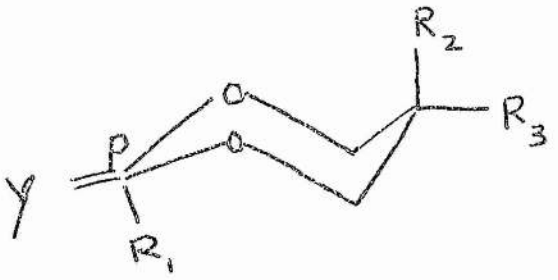

X	Y	R_1	R_2	R_3	J_{BX}	J_{AX}
P	O	Cl	Me	Me	27.5	2.9
P	O	Br	Me	Me	30.0	3.6
P	S	Cl	Me	Me	28.6	4.3

An explanation for this will be suggested later.

Dihedral Angular Dependence

Kainosho[41] has, as was mentioned in chapter 2, obtained values for phosphorus-proton couplings as a function of dihedral angles. From these values he has been able to produce a Karplus like curve shown below in Fig.4.3. for

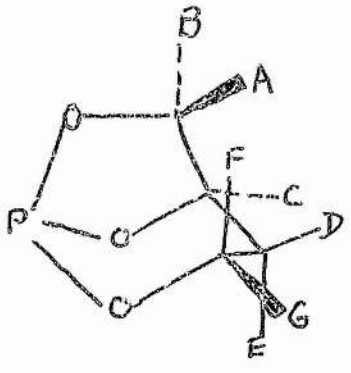

However, X-ray analysis[43] and further calculations gave, for compound 3, $\phi_{POCH_{ax}} = 50^{o}$, $\phi_{POCH_{eq}} = 180^{o}$, for compound 4, $\phi_{POCH_{ax}} = 40^{o}$ $\phi_{POCH_{eq}} = 180^{o}$. These along with values for coupling constants given in Table 4.3. were plotted on this curve and are in reasonable agreement.

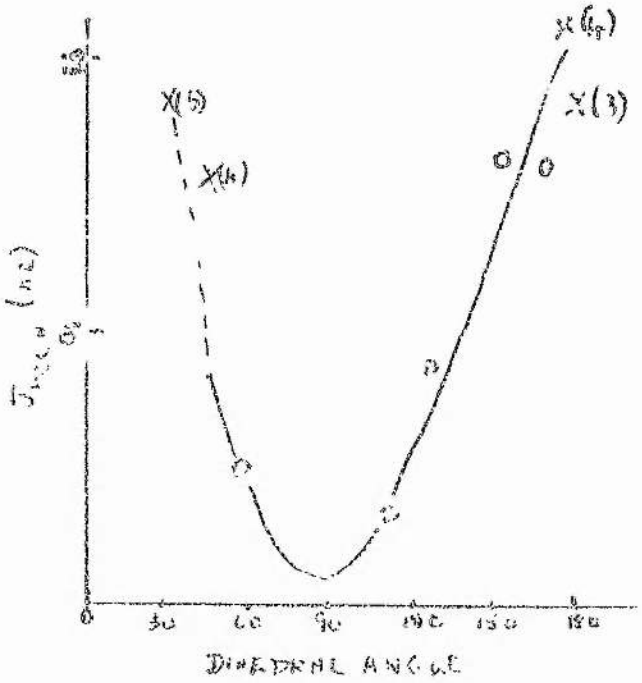

FIG. 4.3

However, this could be deceiving since between dihedral angle values of 30^{o} and 60^{o} one could have a range for J of 5 to 20 Hz and likewise for $\phi = 180^{o}$, J could be any value greater than 10 Hz ! The only large dependence between J and ϕ is in the range $\phi = 60$ to 150^{o} and since dihedral angles for either a boat or chair form do not lie within this range, no startling conclusions can be drawn.

Electronegativity of Substituents Directly Attached to the Phosphorus Atom

Empirical correlations between J_{H-H} and the electronegativity (E_x) of a substituent has been observed for vinyl compounds. Banwell and co-workers[44] found an inverse proportionality with E_x for compounds $CH_2 = CHX$ but Schaefer[45] over a wide range of E_x found a linear correlation between E_x and J_{H-H} for gem, cis and trans protons and for the sum $J_{gem} + J_{cis} + J_{trans}$.

TABLE 4.4.

for 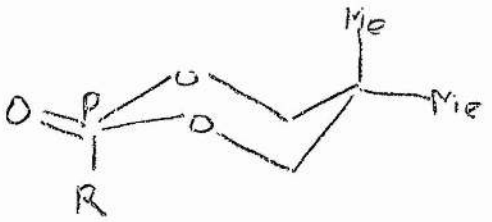

Ref.	R	J_{ax} [a]	J_{eq}	E_x	Ref.
39	CMe_3	2	19	2.3	48
46	Me	7.9	16.2	2.27	48
46	Ph	10.6	12.9	2.5	45
42	Br	3.6	30	2.8	48
46	CCl_3	3.6	15.1	2.84	48
42	Cl	2.9	27.5	3.0	48
47	O Ph	3	21	3.2	48
39	CPh_3	6.6	14.7		
39	CH_2Ph	7.8	14.9	< 2.4	
39	$NHCHMe_2$	6.2	22.4	> 2.0	
39	$NHCMe_3$	7.8	16.3		

a) all values in Hz.

It would help in the present study to attempt a similar correlation for $J_{POCH_{ax}}$ and E_x. Table 4.4. gives results that have been published to date and Figure 4.4. gives a plot of these results.

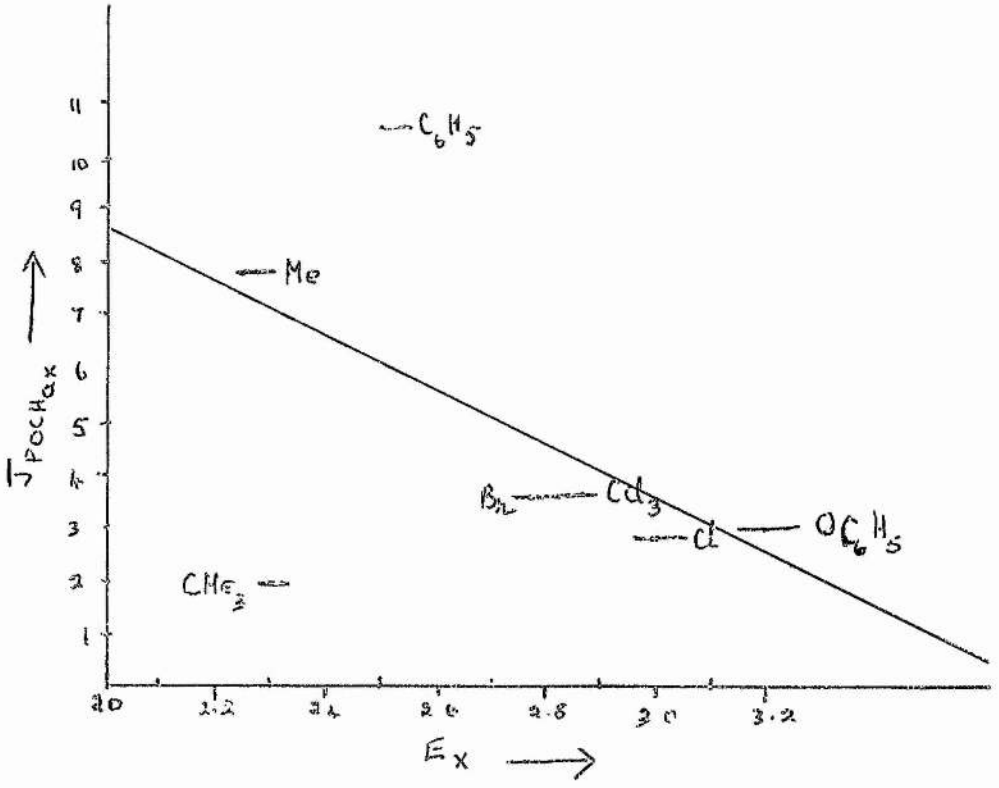

FIGURE 4.4

It would appear that a linear relationship for $J_{POCH_{ax}}$ and E_x does exist. The position of the C_6H_5 values could be explained as due to a wrong E_x, since the phenyl group has been known to act as a donor when bonded to a P-O group.[48] Moreover, looking at Table 4.5 below, it appears that not only is the phosphorus proton coupling constant dependent on the electronegativity of the substituent, but it is also dependent on its orientation. For all the compounds listed in Table 4.5. there is evidence[40,49] that group R lies in the equatorial position and this change of configuration about the phosphorus nullifies any electronegativity effect, a conclusion which is evidenced by previous work.[40,49] Taking both Figures 4.3 and 4.4. and Table 4.5. into account, seems to indicate that the electro-

TABLE 4.5.

Coupling Constants and Electronegativities for

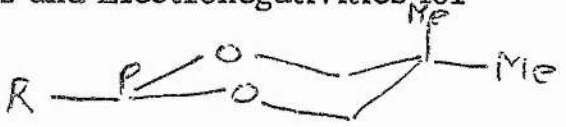

Ref.	R	J_{ax}	J_{eq}	E_x	Ref.
40	Cl	6	10.8	2.8	48
46	Ph	3	10.2	3.0	48
40	$N(CH_3)_2$	3.8	19.6	3.0	48
40	O Ph	2.8	10.8	3.2	48
40	O Me	2.8	10.8	3.7	48
40	F	2.8	10.8	3.9	48

negativity of a substituent in the axial position has a greater effect on vicinal coupling constants than the dihedral angle. In fact, the present results would suggest that the dihedral angular dependence can only be studied in an 'isolated' or unpertubed P - O - C - H system just as Karplus' original quantitative calculations were carried out for an unperturbed H - C - C - H system.[41]

However, in spite of this, a problem does seem to present itself as regards the conformation of the heterocyclic rings in compounds 1 and 3. When the decoupled spectra of compound 3 2-phenyl-2-oxo-1,3,2-dioxaphosphorinane was first obtained on the Perkin Elmer R 10 and R 12 instruments and on the Jeol 100 megacycle instrument, a symmetrical sextet with broad peaks was obtained :

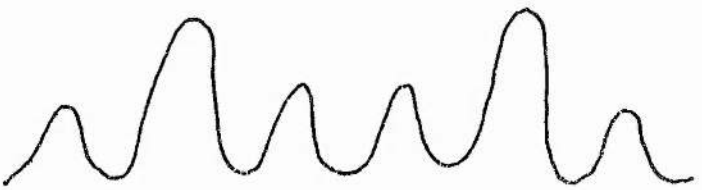

This indicated that J_{AX} was equal to J_{BX} and that both equalled J_{AB} = 11 Hz. X-ray analysis of this compound and its 5,5-dimethyl counterpart was then carried out to see if these couplings could arise from a boat conformation of the heterocyclic ring, since in a boat conformation $\emptyset_{ax} = \emptyset_{eq}$. VerKade and King have reported equal couplings[50] for axial and equatorial protons in a compound with an obvious boat form :

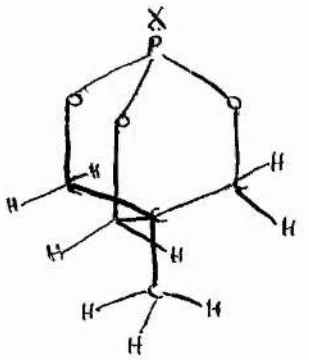

The X-ray analysis indicated a chair form for both compounds in the solid state. The broad-line N.M.R. did not show any conformational change for either 2-phenyl or 2-methyl-2-oxo-1, 3, 2-dioxaphosphorinane. Moreover, when HA 100 spectra (decoupled and expanded) were obtained for compound 3, the improved resolution showed clearly that in $CDCl_3$ $J_{AX} = J_{BX}$ but in C_6D_6 J_{AX} was slightly smaller than J_{BX}. One may conclude from this that either the dihedral angular relationship to coupling constants is meaningless, or that in solution the heterocyclic ring of compound 3 assumes a boat conformation and that of compound 1, a slightly distorted boat conformation. This conformation, though rare, is not impossible. Since a boat conformation is essentially a flexible form, one explanation could be that in solution compound 3 is flipping over from one 'twist-boat' conformation to another. See figure below.

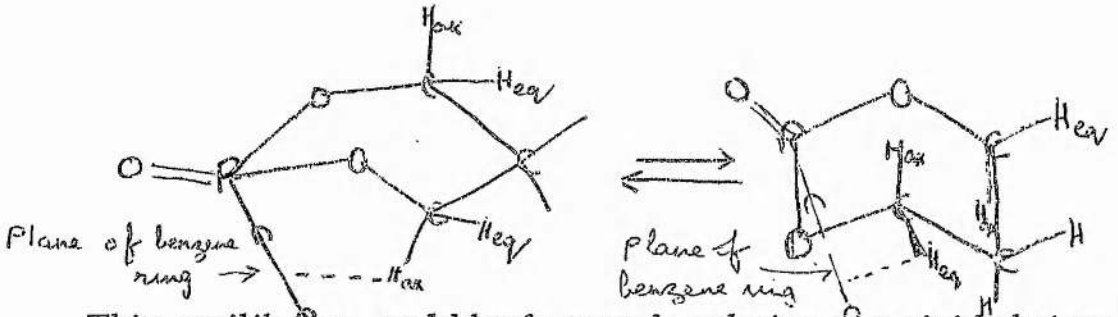

This equilibrium could be favoured, relative to a rigid chair conformation by weak association between axial ring protons and the benzene ring attached to the phosphorus atom (similar to the situation in solvent-solute interactions). The expected up-field shift of the axial protons, arising from such an interaction would be difficult to detect, and in fact, may be cancelled out by other factors such as the interchange of axial-equatorial positions in the flexible boat conformers and change in solvent-solute orientation relative to a chair form. Moreover, in the flipping over process, the mean dihedral angle is equal for both equatorial and axial protons; thus equal phosphorus-proton couplings would be expected. However, no evidence seems to have been found for any such interaction, in other similar molecules.[51, 52] Another possibl explanation for the equal coupling constants may be that the effect of the phenyl ring acting as a donor may just be enough to cancel out the difference between axial and equatorial couplings. Both the above possibilities need to be investigated further before any sound conclusions can be drawn.

The introduction of methyl groups at position 5 in the heterocyclic ring has an obvious effect; in each case the axial-phosphorus coupling is decreased and the equatorial coupling increased. This could be explained by the weak electron donating power of the methyl group or could be due to deformation of the ring since X-ray data shows a change of -10^{o} in the $P-O-C-H_{ax}$ angle when the methyl groups are introduced giving $\phi_{ax} = 41^{o} \pm 4^{o}$. However, such a change should result in an increase in J_{AX} not a decrease as is found. In compound 6 the phenyl group in position 5 increases the P-equatorial coupling relative to compound 3 and decreases the P-axial coupling - thus here the phenyl group seems to be acting as a weak electron donor like the methyl group.

That the geminal coupling J_{AB} remains relatively unaffected by any change in substituents whether at position 2 or position 5, would support evidence that just as for J_{H-F}[53], J_{H-P} is very much more sensitive to substituent groups than J_{H-H}. In fact, results for the 1,3-dioxanes, compounds 9 and 10, show that the J_{AB} coupling is not even affected by the introduction of a phosphorus atom into the ring.

For the 7-membered ring compounds $J_{AX} \approx J_{BX}$. This is to be expected, if one considers the ring to be as predicted by Hanack[54] and Hendrickson[55]

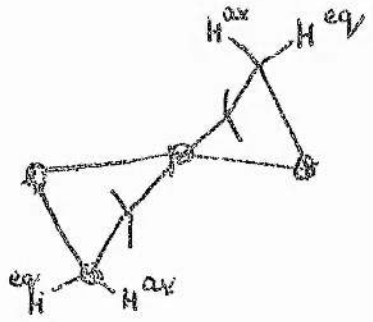

for then the dihedral angle for axial is very small, i.e. J_{AX} will increase and the angle for equatorial $\simeq 160$. Thus there is a possibility of J_{AX} being equal to J_{BX}.

The effect of benzene as a solvent is interesting. There is relatively

no change of any of the coupling constants except J_{AX} and J_{BX}. The effect on the latter seems to vary haphazardly. However, for the unsubstituted phosphorinane ring the P-axial couplings decrease and the P-equatorial coupling increases for 2-methyl compound and decreases very slightly for the 2-phenyl. This can be explained if, as mentioned previously, the solvent molecules complex slightly with the solute molecules; then with the associated diamagnetic ring current of the benzene solvent, the electronic environment of system is altered and the coupling may be 'through space'. as has been suggested.[56] On the other hand, formation of a complex between the solvent and solute may result in a sufficient change in the dihedral angle to alter the coupling constants. If the solvent molecules are position as was suggested previously[57] then ϕ_{ax} would increase with a corresponding decrease in $J_{P\text{-}ax}$ since $\phi_{ax} < 90^{o}$ and $J \alpha \cos\phi$ as is observed. For compound 5 where no solvent molecule can get near to the phosphorus atom, no change is observed. The biggest solvent effect is shown in the $J_{P\text{-}eq.}$ coupling for compound 4 where J_{BX} increases from 12.9 Hz to 15.1 Hz. No reasonable explanation for this seems apparent.

Compared with geminal coupling in cyclohexane of 12.4 Hz, the values for the phosphorinane and dioxane rings 4,6 protons are slightly smaller due to the electronegative hetero atom oxygen in the rings. The geminal coupling for the 5 protons of 2-phenyl-1,3-dioxane is 13.7 Hz and agrees with past experimental results for similar protons.[58] However, in 2-phenyl or 2-methyl-2-oxo-1,3,2-dioxaphosphorinane, there is no evidence of any such large coupling constant. The other proton-proton couplings given in Table 4.3. are all as expected.

Conformational Mobility of the
1,3,2-Dioxaphosphorinance Ring System

Although there have been numerous reports of the rigidity of the dioxaphosphorinane ring and lack of inversion at the phosphorus atom[58,59,60,61] the spectra of all the compounds was studied over the temperature range $-90^{o}C$ to $+200^{o}C$. Apart from the expected broadening of peaks at low

temperature, no change was observed for any of the compounds, indicating that the ring system is a very rigid one although 1,3-dioxane has been shown to be conformationally mobile.[62] This rigidity can probably be attributed to the presence of the heavier phosphorus atom.

Edmundson has reported[63] conformational mobility for trans-5-bromomethyl-2,5-dimethyl-2-oxo-1,3,2-dioxaphosphorinane but the argument is difficult to follow. He has also very recently[64] put forward the view that trans-2-benzyl-5-chloromethyl-5-methyl-2-oxo-1,3,2-dioxaphosphorinane and trans-5-bromo-methyl-2,5-dimethyl-2-oxo-1,3,2-dioxaphosphorinane are conformationally mobile systems. This conclusion is based on changes in the CH_2Ph and CH_2Br patterns over a temperature range $+30^{o}$ to -70^{o}, and on the values of time-averaged coupling constants. However, it would seem that both of these effects can be explained by free rotation of the CH_2Ph and CH_2Br groups (which is to be expected) and not by any ring mobility.

Broad-line N.M.R.[65]

Broad-line N.M.R. of compound 3 at low temperature and ambient indicate that at $140^{o}K$ there was little or no motion taking place. At room temperature there was evidence that motion of either the Ph group or the ring had set in. Motion of such groups normally begins about $200^{o}K$.

Broad-line N.M.R. of compound 4 showed no evidence of the expected end methyl motion at $\sim 125^{o}C$ and as for the previous compound, motion of the phenyl group and ring methylenes set in just below room temperature.

CHAPTER 5

X-Ray Theory

When a beam of x-rays impinges upon a crystal it will be diffracted provided the direction of the incident beam obeys Bragg's Law.

$$2d \sin\theta = n\lambda \qquad (1)$$

where θ is the angle between the incident beam and the (h k l) plane from which the beam is reflected, d is the spacing of the (h k l) planes, n is an integer related to the indices h k l and λ is the wavelength of the radiation.

The amplitude of the scattered wave is called the Structure Factor. If, in the unit cell in the crystal, the nth atom is situated at the point (x_n, y_n, z_n) the structure factor is defined as

$$F(h\ k\ l) = \sum_{n=1}^{N} f_n \exp 2\pi i \quad (hx_n + ky_n + lz_n) \qquad (2)$$

where f_n is the scattering factor of the nth atom and there are N atoms in the unit cell.

The complex form of the expression for F(h k l) arises because the phase of the scattered wave differs from that of the incident wave. But the phase is not an observable or measurable quantity and the only measurable quantity is the intensity of the scattered wave, which is proportional to $|F|^2$. F can be written as

$$F = A + iB$$

and from equation (2)

$$\text{then } A = \sum_{n=1}^{N} f_n \text{ Cos } 2\pi (hx_n + ky_n + lz_n) \qquad (3)$$

$$B = \sum_{n=1}^{N} f_n \text{ Sin } 2\pi (hx_n + ky_n + lz_n) \qquad (4)$$

If $\rho(x\ y\ z)$ is the electron density at the point $(x\ y\ z)$ the amount of scattering matter in the volume element $Vdxdydz$ is $\rho\, Vdxdydz$ and thus

$$F(h\ k\ l) = \int_{x=0}^{1} \int_{y=0}^{1} \int_{z=0}^{1} V\ \rho(xyz) \exp 2\pi i(hx + ky + lz)dx\ dy\ dz \qquad (5)$$

Since a crystal is periodic in three dimensions it can be represented by a three dimensional Fourier series:- and

$$\rho(x\ y\ z) = \sum_{h'}^{\infty} \sum_{k'}^{\infty} \sum_{l'}^{\infty} C(h'k'l') \exp\ 2\pi i\ (h'x + k'y + l'z) \qquad (6)$$

if each Fourier coefficient has 3 integral indices $h'k'l'$

Then (5) and (6) give

$$F(h\ k\ l) = \int_0^1\int_0^1\int_0^1 \sum_{h'}\sum_{k'}\sum_{l'} C(h'k'l') \exp\ 2\pi\ i(h'x + k'y + l'z) \exp 2\pi i (hx + ky + lz) V\ dx\ dy\ dz \qquad (7)$$

Unless $h = -h'$, $k = -k'$, $l = -l'$ this expression is zero. When the above case holds

$$F(h\ k\ l) = \int_0^1 \int_0^1 \int_0^1 C(h'k'l')\ V\ \ dx\ \ dy\ \ dz$$

$$\therefore F(h\ k\ l) = C(\bar{h}\ \bar{k}\ \bar{l})\, V$$

and from equation (6)

$$\rho(x\ y\ z) = \frac{1}{V} \sum_{h}\sum_{k}\sum_{l=-\infty}^{\infty} F(h\ k\ l) \exp\ [-2\pi\ i\ (hx + ky + lz)] \qquad (8)$$

However the difficulty of calculating the phase of the Structure Factor still remains, and in 1934 Patterson[1] produced a Fourier series which used the measurable quantity $|F(h\ k\ l)|^2$ instead of $F(h\ k\ l)$ if $\rho(x\ y\ z)$ is the density of scattering matter at a point $x\ y\ z$ in the crystal then ρ will be very small except near the positions of the

atoms. A function $\rho(x + u, y + v, z + w)$ where u, v and w are constant parameters, represents a distribution similar to $\rho(x\ y\ z)$ but displaced with reference to it. The product $\rho(x\ y\ z) \times \rho(x + u, y + v, z + w)$ will usually be small, but if u, v, w, are the components of the vector between two of the atoms in the structure then one maximum of the distribution $\rho(x\ y\ z)$ coincides with another maximum $\rho(x + u, y + v, z + w)$. This also occurs if u, v and w are zero or any multiples of the lattice translations of the crystal. Patterson took a function

$$P(u\ v\ w) = V \int_0^1 \int_0^1 \int_0^1 \rho(x\ y\ z)\ \rho(x + u, y + v, z + w)\,dx\,dy\,dz \qquad (9)$$

Since P(u v w) is periodic it can be expressed as a Fourier series. From (6) and (9)

$$P(u\ v\ w) = \frac{1}{V} \int_0^1 \int_0^1 \int_0^1 \sum_h \sum_k \sum_l \sum_{h'} \sum_{k'} \sum_{l'} F(h\ k\ l) \exp[-2\pi i(hx + ky + lz)]$$

$$\times F(h'k'l') \exp[-2\pi i(h'x + k'y + l'z)] \exp[-2\pi i(h'u + k'v + l'w)]\,dx\,dy\,dz \qquad (10$$

The right hand side of this equation again equals zero, unless

$h = -h'$, $k = -k'$, $l = -l'$

If this is the case then

$$P(u\ v\ w) = \frac{1}{V} \sum_h \sum_k \sum_{l=-\infty}^{+\infty} F(h\ k\ l)\ F(\bar{h}\ \bar{k}\ \bar{l}) \exp[-2\pi i(h'u + k'v + l'w)] \qquad (11)$$

But $F(h\ k\ l)$ and $F(\bar{h}\ \bar{k}\ \bar{l})$ are complex conjugates and therefore

$$P(u\ v\ w) = \frac{1}{V} \sum_h \sum_k \sum_{l=-\infty}^{+\infty} \left|F(h\ k\ l)\right|^2 \exp[2\pi i(hu + kv + lw)]$$

For all positive values of u, v, w, P is real; therefore

$$P(u, v\ w) = \frac{1}{V} \sum_h \sum_k \sum_{l=-\infty}^{+\infty} \left|F(h\ k\ l)\right|^2 \cos[2\pi\ (hu + kv + lw)] \qquad (12)$$

This is the Patterson series, and it can be seen that the coefficients are now proportional to the intensities of the spectra, that is to a measurable quantity. When this series is evaluated it gives a density distribution which

is periodic with the periodicity of the crystal, has maxima at the origin and at points related to it by lattice translations of the crystal and subsidiary maxima at vector distances from the origin equal to the distances between every pair of atoms in the crystal. It can thus be used to calculate the positions of atoms in the unit cell. This enables a molecular structure to be postulated, and the structure factors arising from this structure are progressively improved until they match those obtained experimentally.

In other words, the determination of a crystal structure involves postulating a structure whose theoretically calculated diffraction pattern is similar to that obtained experimentally.

In practice the Patterson series can be difficult to interpret, peaks can overlap, too much symmetry can exist and a very heavy atom can swampt the rest of the peaks. Harker[2] however has shown that in some cases the Patterson can be less difficult to interpret when the series is of crystals with certain symmetry elements. For example, if a crystal has a 2-fold rotation axis, say the b-axis, then for any atom with co-ordinates x y z there is another with co-ordinates $\bar{x}, \bar{y}, z$ and the vector between these 2 atoms has components (2x,0,2z). The position of the corresponding peaks can thus be found from the y = o plane of the Patterson, this plane is called the Harker Section. If the crystal is in space group $P2_1$ then for every atom at (x y z) there is one at $(\bar{x}, y + \frac{1}{2}, \bar{z})$ and so when $y = \frac{1}{2}$ (Harker Section) the peaks due to vectors from these 2 atoms can be identified. In both

structures analysed the Harker section was used to identify peaks and vectors.

The quantity actually measured in X-ray analysis gives the integrated Intensity I (h k l) of the diffracted beam, for each reflection. This is related to the observed Structure Factor amplitude $|F_o(h\ k\ l)|$ by the equation:
(calculated on the basis of the kinematic theory and assuming a perfectly mosaic crystal)

$$I(h\ k\ l) = E(h\ k\ l)\omega/I_o = QdV = \left(\frac{Ne^2F}{mc^2}\right)^2 \quad Lp\ \lambda^3 dv \qquad (13)$$

where E(h k l) is total diffracted energy at h k l, I_o is the intensity of the incident X-ray beam, dV is the volume of crystals, this is assumed small and absorption effects are therefore neglected . ω is the angular velocity of the crystal, which must be rotated through the region of the Braggs reflection and N is the number of unit cells per unit volume. p the polarisation arises because the original expression assumes a plane polarised incident X-ray beam. The characteristic incident beam is however unpolarised and there is, therefore a reduction in intensity by a factor p which

$$= \tfrac{1}{2}[1 + \cos^2 2\theta]$$

L is the Lorentz factor and is a measure of the relative time opportunity for the various crystal planes to reflect X-rays. It is therefore dependent on the experimental method. For equi-inclination Weissenberg geometry, the L factor equals $1/\cos^2\mu \sin\gamma$, where the axis of rotation of the crystal makes an angle $(\pi/2 - \mu)$ with the incident beam and where γ is the projection on zero level of the angle 2θ between the incident and reflected beams. Therefore with radiation of wavelength equation(13) can be rearranged and gives $|F_o(h\ k\ l)|^2 = \text{constant} \times (LP)^{-1} I(h\ k\ l)$ (14)

Hence the Patterson series can be evaluated using values of $|F_c(h\ k\ l)|^2$ obtained from equation (14).

The calculated Structure Factors are obtained from equation (4) which includes the scattering factor f_n. This latter is a measure of the efficiency of the nth atom in scattering X-rays and is defined in such a way that the atom scatters f times as much as a single electron. The scattering factor is also a function of $\frac{\sin\theta}{\lambda}$ and as θ goes to zero f_n goes to z_n where z_n is the number of electrons in the atom. f_n decreases if θ increases because waves scattered by electrons in different parts of the atom will interfere destructively. International Tables for X-ray crystallography[4] give values for atomic scattering factors and curves, for most atoms, calculated by using various atomic models. However, these models assume that the atom is stationery and at rest and that the electron density is distributed spherically and symmetrically. Thermal motion arising from temperature exists and the scattering or form factor f_n must be modified to take it into account. Thermal motion will also reduce $F_c(h\ k\ l)$ because two equivalent atoms will no longer scatter in phase, since they are displaced from their true positions. The modified scattering factor is given by $f'_n = f_o \exp\left[-B \sin^2\theta/\lambda^2\right]$ (15) where B the temperature factor $= 8\pi^2\bar{\mu}_n^2$, $\bar{\mu}_n^2$ being the mean square atomic displacement[4,5]. B is difficult to estimate or calculate theoretically and may be found for each atom by comparing $|F_o(h\ k\ l)|$ with $|F_c(h\ k\ l)|$ for successive refinements in a trial structure or from an electron density map.[6] Equation (15) however assumes isotropic thermal vibration and in refining a structure Cruickshank has shown that it is necessary to assume ellipsoidal anistropic atomic motion. The scattering factor now becomes

$$f_{on} \exp - \left[B_{11}h^2 + B_{22}k^2 + B_{33}l^2 + B_{12}hk + B_{23}kl + B_{13}hl\right] \qquad (16)$$

The six temperature factors for each atom define the principal axes and direction cosines of the ellipsoid which is one of vibration in real and reciprocal space.

Refinement

The method of least squares can be used to refine a structure. This method[8] varies the atomic parameters so that

$$R = \sum W(h\ k\ l)(|F_o(h\ k\ l)| - |F_c(h\ k\ l)|)^2$$

where $W(h\ k\ l)$ is the weight for each term, $F_o(h\ k\ l)$ the observed structure factor and $F_c(h\ k\ l)$ is the calculated structure factor. The summation is over the set of crystallographically independent observed planes. R can also be written as

$$R = \sum W(h\ k\ l)\ \Delta^2(h\ k\ l)$$

where $\Delta(h\ k\ l) = |\,|F_o(h\ k\ l)| - |F_c(h\ k\ l)|\,|$.

If $u_1\ u_2\ \ldots\ u_n$ are the n parameters occurring in the $|F_c|$ whose values are to be determined then R will be a minimum when

$$\frac{\partial R}{\partial u_j} = 0, \quad (j = 1,2, \ldots, n)$$

that is when

$$\sum W(h\ k\ l)\ \Delta(h\ k\ l)\ \frac{\partial \Delta(h\ k\ l)}{\partial u_j} = 0 \qquad (17)$$

The n parameters may also include temperature factors, scale factors, extinction coefficients, as well as atomic co-ordinates.

Equation (17) alone must be satisfied by the chosen parameters. For a

trial set of values of the u_j close to the correct set, the normal equations for the corrections ϵ_j to the parameters u_j are the n simultaneous linear equations

$$\sum_{i=1}^{n} \epsilon_i \left\{ \sum W(h\ k\ l)\ \frac{\Delta(h\ k\ l)}{u_j}\ \frac{\partial\Delta(h\ k\ l)}{u_i} \right\}$$

$$= - \sum W(h\ k\ l)\ \Delta(h\ k\ l)\ \frac{\partial\Delta(h\ k\ l)}{\partial u_j} \qquad (18)$$

$$(j = 1,2, \ldots\ldots\ldots, n)$$

where the $\partial\Delta(h\ k\ l)/\partial u_j$, etc., are evaluated for the trial parameter values. In equation (18)

$$\frac{\partial\Delta}{\partial u_j} = - \frac{\partial|F_c|}{\partial u_j}$$

if the above representation for R is used.

Solution of the matrix arising from equation (18) is simplified by making some assumptions

i) no interaction between parameters of different atoms.
i.e. terms of the type $\frac{\partial|F_c|}{\partial x_i} \cdot \frac{\partial|F_c|}{\partial x_j} = 0$ for $i \neq j$

ii) no interaction between the co-ordinate parameters and temperature parameters for the same atom, i.e. terms of the type

$$\frac{\partial|F_c|}{\partial x_i} \cdot \frac{\partial|F_c|}{\partial \beta_j} = 0$$

This is called the block diagonal approximation.[9]

The shifts are multiplied by a fudge or damping factor because the calculated shifts are generally too large. The iterative procedure of

least squares refinement is followed until $\sum w_n \Delta_n^2$ has minimised, an indication of the agreement between F_o and F_c being given by R, the reliability factor

$$= \frac{\sum \left| |F_o| - |F_c| \right|}{\sum |F_o|}$$

In carrying out a refinement the choice of weighting scheme is important, since a good weighting scheme gives the least squares method an advantage over the Fourier method in accuracy, but a bad one can give very misleading results. In order to obtain the most accurate parameters with correct standard deviations

$$w_n(h\ k\ l) = 1/\sigma_n^2(h\ k\ l) \text{ where } \sigma_n^2$$

is the variance of $\Delta_n = (|F_o| - |F_c|_n)$.

In practice absolute estimates of the weights are usually not known in advance and relative estimares are made, taking into account both the accurac of $|F_o|$ and the appropriateness of the calculated model on which the $|F_c|$ are based. The weights are often estimated by approximating to a simple function of $|F_o|$ since the uncertainties are often more dependent on random errors in $|F_o|$ than on any other factor. It is important to ensure that values of $\sum_n W\Delta_n^2$ are constant for any group of $|F_o|$'s and the one used in refining the second structure in this present work was one derived by Hughes[8]

$$W = 1 + [(kF_o - F^{**}/F^*)^2]^{-1} \text{ where } F^* = 8F_{min} \text{ and } F^{**} = 5F_{min}$$

The weighting scheme used in the first structure (diffractometer data) was that devised by Killean and Lawrence[10]. This calculates absolute weights by taking into account random errors which are encountered in a diffractometer experiment. These errors are due to counting statistics, random setting errors and random errors arising from errors in the scattering or form factors caused by bonding between atoms. If the first two errors are taken into account it has been shown[11] that

$$\frac{1}{W(\underline{h})} = \sigma_1^2(\underline{h}) + \sigma_2^2(\underline{h}) \quad \text{where } \sigma_1^2(\underline{h})$$

is the variance of $F(\underline{h})$ due to counting statistics alone and $\sigma_2^2(\underline{h})$ the variance due to random instrumental setting errors. The latter are of the form $\sigma_2(\underline{h}) = c^2 |F(\underline{h})|^2$ where c is a constant. An error in the calculated structure factor arises from the errors in the scattering factor curves and Killean and Lawrence take this into account and derive a $\sigma_g^2(\underline{h})$ term which they include in the expression for $\frac{1}{W(\underline{h})}$. The error in the scattering factor curves is of two main types, the first has a systematic effect on $F_s(\underline{h})$ and is due to the isolated atom model which is used to compute the curves, the second type has a random effect upon the

structure factors and arises because each atom will have its electron cloud distorted in a different way from the free-atom shape. This is highly assymmetric and arises when atoms are bonded to one another. Killean and Lawrence[10] take an expression

$$F(\underline{h}) = \sum_{\underline{r}} [f(\underline{h}) + \delta(\underline{h})] \exp 2\pi i \underline{h}.\underline{r} \text{ where}$$

$f(\underline{h})$ is the "isolated atom" scattering factor and $\delta(\underline{h})$ is the correction to be applied to $f(\underline{h})$ due to the bonding of the atom. They then assume that $|\delta(\underline{h})| = k\, f(\underline{h})$ and

hence $F(\underline{h}) = \sum_{\underline{r}} f(\underline{h}) \exp 2\pi i \underline{h}.\underline{r} + \sum_{\underline{r}} k s_j f(\underline{h}) \exp 2\pi i \underline{h}.\underline{r}$

where $s_j = \pm 1$ since $\delta(\underline{h})$ can be positive or negative.

The second term of this expression gives a variance

$$\sigma_3^2 (|F(\underline{h})|) = k^2 \langle \{f(\underline{h})\}^2 \rangle = k^2 \langle |F(\underline{h})|^2 \rangle$$

and this is a measure of the variance of $|F_c(\underline{h})|$ due to the bonding of the atoms. Thus now

$$\frac{1}{W(\underline{h})} = \sigma^2(\underline{h}) = \sigma_1^2(\underline{h}) + \sigma_2^2(\underline{h}) + \sigma_3^2(\underline{h})$$

$$= \frac{K}{4Lp} \frac{(I + B)}{(I - B)} + c^2 |F(\underline{h})|^2 + k^2 \langle |F(\underline{h})|^2 \rangle$$

where $\sigma_1^2(\underline{h})$ is described for a constant time experiment and I is the integrated peak count and B the background count and k is the average fractional error in the scattering curves due to the environment of the atoms.

The G-factor for a structure is defined[12] as

$$G^2 = \frac{\Sigma_{\underline{h}} |\Delta(\underline{h})|^2}{\Sigma_{\underline{h}} |(F(\underline{h})|^2}$$

$$\text{thus } G^2 = \sum_{\underline{h}} \frac{[\sigma_1^2(\underline{h}) + \sigma_2^2(\underline{h}) + \sigma_3^2(\underline{h})]}{\Sigma |F(\underline{h})|^2}$$

$$= S^2 + C^2 + k^2$$

or $G^2 = S^2 = c^2 + k^2 = M$. Since c and k are taken as constants then $(G^2 - S^2)$ should have the same value M over ranges of

The weight of a structure factor is now given by

$$\frac{1}{W(\underline{h})} = \frac{K}{4Lp}\frac{(I + B)}{(I - B)} + (M - k^2)\,|F(\underline{h})|^2 + k^2 \langle |F(\underline{h})|^2 \rangle$$

If a structure has been refined using a reasonable weighting scheme then the $|\Delta(\underline{h})|$ from the last cycle of refinement can be combined with various sets of weights obtained by allowing k^2 to vary from zero to M. The value of k^2 which gives the minimum value of $\Sigma w(\underline{h})\ |\Delta(\underline{h})|^2$ at this stage is then used to continue the refinement with weights on the absolute scale. At the conclusion of refinement if $\sigma_1(\underline{h})$, $\sigma_2(\underline{h})$ and $\sigma_3(\underline{h})$ are an accurate estimate of the random errors present then

$$\frac{\Sigma w(\underline{h})\ |\Delta(\underline{h})|^2}{m - n} \rightarrow 1$$

where m is the number of independent structure factors and n is the number of parameters being refined.

Linear Diffractometer

A Hilger and Watts linear diffractometer was used to collect intensity data for the first structure, that of 2 - phenyl - 2 - oxo - 5,5, - dimethyl - 1,3,2 - dioxaphosphorinane. This section describes the mechanical parts of the instrument and the techniques employed when operating the diffractometer.

The linear diffractometer[13] is an instrument for "automatic" collection of single crystal diffracted intensities. Basically it is a mechanical

FIGURE 5.1

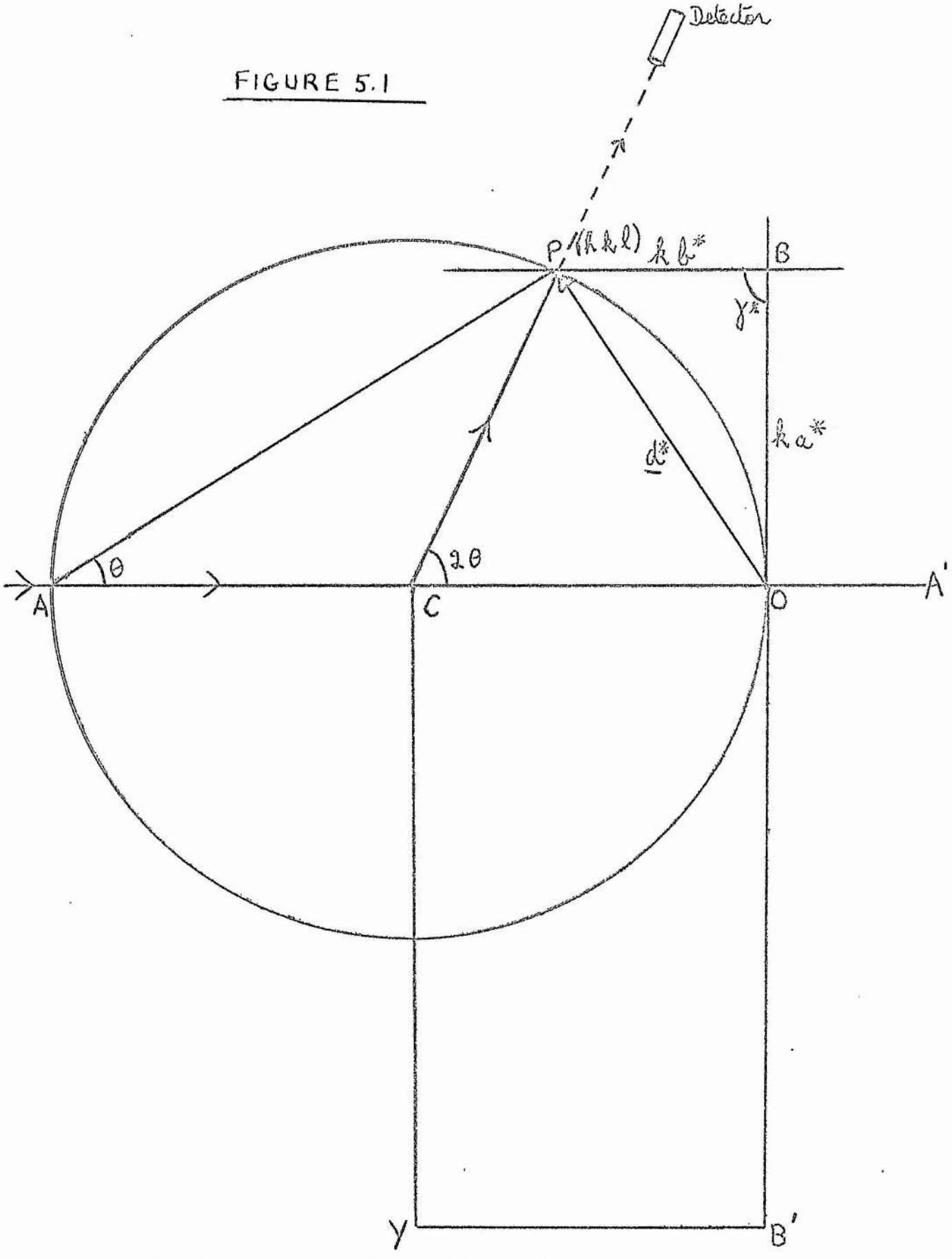

analogue of the Ewald sphere construction of a reciprocal lattice.[14]

According to Braggs law ($2d \sin\theta = n\lambda$) the condition for a group of planes [h k l] to diffract radiation, wavelength λ, is equivalent to the requirement that the reciprocal lattice point P(h k l) lies on the surface of the Ewald sphere of reflection.[14]

A horizontal section of the Ewald sphere is represented in Figure 5.1 The figure also indicates the two dimensional arrangement of the diffractometer when P(h k l) is in the reflecting position. The direction of the incident beam is along ACO. C is the crystal (at the centre of the Ewald sphere) and O is the origin of the reciprocal lattice. A'OA and B O B' are two of the principal axes of the reciprocal lattice and so the figure represents $\underline{a}^*$ $\underline{b}^*$ plane. OP is the reciprocal lattice vector $\underline{d}^*$ of the reflection P(h k l) and equals $h\underline{a}^* + k\underline{b}^* + l\underline{c}^*$ with magnitude $\frac{1}{d(h\ k\ l)}$ where d(h k l) is the spacing of the h k l crystal planes represented by AP, perpendicular to $\underline{d}^*$. CP is the direction of the reflected X-ray beam corresponding to the reciprocal lattice point P(h k l) which lies in the surface of the sphere of reflection.

On the linear diffractometer three slides represent the two reciprocal axes and the real axis C. The motion of the crystal and the detector are linked to C. The detector of fixed length ($\equiv$ 1 r.l.u.) is aligned with the bar CP. The crystal is pivoted at C, independently of the counter and is linked by means of the parallelogram COB'Y to the motion of the carriage B along either slide OB or BP which represent $\underline{b}^*$ and $\underline{a}^*$ respectively. These slides OB and BP are pivoted at O and P, with OB = k $\underline{b}^*$ and BP $h\underline{a}^*$ for reflection P. The carriage B is moved linearly along either slide by driving

FIGURE 5.2

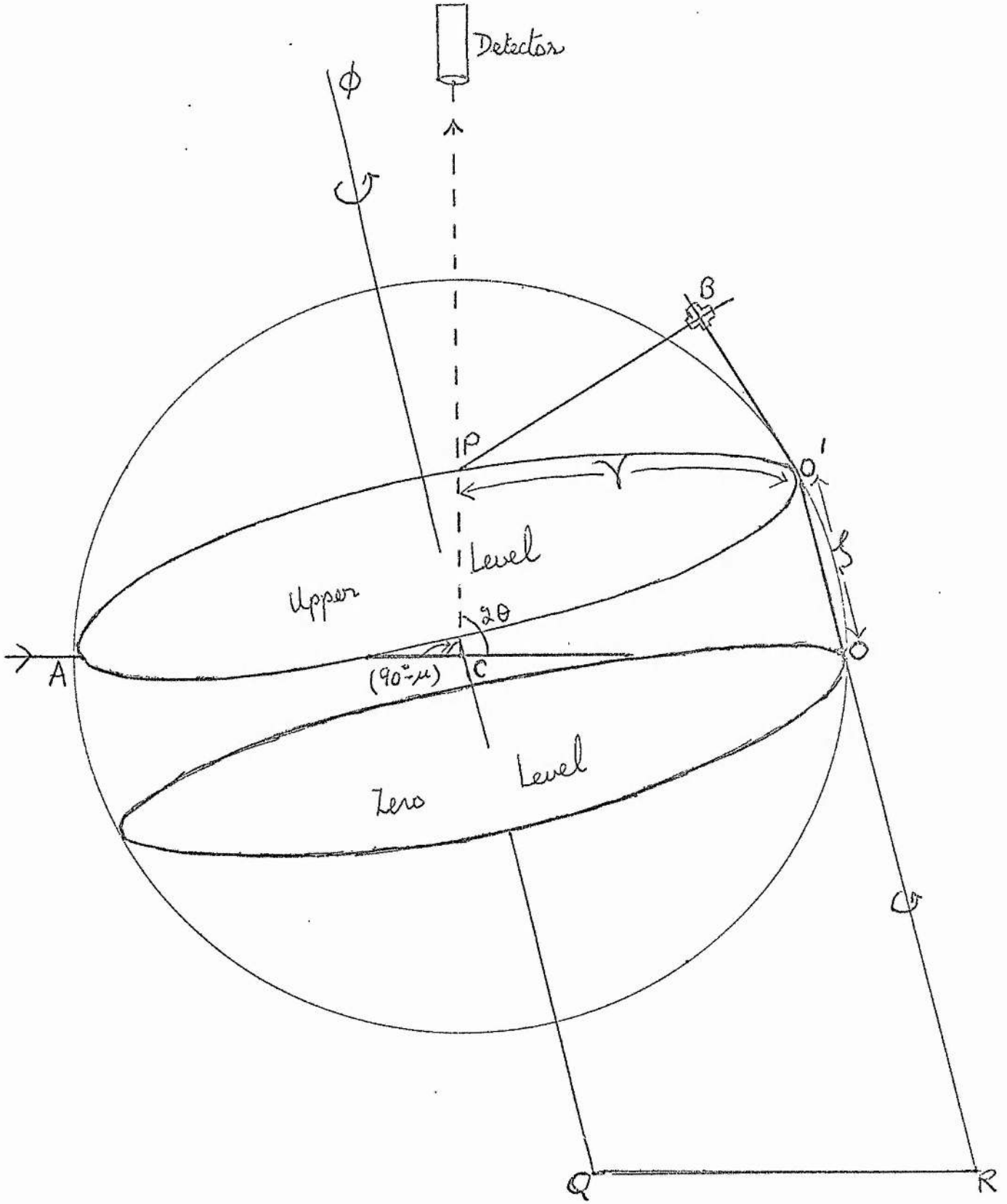

the slides, the counter arm and crystal follow, rotating about the goniometer axis, and as reciprocal lattice points successively cut the surface of the Ewald sphere, the detector is always at the correct angle 2θ to the incident beam.

The extension of the above to upper level data collection is shown in Figure 5.2. Equi-inclination geometry is used since then the upper levels are similar to the lower levels. A third slide OO' is perpendicular to the other two. It is kept parallel to the crystal axis C by means by the parallelogram linkage CQRO, this linkage also ensures equal rotation about CQ and OO'. On the diffractometer the X-ray beam is fixed and so the whole system of Figure 5.2 is tilted to give the correct height of the level AO'P; $\zeta = \frac{l\lambda}{c}$(r.l.u) = OO'. The angle tilt can be independently set at $\mu = \sin^{-1}\zeta/2$ so that the counter is put in the correct orientation at an angle $(90^{\circ} - \mu)$ to the goniometer axis. For each level, once ζ and u have been set, only v and ϕ, the angular positions of the counter and crystal respectively, are changed as P moves round the circle AO'P. P is moved round by the usual method of linearly driving O'B and BP, the counter moving round the cone of semi-angle $(90^{\circ}-\mu)$.

When the reciprocal lattice of the crystal is correctly orientated with respect to the slide system, the normal procedure for measurement of the reflections is to move along successive reciprocal lattice rows on each level, while the stepping slide is kept at the appropriate value of $h\underline{a}^*$ or $k\underline{b}^*$, and moves in equal steps of $\underline{b}^*$ or $\underline{a}^*$ r.l.u. along the other scanning slide. When the counter arm reaches a preset limit switch V during a scan, the next intensity measurement is completed and the stepping

slides moves one translation. Scanning then continues and the process is repeated automatically until the whole level is recorded in this zig-zag fashion.

The integrated intensity of each reflection is measured by a stationary detector - moving crystal technique[15]. An independent constant speed mechanism[16] is used to oscillate the crystal about the axis through the region of the Bragg reflection, enabling the usual equi-inclination Weissenberg Lorentz factor to be used. During each measuring cycle an initial stationary background count b is taken for time t on one side of the reflection, a time 2t is spent counting the integrated peak N as the crystal oscillates and then a second background is measured for time t on the other side. The crystal then returns to its original position. The corrected intensity of the reflection is thus $N = (b + b')$. In practice two oscillation cycles are carried out on each reflection using a balanced filter unit.[17] This introduces between the crystal and the detector an α filter for the first cycle and a β filter for the second (Strontium and Zirconium respectively for the Molybdenum radiation). The absorption edges of the filters bracket the $K\alpha$ line of the radiation used and thus the difference between the two background corrected integrated intensities gives the diffracted characteristic radiation. With the Molybdenum radiation, a scintillation counter was used as the detector. An I.B.M. card punch was used to output the results; the indices h,k,l of the reflection, together with $b_1, N_1, b'_1, b_2, N_2, b'_2$.

Photographic Method of Integrating Intensities

Since the 2nd crystal had to be kept at a low temperature, the linear diffractometer could not be used to collect intensity data and instead an integrating Nonius Weissenberg camera[18] was used.

For each equi-inclination Weissenberg level it is necessary to set :

a) the equi inclination angle

$$\mu = \mathrm{Sin}^{-1}(\zeta/2) = \mathrm{Sin}^{-1}\left[\mathrm{Sin}\left[\tan^{-1}(2Y/D_F)\right]/2\right].$$

Where ζ is the height of the level in reciprocal lattice units (r.l.u.) obtainable from a rotation photograph, Y is the rotation film layer line height in mm. and D_F is the diameter of the film cassette.

b) the shift of the layer line screens of the zero level position. This shift = Stan μ where S is the effective radius of the screens (mean of the internal and external radii).

The integrating mechanism on the camera performs two movements at the end of every usual Weissenberg film translation by means of turning a pinwheel with 14 notches through 1 notch.

(1) A small horixontal translation parallel to the goniometer axis

(2) A small vertical rotation about the goniometer axis.

After one complete rotation of the pinwheel the film has traversed 14 times and 14 small displacements have been made in both directions and the rotational position of the film cassette returns to its original position.

The horizontal displacement may be continued up to 30 times more, when

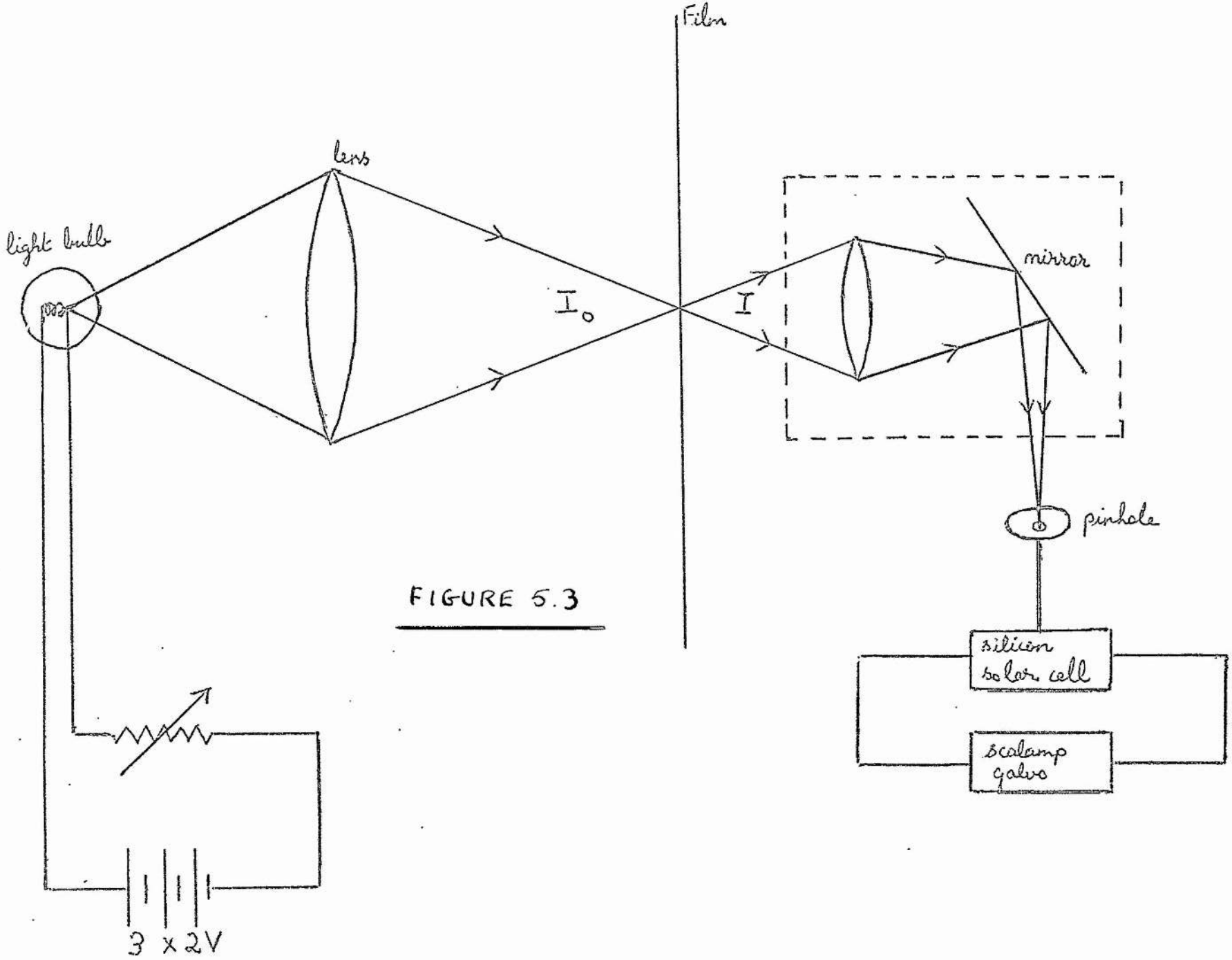
Film
lens
light bulb
I_o
I
mirror
pinhole
silicon solar cell
scalamp galvo
3 x 2V

FIGURE 5.3

the cassette begins to translate in the opposite directions for a further 14 x 30 small translations until back at its original position. For one rotation of the pinwheel, the rotational displacement is equal to the total vertical displacement b and the translational movement is equal to one horizontal step a and up to 30 or multiples of 30 translational steps may be taken per exposure. Thus a complete integration cycle consists of 14 x 30 = 420 translations. Exposure time t for a complete cycle is given by

$$t = \frac{420 \times \Delta\theta}{2 \times 60} \text{ minutes}$$

where $\Delta\theta$ is the oscillation angle of the crystal in degrees.

2 is the number of degrees per m.m. film displacement and 60 is the speed of the film translation mechanism in mm/min (equal to 2.r.p.m. for the driving unit).

The size of the crystal and the setting on the camera determine the size of the integrated plateau whose intensity is to be measured.

For a reflection recorded on film, the integrated Intensity I(B) of X-rays striking the film is the effective intensity of the reflection in the plateau region. This is linearly proportional to the effective film blackening or optical density D of the plateau and is measured with a Nonius microdensitometer. The schematic diagram of the latter is shown in Figure 5.3.

The Density D at any point is defined by $\text{Log}_{10}(I_o/I_T)$ where I_o is the incident intensity and I_T is the transmitted intensity received

by a solar cell and causing a deflection on the galvanometer.

The effective optical density of the plateau =

density of plateau - density of background

$$= \log_{10}(I_o/I_p) - \log_{10}(I_o/I_B)$$

$$= \log_{10}(I_B/I_P) = \log_{10}(B/P)$$

since I_B and I_p are linearly proportional to the deflections B and P on the galvanometer.

Thus for any reflection $I(\underline{h})$ is proportional to $\log_{10}$ (B/P) and for a constant I_o for one film, a set of relative intensities recorded on the film can be obtained. The film is inserted in a holder and can be moved by hand vertically or horizontally. A dummy film is indexed and fixed above the film and aligned with it. A pointer indicates the spot to be measured. I_o was chosen for each film sothat on the lightest portion the galvanometer deflection was a maximum. The peak plateau region of each reflection was found by moving the film slowly until the galvanometer showed a minimum recording. The film was then moved vertically to either side to obtain background readings B_1 and B_2 the mean of these B was used in calculating the intensity. By this method white radiation streaks if present are included in the background.

CHAPTER 6

X-RAY EXPERIMENTAL AND RESULTS

Having studied the N.M.R. spectra and resulting coupling constants of a range of phosphorus heterocyclics, it was decided to undertake crystal structure analysis of two of these compounds, namely, 2-phenyl-2-oxo-1,3,2-dioxaphosphorinane and 5,5-dimethyl-2-phenyl-2-oxo-1,3,2-dioxaphosphorinane. The purpose of this analysis was to obtain non-ambiguous information on the conformation of the phosphorinane ring and the configuration around the phosphorus atom. Also, it would be possible to calculate dihedral angles for the P-O-C-H system, using the co-ordinates obtained. Figure 6.1. shows the chemical constitution of 5,5-dimethyl-2-phenyl-2-oxo-1,3,2-dioxaphosphorinane and the labelling used throughout the rest of the chapter.

FIGURE 6.1.

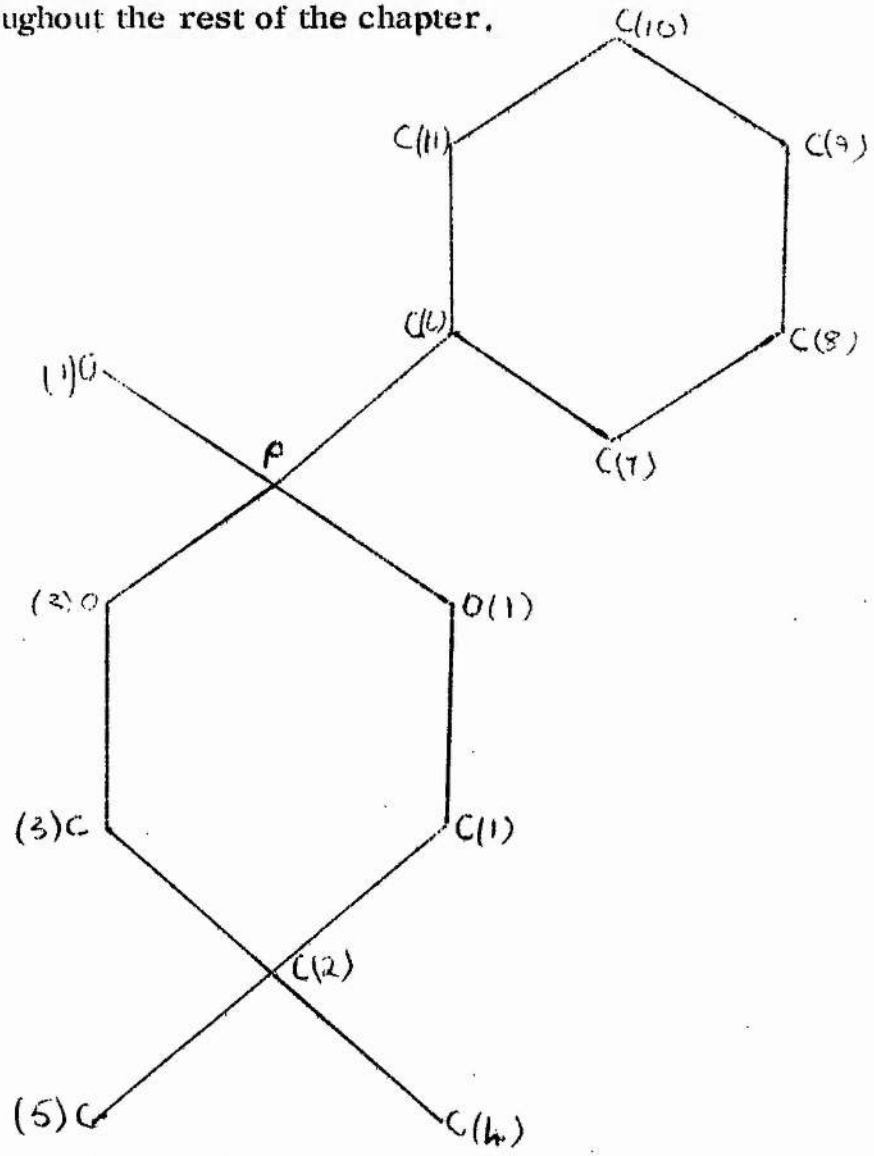

Two well formed crystals of approximate dimensions 0.5 mm x 0.2 mm x 0.1 mm were used in the X-ray analysis of 2-oxo-2-phenyl-5,5-dimethyl-1,3,2-dioxaphosphorinane. They were mounted on a standard goniometer one about the b axis and the other about the c axis. Unit cell dimensions were obtained from the rotation and zero layer Weissenberg photographs.

The photographs were taken at room temperature and copper radiation was used. (λ = 1.5418Å).

Two angles of the unit cell were 90.0° showing the cell to be monoclinic and all oko reflections for k odd were absent. The space group must therefore be $P2_1$ or $P2_1/m$. The rest of the crystal data is as follows:-

Molecular formula $C_{11}H_{15}O_3P$, m.p. 104°C, M.W. 226.22 a.m.u. monoclinic

a = 5.82 ± 0.02, b = 10.23 ± 0.03, c = 9.70 ± 0.02 Å

β = 99.0° ± 5'

V = 570.42 A^3

Density calculated = (1.32 ± 0.02) gm cm^{-3}

Density observed = (1.30 ± 0.05) gm cm^{-3}

z, number of molecules per unit cell = 2

μ for Mo Kα = 0.23 cm^{-1}

Equi-inclination intensity data was then collected for k = 0⟶9 on a Hilger and Watt's linear diffractometer with the crystal mounted about the b axis. As mentioned previously, the balanced filter technique was used with molybdenum Kα radiation (λ = 0.710 Å) and a 30 second oscillation motor. The data were reduced to structure factors by correcting for Lorentz and polarisation effects, using a programme written in Fortran IV for an 1130 I.B.M. computer. No corrections for

FIGURE 6.2

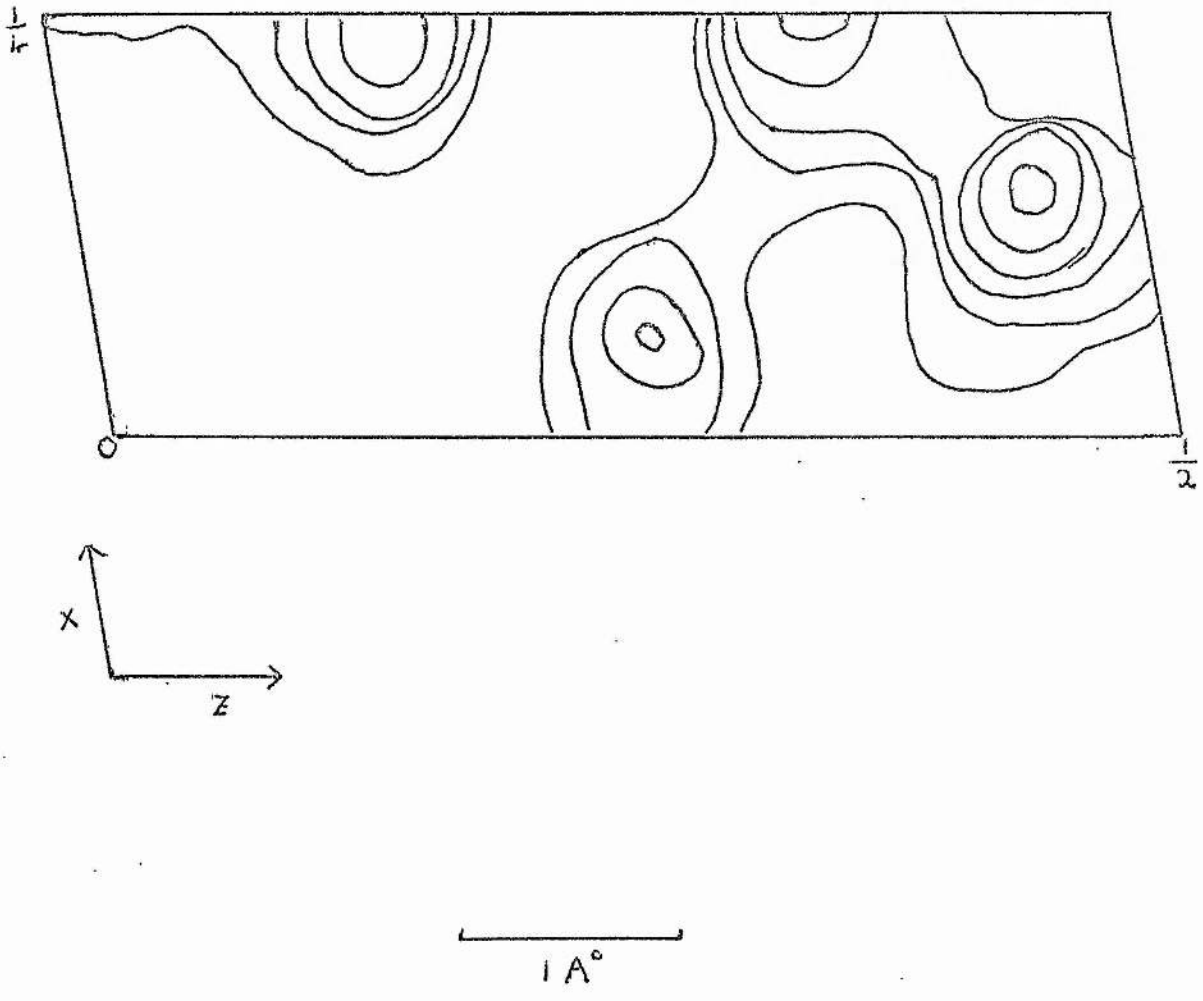

absorption were made. The total number of reflections recorded with net counts greater than zero was 635.

STRUCTURE DETERMINATION

A three-dimensional unsharpened Patterson function obtained from a 1620 I.B.M. computer, using a programme written by G.A. Mair was difficult to interpret initially. Phosphorus is a fairly heavy atom and since peak heights are proportional to the product of the atomic numbers of the atoms forming the vector, phosphorus-oxygen and phosphorus-carbon vectors can be expected to be much higher than oxygen-carbon or carbon-carbon vectors. In the present structure phosphorus is bonded to four atoms, three oxygen and one carbon. Thus the first stage in analysis was to look for three phosphorus-oxygen and one phosphorus carbon vectors at about 1.5 Å from the origin with known geometry. There were however only two present:

x_1/a	y_1/b	z_1/c	x_2/a	y_2/b	z_2/c
+0.20	+0.09	+0.10	+0.12	-0.087	-0.10

If symmetry related peaks at $\bar{x}_1$, y_1 and $\bar{z}_1$ and $\bar{x}_2$, y_2 $\bar{z}_2$ were considered we got four vectors with correct geometry. Using a model and putting the phosphorus atom on the highest peak on the Harker section (see Figure 6.2) $y = \frac{1}{2}$, the above vectors could be identified and co-ordinates of the atoms in the ($P\text{-}O_3C$) group could be calculated. At this stage the possibility of space group $P2_1/M$ could be excluded.

Table 6.1

Co-ordinates obtained from Patterson for

$P(O_3-C)$ group[a]

	x	y	z[b]
Phosphorus	0.2417	0.0000	0.1542
Atom I	0.0667	0.0917	0.0792
Atom II	0.0833	-0.0917	0.2542
Atom III	0.3625	-0.0875	0.0542
Atom IV	0.4340	0.0958	0.2542

[a] Carbon atom not identified at this stage

b Values are given in fractional co-ordinates

A structure factor calculation based on the co-ordinates given in Table 6.1, calculated from the four vectors gave a reliability factor R, (defined in the last chapter) of 0.40. The resulting Fourier summation enabled the carbon atom of the P-(O_3-C) group to be identified and gave also the positions of the remaining ten carbon atoms. These, indicated a chain conformation for the phosphorinane ring and an axial position for the phenyl group. Least squares refinement (8 cycles) using a Hughes weighting scheme and isotropic temperature factors reduced R to 0.15.

REFINEMENT.

Further refinement was carried out using the absolute weighting scheme[1] mentioned previously. This gives a weight $W(\underline{h})$ for each structure factor $|F(\underline{h})|$ having a variance $\sigma^2(\underline{h})$ of

$$W(\underline{h}) = \frac{1}{\sigma^2(h)} = \frac{K}{4LP} \frac{(I + B)}{(I - B)} + C^2 |F(\underline{h})|^2 + k^2 \langle \tfrac{1}{4} |F(\underline{h})|^2 \rangle$$

where I is the integrated peak count, B is the background count, C is the fractional error in $F(\underline{h})$ and k is the average fractional error in the scattering curves due to bonding electrons.

Since, each integrated reflection was measured for only 15 secs., the variance of $|F(\underline{h})|$ due to counting statistics was fairly large and, assuming values of C and k of 0.0025 and 0.0010 respectively, the theoretically expected R - index[2] given by $R = \frac{2}{\pi} \frac{\sum_h \sigma(h)}{\sum_h |F(\underline{h})|}$ was 0.11.

When the structure was refined using this weighting scheme with the assumed values of C and k a final R-factor of 0.134 was obtained. The value of $\sum_h \frac{W(\underline{h}) |\Delta \underline{h}|^2}{M-N}$ where M represents the number of observations and N the number of variables, was 1.24. Corrected values of C and k were then calculated using the G-Index defined in Chapter 5 as $G^2 = S^2 + C^2 + k^2$.

At this point of refinement, $G^2 = 0.0200$ and $S^2 = 0.0153$, $\therefore$ $C^2 + k^2 = 0.0047$. Various values of $\sum_h \frac{W(h) |\Delta(h)|^2}{M-N}$ were then calculated for values of C and k subject to $C^2 + k^2 = 0.0047$ and the minimum value occurred when $C^2 = 0.0027$ and $k^2 = 0.0020$.

Further refinement using these values gave a final R-index of 0.119 and a final value of $\sum_h \frac{W(\underline{h}) |\Delta(\underline{h})|^2}{M-N}$ of 0.99. The theoretical value of this term is unity, thus the value obtained justified the choice of the weighting scheme. Moreover, the final R-index agrees with the theoretically accepted value. This value could of course have been reduced by increasing the time taken to measure each reflection but it was felt that sufficient accuracy for the purpose of the analysis could be obtained using the 30 sec. motor. The final value of k = 0.04 suggests about a 4% error in the form factors due to bonding.

Table 6.2 gives the final co-ordinates and their standard deviations and calculated positions of the methylene and benzene ring hydrogens. Table 6.3 gives the anisotropic temperature parameters and Table 6.4* the structure factors, observed and calculated.* In appendix.

Table 6,2

Final co-ordinates and standard deviations*

Atom	x/a	y/b	z/c
P	0.2320 (10)	-0.0008 (7)	0.1024 (6)
O (1)	0.0721 (23)	-0.0937 (14)	0.0715 (13)
O (2)	0.1067 (32)	-0.0937 (18)	0.2392 (14)
O (3)	0.3766 (24)	-0.0736 (15)	0.0613 (13)
C (1)	0.1535 (40)	0.1631 (21)	-0.0393 (23)
C (2)	0.2538 (44)	0.0753 (23)	-0.1407 (21)
C (3)	0.4560 (33)	-0.0008 (30)	-0.0519 (20)
C (4)	0.0696 (45)	-0.0213 (25)	-0.2062 (23)
C (5)	0.3702 (47)	0.1519 (29)	-0.2492 (24)
C (6)	0.440 (38)	0.0963 (19)	0.2802 (17)
C (7)	0.3469 (42)	0.2142 (19)	0.3275 (22)
C (8)	0.4895 (52)	0.2838 (26)	0.4224 (21)
C (9)	0.7074 (44)	0.2376 (30)	0.4727 (21)
C (10)	0.7974 (46)	0.1234 (24)	0.4221 (18)
C (11)	0.6582 (37)	0.0548 (23)	0.3198 (19)

* given in brackets

Table 6.2 Continued

Calculated positions of the methylene and benzene ring hydrogen atoms

Atom	x/a	y/b	z/c
H (1)	0.0154	0.2189	-0.0969
H (1)	0.2894	0.2302	0.0058
H (3)	0.5902	0.0689	-0.0058
H (3)	0.5361	-0.0664	-0.1160
H (7)	0.1658	0.2447	0.2864
H (8)	0.4297	0.3760	0.4616
H (9)	0.8143	0.2915	0.5566
H (10)	0.9777	0.0910	0.4629
H (11)	0.7184	-0.340	0.2679

Table 6.3

Final anisotropic temperature factors x 10^5,

defined as exp $(-\sum_i \sum_j B_{ij} h_i h_j)$

	B_{11}	B_{22}	B_{33}	B_{23}	B_{13}	B_{12}
P	2261	896	915	-678	-26	-296
O (1)	2022	892	1241	-285	-202	-315
O (2)	6843	1334	943	380	1162	-488
O (3)	2905	1135	1071	67	85	-149
C (1)	4045	596	1266	133	-950	599
C (2)	5157	857	756	-37	-223	1352
C (3)	2067	2129	1357	-692	1152	-2363
C (4)	5698	933	1307	-1228	71	619
C (5)	5109	1871	1113	20	1820	-2368
C (6)	3869	799	302	-273	-54-	-263
C (7)	5600	578	1253	304	3822	-252
C (8)	8081	1301	610	-1515	2313	-3376
C (9)	4192	2326	587	508	-1217	-2957
C (10)	6545	1231	329	-784	542	-2832
C (11)	2356	1543	882	1428	126	1111

Table 6.5

Bond lengths and standard deviations based on co-ordinates from Table 6.2

Bond	length	Standard deviation
P-O (1)	1.53 Å	0.02 Å
P-O (2)	1.47	0.02
P-O (3)	1.57	0.02
P-C (6)	1.82	0.02
O (1)-C (1)	1.43	0.02
O (3)-C (3)	1.46	0.02
C (1)-C (2)	1.51	0.03
C (2)-C (3)	1.55	0.03
C (2)-C (4)	1.52	0.04
C (2)-C (5)	1.55	0.03
C (6)-C (7)	1.43	0.03
C (7)-C (8)	1.34	0.03
C (8)-C (9)	1.37	0.04
C (9)-C (10)	1.40	0.03
C (10)-C (11)	1.37	0.03
C (6)-C (11)	1.33	0.03

TABLE 6.6.

	angle	standard deviation
O(1)-P-O(2)	113.1°	0.9°
O(1)-P-P(3)	106.2°	0.8°
O(2)-P-O(3)	111.4°	0.9°
O(1)-P-C(6)	107.6°	0.9°
O(2)-P-C(6)	111.7°	0.9°
O(3)-P-C(6)	106.5°	0.9°
P-O(1)-C(1)	119.7°	0.8°
P-O(3)-C(3)	118.3°	0.8°
O(1)-C(1)-C(2)	113.8°	1.7°
O(3)-C(3)-C(2)	111.8°	1.5°
C(1)-C(2)-C(3)	105.8°	1.8°
C(1)-C(2)-C(4)	109.8°	2.0°
C(1)-C(2)-C(5)	113.2°	1.9°
C(3)-C(2)-C(4)	109.8°	2.0°
C(3)-C(2)-C(5)	104.8°	2.0°
P-C(6)-C(7)	114.3°	1.7°
P-C(6)-C(11)	120.1°	1.6°
C(6)-C(7)-C(8)	116.2°	2.0°
C(7)-C(8)-C(9)	120.1°	2.0°
C(8)-C(9)-C(10)	122.6°	2.0°
C(10)-C(11)-C(6)	118.2°	2.0°
C(11)-C(6)-C(7)	124.7°	2.0°

TABLE 6.7.

Dihedral Angles[a]

[a] calculated from co-ordinates of Table 6.2.

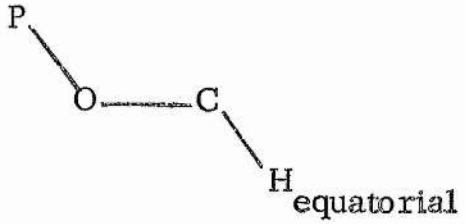

$180^\circ \pm 4^\circ$

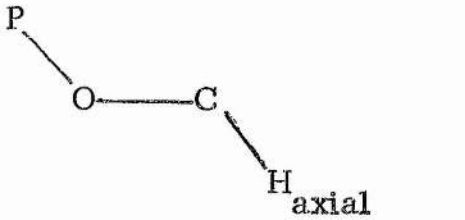

$41^\circ \pm 4^\circ$

MOLECULAR GEOMETRY

In the solid state the phosphorinane ring has a chair conformation which is slightly flattened compared with the cyclohexane ring. The arrangement around the phosphorus atom is approximately tetrahedral with the phenyl group lying in the axial position and the phosphorus-oxygen double bond lying in the equatorial position. This configuration occurs also in methoxy[3], hydroxy[4] and phenoxy[5] derivatives of the compound, which indicates that this is the sterically preferred conformation.

Bond lengths and valency angles are listed in Tables 6.5 and 6.6. The single bonded phosphorus-oxygen distance (mean 1.55 Å) and double bonded phosphorus-oxygen distance (1.48 Å) agree with those found in several structures. Kraut and Jensen[6] allot values of 1.56 Å and 1.49 Å, respectively to these bonds. They have also observed that oxygen-phosphorus-oxygen angles increase with decreasing oxygen-phosphorus distances, it can be seen that this is confirmed by the present results. Large valency angles for oxygen atoms have been found in organic phosphates[7] and this is the case in the present structure. This increase in the interior C-O-P angles, mean value 119°, compared with 111° in cyclohexane[8] causes the phosphate end of the ring to be slightly flattened. Calculated dihedral angles are given in Table 6.7.

FIGURE 6.3

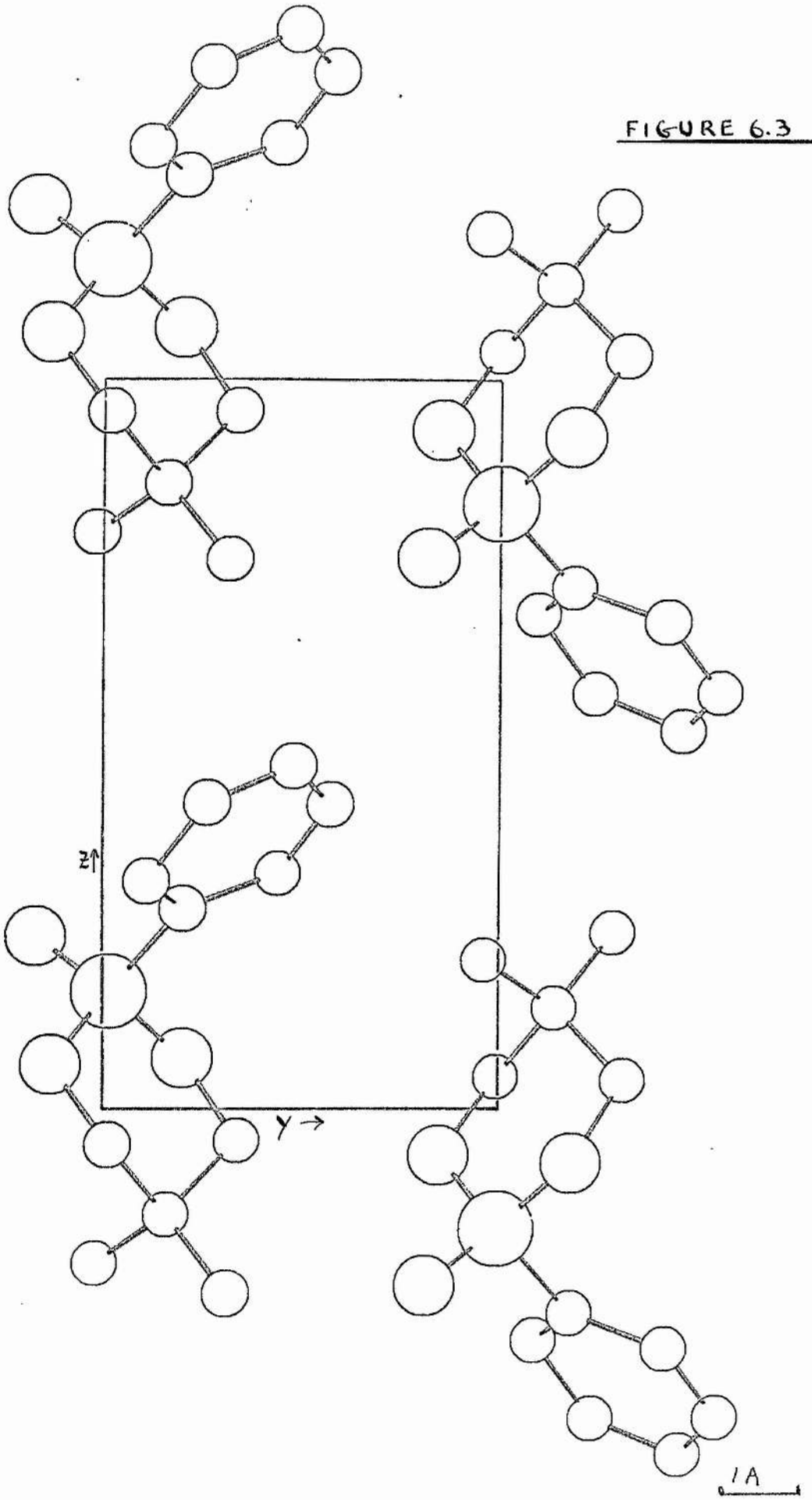

The carbon valency angles are normal except for the C-C-C angle in the heterocyclic ring which is unusually small 105°. However since carbon co-ordinates are most seriously affected by series termination effects, small deviations in carbon valency angles or carbon bond lengths are of doubtful significance. Bond distances in the benzene ring give an average value of 1.37 Å and bond angles an average value of 119°. Figure 6.3 shows a packing of the structure projected along the a axis. No particularly short intermolecular distances are found, see Table 6.8. The shortest distance (3.40 A°) is between C(9) (central molecule at (x, y, z) and C(5) belonging to molecule at x, y, z + 1.

Table 6.8

Shortest intermolecular distances

atom of molecule x, y, z.	atom of other molecule	distance in A°	symmetry relations
C(9)	C(4)	3.40	x y z + 1
C(1)	O(2)	3.45	$\bar{x}$ y + ½ $\bar{z}$
C(5)	O(2)	3.83	$\bar{x}$ y + ½ $\bar{z}$
C(10)	C(5)	4.05	x y z + 1
C(2)	O(2)	4.08	$\bar{x}$ y + ½ $\bar{z}$
C(1)	O(3)	4.13	$\bar{x}$ y + ½ $\bar{z}$
O(1)	O(3)	4.45	$\bar{x}$ y + ½ $\bar{z}$

During the preliminary investigations on the crystals of 2-oxo-2-phenyl-1,3,2-dioxaphosphorinane, it was found that they were unstable and seemed to liquify on a glass surface at room temperature although the melting point of the substance was 40-45°C. Figure 6.4 below gives the chemical constitution of the compound and the numbering used throughout.

FIGURE 6.4

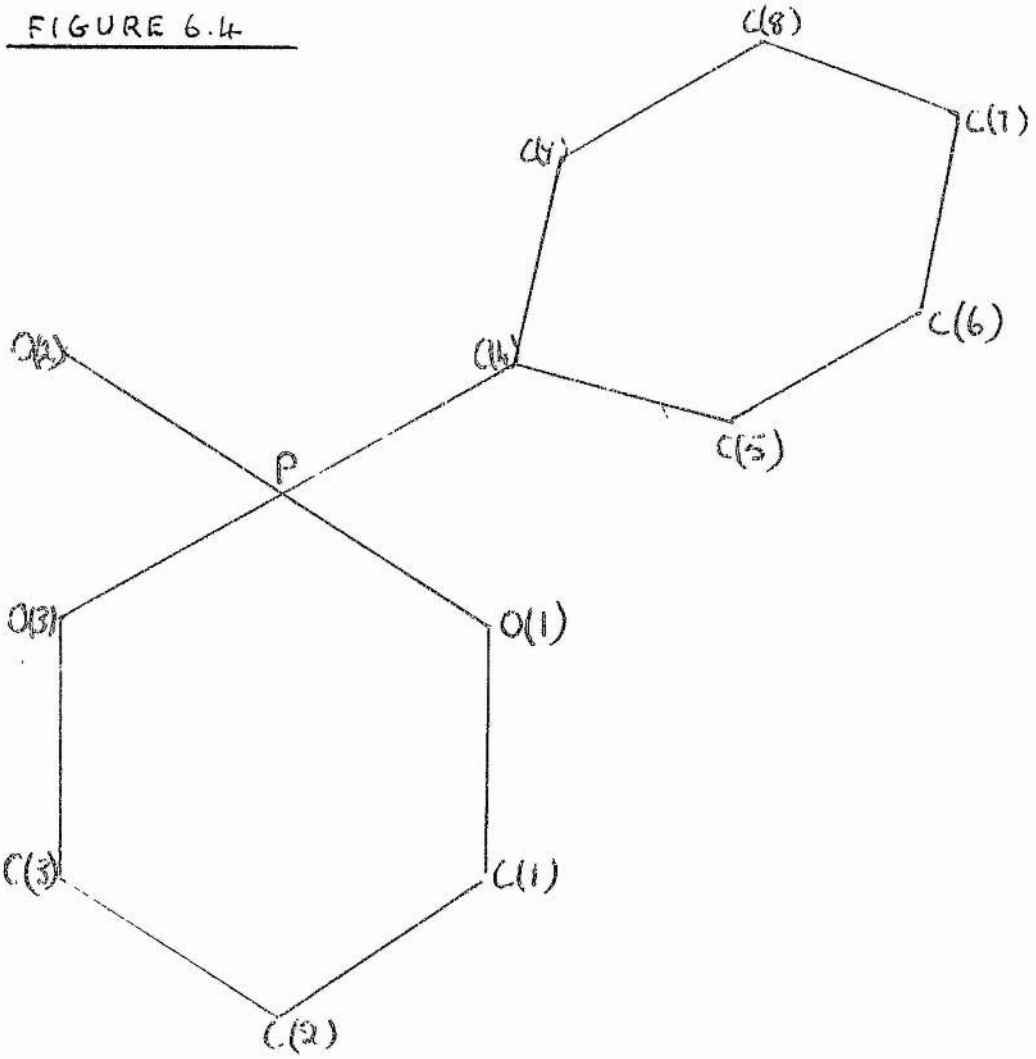

FIGURE 6.5.

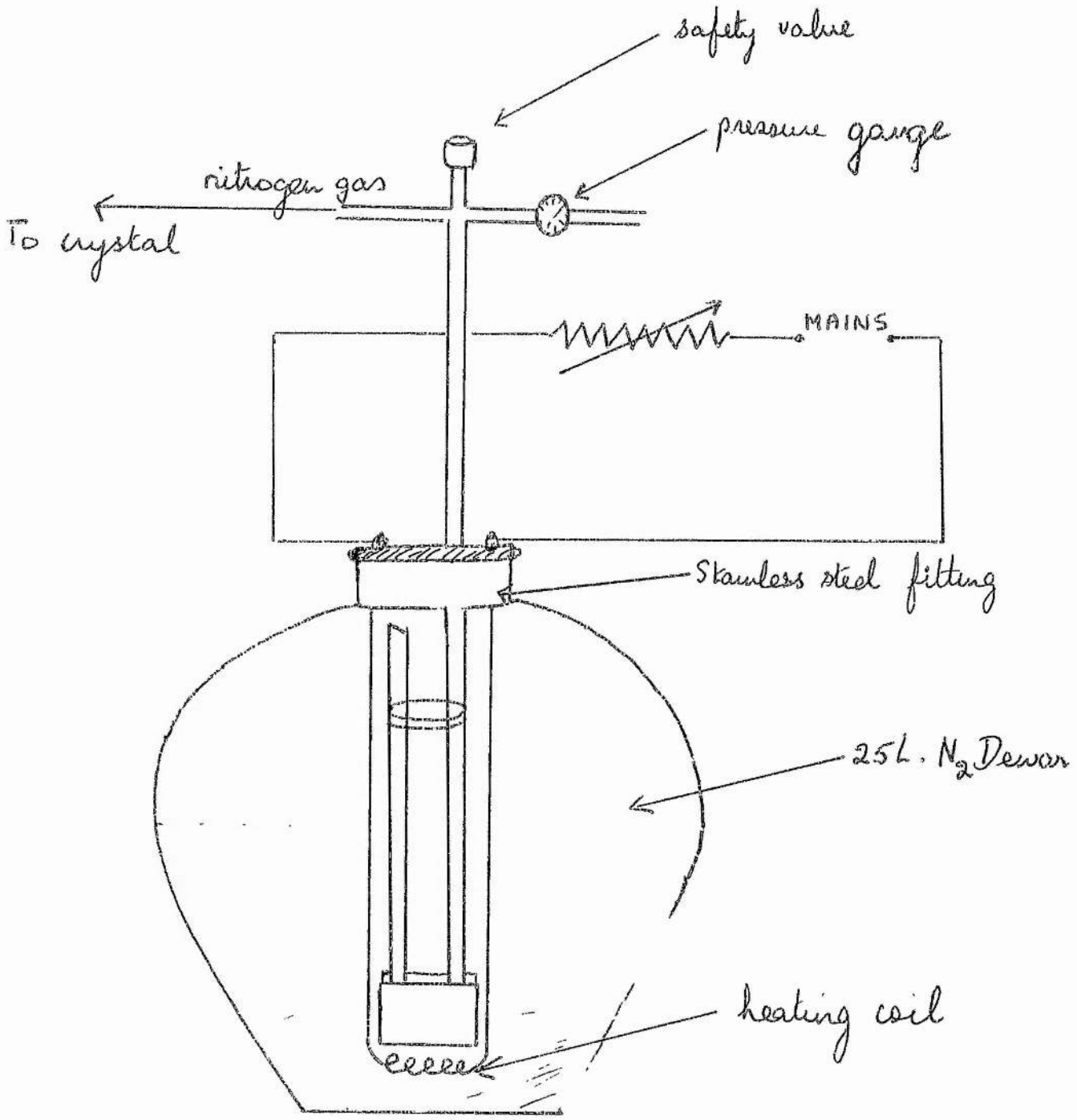

CRYSTAL COOLING DEVICE

Designed by : R. H. Mitchell
Made by : Derek Jones

School of Physical Sciences, University of St. Andrews.

To maintain this temperature around the crystal during data collection, a simple cooling device was constructured see Figure 6.5. Cold nitrogen gas was boiled off from a large dewar using a small heating coil, then passed through a glass walled dewar flask and over the crystal mounted on a goniometer. The rate of flow of the nitrogen and hence the temperature round the crystal, was controlled by varying the current through the coil. The temperature round the crystal was maintained at about $-10^{o}C$, low enough to ensure crystal stability. During the data collection a slight amount of frost was deposited on the tubes and it was felt that this coupled with possible temperature fluctuations in the crystal would limit the accuracy of the final structure.

A crystal of approximate dimensions 0.2 mm x 0.2 mm x 0.2 mm, sealed in a beryllium glass capillary was mounted about the b axis. Unit cell dimensions were determined from rotation and zero level Weissenberg photographs using CuKα radiation (λ = 1,5418 A). Integrated equiinclination Weissenberg photographs were taken for k = $0 \rightarrow 6$ using the Nonius low-temperature divided camera with a multi-layer (5) pack. The intensities were then measured on the Nonius single spot microdensitometer. The intensities on each layer were calculated and placed on the same scale and the scale factors between layers obtained from a second crystal mounted about the c axis. The data was then reduced to structure factors by applying Lorentz and polarisation factors. No correction for absorption was made and the total number of

FIGURE 6.6

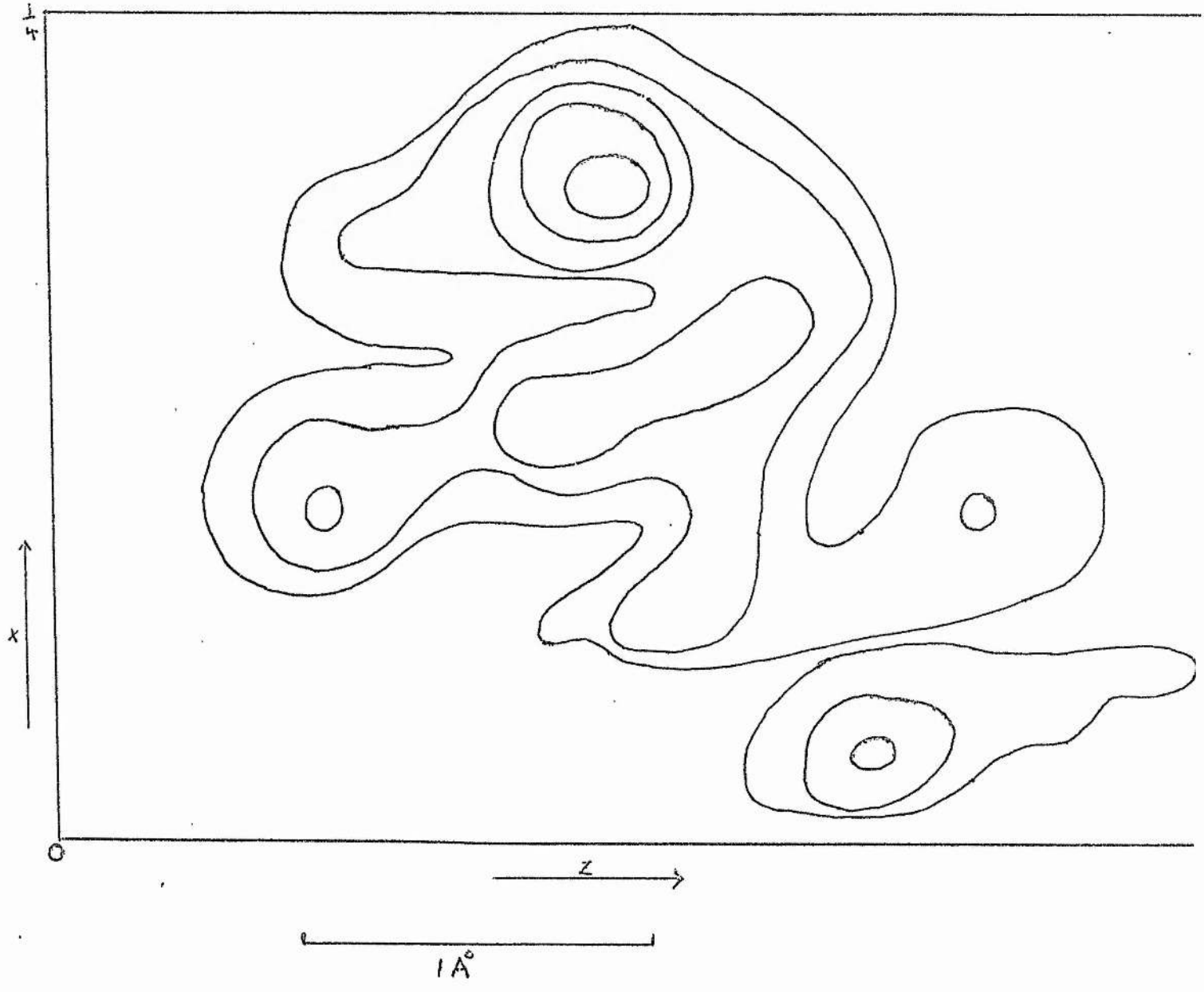

reflections was 462. Complete Crystal Data is as follows:-

Molecular formula $C_9H_{11}O_3P$, m.p. 49-50°C,

M.W. 198.16 a.m.u.

Monoclinic

$a = 9.72 \pm 0.03$, $b = 7.61 \pm 0.03$, $c = 6.60 \pm 0.03$ A°

$\beta = 90.5^{\circ} \pm .5'$

$V = 488.20$ A^3

Density calculated = $(1.35 \pm .02)$ gm cm^{-3}

Density observed = $(1.30 \pm .05)$ gm cm^{-3}

$Z = 2$

μ(CuKα) = 2.33 cm^{-1}

Absent spectra: OKO when K is odd

Space Group: $P2_1$

STRUCTURE DETERMINATION

A three dimensional unsharpened Patterson was calculated, as for the previous structure. The largest peak on the Harker Section $y = \frac{1}{2}$ was assumed to correspond to the vector between the two phosphorus atoms in the unit cell, see Fig. 6.6. Three peaks at about 1.5 Å from the origin of the Patterson function were taken to be the intramolecular vectors between the phosphorus and oxygen atoms. Thus the positions of the phosphorus atom and the oxygen atoms in the unit cell were

TABLE 6.9.

INITIAL CO-ORDINATES FROM PATTERSON

	x/a	y/b	z/c
P	0.208	0.000	0.242
0 (1)	0.142	0.100	0.066
0 (2)	0.216	-0.190	0.233
0 (3)	0.150	0.082	0.416

TABLE 6.15.

DIHEDRAL ANGLES [a]

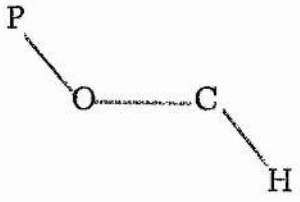

equatorial $180^{o} \pm 4^{o}$

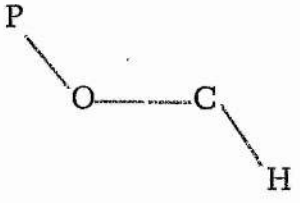

axial $50^{o} \pm 4^{o}$

[a] Calculated from co-ordinates of Table 6.10.

Table 6.10

Final co-ordinates and standard deviations

	x/a	y/b	z/c
P	0.2065(6)	0.0023	0.2288(10)
O(1)	0.1597(19)	0.1194(27)	0.0323(27)
O(2)	0.1811(17)	0,1848(28)	0.1945(23)
O(3)	0.1171(17)	0.0845(24)	0.4047(25)
C(1)	0.1437(27)	0.3271(43)	0.0717(40)
C(2)	0.0485(32)	0.3554(45)	0.2404(48)
C(3)	0.1054(29)	0.2561(43)	0.4290(42)
C(4)	0.3876(30)	0.0703(40)	0.2823(46)
C(5)	0.4226(32)	0.0613(38)	0.4896(46)
C(6)	0.5569(34)	0.0833(42)	0.5337(46)
C(7)	0.6595(30)	0.1272(43)	0.3843(44)
C(8)	0.6185(30)	0.1332(42)	0.1785(43)
C(9)	0.4709(30)	0.0850(43)	0.1421(44)

*Standard deviations. All values are given in fractional co-ordinates.

Table 6.10 Continued

Calculated positions of hydrogen atoms

Atom	x/a	y/b	z/c
H (1)	0.098	0.306	-0.067
H (1)	0.239	0.364	0.102
H (2)	0.055	0.300	0.210
H (2)	0.039	0.495	0.255
H (3)	0.038	0.301	0.558
H (3)	0.206	0.326	0.459
H (5)	0.349	0.160	0.580
H (6)	0.596	0.089	0.691
H (7)	0.765	0.152	0.419
H (8)	0.690	0.032	0.045
H (9)	0.448	0.092	-0.019

Table 6.13

Bond lengths and standard deviations

based on co-ordinates from Table 6.10

Bond	Length	Standard Deviation
P-O(1)	1.62	0.01
P-O(2)	1-46	0.02
P-O(3)	1.58	0.02
P-C(4)	1.85	0.02
O(1)-C(1)	1.48	0.03
O(3)-C(3)	1.49	0.03
C(1)-C(2)	1.49	0.04
C(2)-C(3)	1.52	0.04
C(4)-C(5)	1.37	0.04
C(5)-C(6)	1.39	0.04
C(6)-C(7)	1.41	0.04
C(7)-C(8)	1.44	0.04
C(8)-C(9)	1.37	0.04
C(9)-C(4)	1.36	0.04

Table 6.11

Temperature Factors - Isotropic

O(1)	4.99(40)	C(4)	4.38(66)
O(2)	4.62(40)	C(5)	2.37(69)
O(3)	3.63(37)	C(6)	5.17(63)
C(1)	4.59(64)	C(7)	4.79(62)
C(3)	4.60(54)	C(8)	4.17(63)
C(2)	5.61(75)	C(9)	5.84(62)

Anisotropic

	B_{11}	B_{22}	B_{33}	B_{12}	B_{13}	B_{23}
P	399(57)	1612(113)	1908(157)	-284(89)	116(72)	-511(139)

Table 6.14

Intramolecular bond angles and standard deviations

Angle	Angle in degrees	Standard Deviation in degrees
O(1)-P-O(2)	109.0	1.7
O(1)-P-O(3)	102.6	1.6
O(1)-P-C(4)	107.2	1.7
O(2)-P-O(3)	112.7	1.8
O(2)-P-C(4)	118.0	1.9
O(3)-P-C(4)	105.9	1.6
P-O(1)-C(1)	116.0	1.8
P-O(3)-C(3)	119.2	1.9
P-C(4)-C(5)	116.0	1.6
P-C(4)-C(9)	119.9	2.8
O(1)-C(1)-C(2)	115.1	2.7
O(3)-C(3)-C(2)	109.4	2.6
C(1)-C(2)-C(3)	107.5	2.6
C(4)-C(5)-C(6)	116.4	2.5
C(5)-C(6)-C(7)	121.8	3.0
C(5)-C(4)-C(9)	122.8	3.5
C(6)-C(7)-C(8)	120.0	3.0
C(7)-C(8)-C(9)	115.9	2.9
C(8)-C(9)-C(4)	122.6	3.5

found and a structure factor calculation based on these positions gave a reliability index of 0.40. Table 6.9 gives the initial co-ordinates of these atoms. From the resulting Fourier summation the positions of the carbon atom bonded to the phosphorus atom and of the rest of the atoms in the phosphorinane ring were obtained. A further structure factor calculation and Fourier summation gave the co-ordinates of the remaining atoms in the benzene ring. The reliability factor for all the atoms was now 0.28. The structure was refined by the least square technique using the block diagonal approximation and a Hughes weighting scheme.

Refinement with isotropic temperature factors gave a reliability index of 0.17. When anisotropic temperature factors were applied this index fell to 0.14 but negative B_{ii}'s and large standard deviations were obtained for the co-ordinates of one of the carbon atoms C(1). It was thought that this could be due to wrong positioning of these atoms but a Fourier calculation with structure factors and phases obtained from putting in the positions of all atoms except C(1), C(2) and C(3) showed these latter to be in the same place as before.

In an attempt to find the source of the error, Lorenz-polarisation factors were recalculated and checked, but these were in agreement with previous calculations. A full matrix refinement programme on a 360 I.B.M. computer which allowed scale factors, co-ordinates and temperature factors to be varied at will, was now used and it was found that each layer needed to be separately scaled. This was done and with isotropic temperature factors and co-ordinates varying for four cycles the structure

FIGURE 6.7

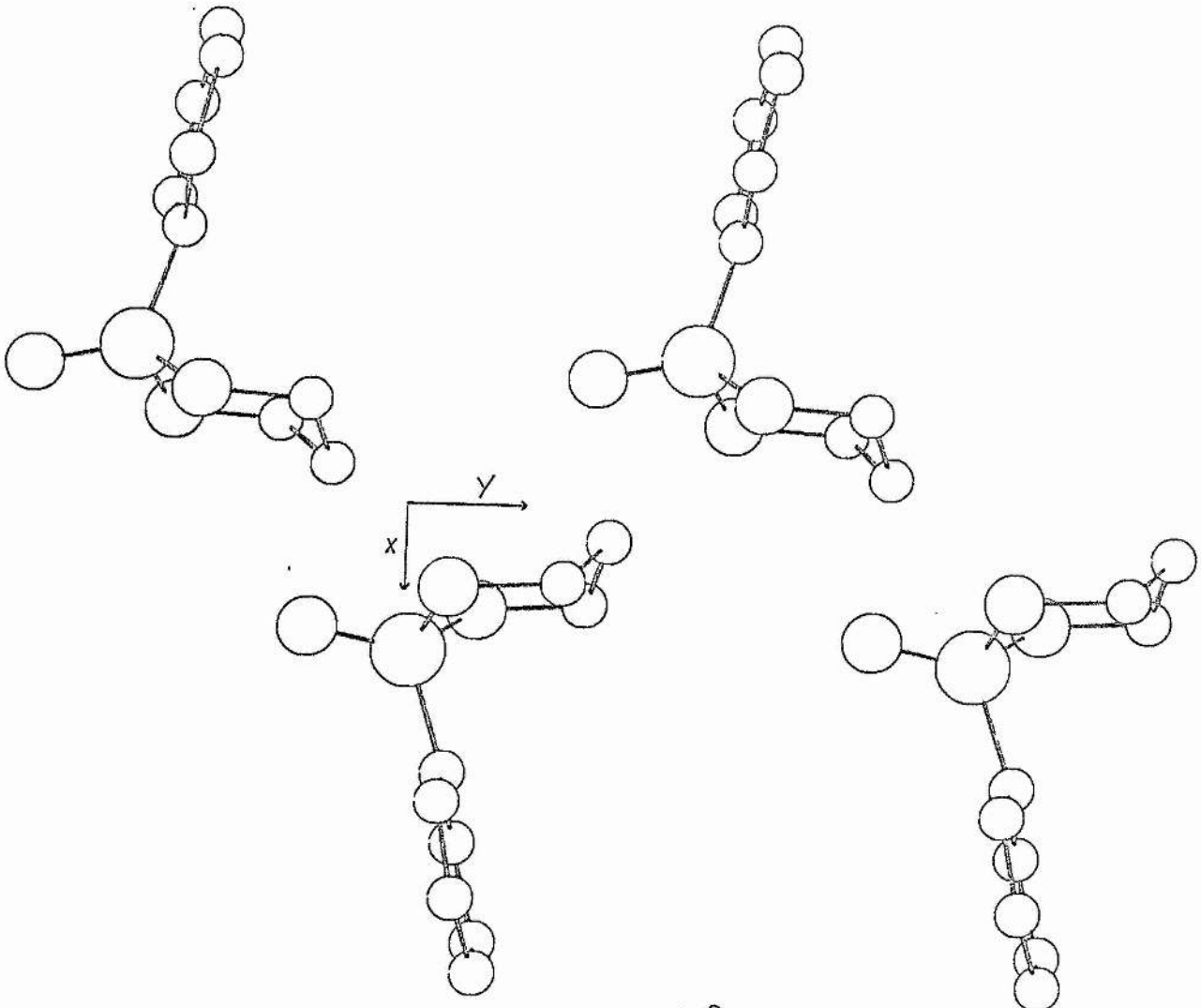

Table 6.16

Shortest Intermolecular distances

Atom of molecule at x y z	atom of other molecule	distance in Å	Symmetry relation
C (2)	O (1)	3.33	$\bar{x}$ y + ½ $\bar{z}$
C (1)	O (2)	3.87	"
C (3)	P	3.99	"
C (2)	O (2)	4.07	"
O (1)	O (2)	4.09	"

factor calculation gave a reliability index of 0.18. Anisotropic temperature factors were introducec for phosphorus and the index fell to 0.165. However discrepancies appeared in isotropic temperature factors for two atoms in the benzene ring:- C(5) had an isotropic temperature factor of 0.9 and C(9) one of 6.6. When the $\bar{1}$ 0 1 reflection was removed on the grounds of back stop error from the structure factor calculation the C(5) value rose to 1.9. Further checking of data and original integrated Weissenburg photographs showed that on the zero level eleven observed structure factors were in error due to original errors in intensity measurements. These eleven structure factors were removed and on one cycle an R-factor of 0.15 and isotropic temperature factors given in Table 6.11 were obtained.

At this stage it appeared evident that the probable source of errors which had resulted in negative anisotropic temperature factors originated from three things,

1. poor quality data which was thought to be due to (a) background shading on photographs, (b) non-uniform integrated spots and (c) mis-reading of the galvanometer in a few cases.
2. varying temperature conditions for integrated Weissenberg experiments. The temperature depended on the nitrogen flow and there was no way of ensuring that this remained constant.
3. the glass tube in which the crystal had to be placed during the X-Ray experiments. This would increase absorption and no correction could be made for it.

In view of the above systematic errors it was felt that the only

justification for refining the structure further would be recollection of data. This was not feasible at this stage and since it seemed that the evidence for the phosphorinane ring having a chair and not a boat form was sufficiently established, the refinement process was stopped. Table 6.10 gives the final co-ordinates and their standard deviations and Table 6.12 (in Appendix I) the final structure factor calculation.

MOLECULAR GEOMETRY

Bond lengths and angles with their standard deviations are given in Tables 6.13 and 6.14 and Figure 6.7 shows a view of the structure projected down the c-axis using the method and programme of Cole and Adamson[10]. Apart from the conclusion that the phosphorinane ring has a chair conformation and that the benzene ring and double bonded oxygen again lie in the axial and equatorial positions respectively, any other detailed analysis of the molecular geometry is meaningless since the structure has now been sufficiently refined.

ISOTROPIC TEMPERATURE FACTORS

On observation of Table 6.11 it would seem that the standard deviations are very small. However these are deceptive, as is usually the case in a full matrix least square refinement. Calculation of the mean value of the isotropic temperature factors gave a value of 4.45 ± 0.48 and a standard deviation for each factor of 1.18.

CONCLUSION

This work, though it may not have proved or disproved in a conclusive way many of the theories involved, has, it seems, opened the way for further research into many fields. Research that should be systematic, based on sound theories and showing quantitative as well as qualitative results.

It has been seen that if further dipole moment measurements of dioxaphosphorinanes are carried out, this will pave the way for satisfactory and convincing explanations for the axial-equatorial shift inversion.

As regards factors influencing phosphorus proton coupling constants, a lot of work needs to be done. Work that will incorporate compounds with a wider range of both dihedral angles and electronegativities of substituents. The work that has been done to date seems a reasonable foundation e.g. something along the lines similar to those which VerKade investigated on the compound

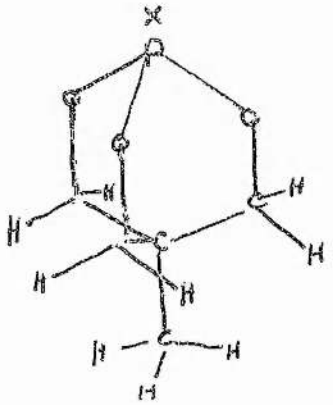

and which is an obvious system for attaching substituents, leading to non-ambiguous results.[67]

Suggestions[68] have been made that the half-width of methyl peaks could be used to ascertain conformation and this would seem very plausible from the present results.

The big question as to whether coupling is 'through space' or 'through bond' still remains unanswered.

Finally, the X-ray crystal analysis that has been carried out has, I think, given invaluable help in sorting out ambiguous results that Nuclear Magnetic Resonance, while bringing them to light, is as yet only beginning to provide the answer.

APPENDIX I

STRUCTURE FACTOR CALCULATIONS FOR

1) 5,5-dimethyl-2-phenyl-2-oxo-1,3,2-dioxaphosphorinane

2) 2-phenyl-2-oxo-1,3,2-dioxaphosphorinane

TABLE 6.4.

FINAL STRUCTURE FACTOR CALCULATION
USING PARAMETERS FROM TABLES 6.2 & 6.3

100 | $F_{calc.}$ *100 | $F_{obs.}$ *		100 | $F_{calc.}$ |00 | $F_{obs.}$ |		100 | $F_{calc.}$ |00 | $F_{obs.}$ |	
0 0 L		0 1 L		0 2 L	
1	1717	3322	1	3621	4185	1	5481	5202
2	1260	604	2	3675	3603	2	2652	2433
3	807	811	3	1884	1837	3	2258	2111
4	1018	852	4	625	695	4	1161	1036
5	423	207	5	335	205	5	1210	1087
6	566	502	6	1092	1279	6	667	709
8	1220	1097	7	950	854	7	856	885
9	881	799	8	664	636	8	512	497
10	708	804	9	458	741	9	945	914
			10	605	535			
0 3 L			0 4 L			0 5 L		
2	1574	1588	2	315	453	2	566	803
4	1033	1039	3	1845	1811	3	841	739
5	1063	1190	4	1579	1687	4	1506	1527
6	403	437	5	694	727	5	3114	2995
7	472	469	6	2066	1991	6	1205	1064
8	1082	986	7	891	1010	7	846	1010
						8	610	426
						10	497	392
0 6 L			0 7 L			0 8 L		
2	536	720	3	704	736	3	1141	1007
3	1082	991	4	2012	2083	4	374	248
4	418	452	5	1697	1659	6	482	523
5	1255	1443	6	571	605	7	448	368
6	1442	1297	8	689	940			

* POSITIONS SHOULD BE REVERSED

TABLE 6.4. (continued)

100 | F_{obs} |	100 | F_{calc} |
1 0 L	
0 1614	1690
1 645	222
-1 2617	2906
2 3045	2952
-2 1899	1780
3 1294	1340
-3 2539	2588
-4 526	325
5 1820	1880
6 551	551
-6 453	355
7 827	870
-8 694	836
9 566	355
10 772	677
1 1 L	
0 6106	5639
1 4654	4693
-1 5781	5647
2 733	617
-2 3985	3711
3 2140	1867
-3 3783	3674
4 841	858
-4 659	714
5 979	975
-5 482	572
6 1077	993
-7 571	657
9 787	786
10 562	648
1 2 L	
0 1141	835
1 4669	4493
-1 1009	1101
2 6017	5255
-2 4212	4083
3 2337	2354
-3 1151	944
4 2219	2042
-4 1707	1711
5 1033	1084
-5 1407	1278
-6 679	567
7 610	629
-7 713	638
8 689	695
-8 1097	1049
10 802	819
1 3 L	
0 1373	1404
1 522	421
-1 1442	1316
2 1791	1696
-2 502	502
3 2499	2324
-3 5412	5531
4 581	594
-4 2691	2652
-5 1510	1673
6 1009	1029
-6 841	813
7 1304	1240
-8 827	1001
9 605	640
1 4 L	
0 1196	1094
1 2598	2384
-1 925	1031
2 2854	2586
-2 1304	1343
3 1068	1032
-3 266	171
4 1333	1309
-4 1383	1419
5 1899	1911
-5 1589	1569
6 772	627
7 551	331
-7 738	1129
8 743	646
-8 1225	1327
1 5 L	
0 1127	1333
1 669	664
-1 458	458
2 1097	1148
-2 1220	1075
-3 1422	1390
4 905	961
-4 1584	1532
5 704	638
-5 541	752
6 969	1008
-6 1535	1565
7 669	856
8 1569	1237
10 512	420

TABLE 6.4. (continued)

100| $F_{obs.}$ |	100| $F_{calc.}$ |	100| $F_{obs.}$ |	100| F_{calc} |	100| $F_{obs.}$ |	100| F_{calc} |
1 6 L		1 7 L		1 8 L	
1	595	633	0	413	493	0	221	291
2	836	745	1	399	583	-1	708	791
-2	763	690	-1	438	497	2	1205	1223
-3	349	357	2	408	519	-2	590	689
4	1668	1618	-2	669	720	3	325	351
-4	1402	1559	3	1319	1162	4	561	741
5	1727	1750	-3	1058	1141	-4	389	692
-5	1643	1795	4	585	602	5	1058	1064
6	1274	1319	-4	802	935	8	536	679
-6	453	588	-5	600	676	9	630	473
-7	969	950	6	777	843			
			-6	590	783			
			7	526	489			
			-7	517	284			
2 0 L		2 1 L		2 2 L	
0	1373	1362	0	1048	1100	0	1028	998
-1	1309	1302	1	2386	2185	1	1225	1178
-2	1255	1284	-1	2199	2107	-1	782	730
3	2814	3050	2	3331	3267	2	1727	1702
-3	708	781	-2	2022	1764	-2	1397	1269
4	1491	1468	3	1004	895	3	1619	1666
-4	871	836	-3	359	362	-3	2637	2500
6	1294	1394	4	1515	1445	4	1087	1026
-6	2150	2318	-4	1565	1578	-4	3218	2913
7	881	793	5	1068	1184	-5	1491	1499
-7	1328	1378	-5	871	718	-6	1048	930
8	4694	365	6	630	547	7	1358	1376
-8	654	455	-6	802	839	-7	699	772
			7	940	799	-8	620	437
			-7	787	772			
			8	640	536			
			-8	1122	969			

TABLE 6.4. (continued)

	100|F obs.|	100|F calc|
	2 3 L	
0	787	810
-1	979	969
1	3651	3324
2	4704	4600
-2	477	492
3	1692	1328
-3	1402	1483
4	389	529
-4	1663	1777
-5	940	954
-6	886	1036
7	728	522
-7	1225	1515
8	541	738
-8	950	887
9	600	251

	100|F obs.|	100|F calc|
	2 4 L	
0	1210	1345
1	699	882
-1	866	930
2	920	1025
-2	1343	1317
3	1018	937
-3	2932	2815
4	1998	1902
5	467	214
-5	640	490
6	935	1063
-6	1348	1533
7	861	1046
-7	841	900

	100|F obs.|	100|F calc|
	2 5 L	
0	581	697
1	2042	2077
-1	2184	2085
2	1506	1401
-2	1747	1603
3	807	829
4	581	735
-4	891	766
5	925	857
7	1186	1207
-8	841	651

	2 6 L	
0	1328	1286
1	772	687
-1	482	605
-2	728	624
3	600	611
-3	664	715
4	536	308
-4	335	377
-6	635	417
7	654	527

	2 7 L	
1	689	799
-1	1466	1364
2	1117	1180
-2	1653	1407
-3	526	360
-4	723	878
5	605	578
6	502	478
7	605	619
8	807	731
9	556	293

	2 8 L	
0	620	517
1	974	899
2	512	436
-2	822	872
3	630	551
-3	1319	1449
4	502	364
-4	507	597
5	428	531
-5	448	253
-6	389	288
-8	664	281

TABLE 6.4. (continued)

10ℓ | $F_{obs.}$	10ℓ | F_{calc}	10ℓ | $F_{obs.}$	10ℓ | F_{calc}	10ℓ | $F_{obs.}$	10ℓ | F_{calc}
3 0 L		3 1 L		3 2 L	
1 344	272	0 1063	1157	-1 1146	1130
-1 359	351	1 413	441	2 1437	1258
-2 1181	1199	-1 679	733	-2 974	793
3 561	330	2 531	691	3 758	793
-3 1476	1498	-2 571	734	-3 831	687
4 1028	1120	3 2239	2392	4 1127	1270
-4 1545	1579	-3 768	811	-4 1314	1184
5 2106	2268	4 2745	2645	5 768	807
-5 433	470	-4 423	422	-5 1102	1239
-6 428	147	-5 950	877	-6 831	655
-7 1461	1571	6 969	1276	7 886	709
8 630	512	-6 2155	2266	-7 1102	881
		7 940	799	9 522	491
		-7 1510	1560		
3 3 L		3 4 L		3 5 L	
0 1358	1457	0 379	369	0 1653	1726
-1 320	245	1 1205	1141	1 546	643
-2 925	955	-1 2396	2511	-1 886	973
3 664	793	2 1353	1417	2 497	435
-3 1683	1451	-2 1633	1555	-2 1412	1409
4 664	790	-6 418	242	3 625	665
5 517	246	8 812	709	-3 581	665
6 679	859	-8 802	783	-4 389	236
-6 846	845			5 704	532
7 659	906			6 502	209
-7 458	488			-6 438	440
8 517	387				
3 6 L		3 7 L		3 8 L	
0 841	826	0 600	722	0 541	497
1 910	1009	1 856	803	1 576	584
-1 2273	2369	-1 413	172	-1 787	907
2 841	845	2 448	337	2 738	851
-2 2037	2163	-3 753	691	-2 787	810
4 649	403	5 428	571	5 625	425
-4 625	682	9 610	500	8 517	525
-5 477	177				
6 507	423				
-7 433	397				
8 718	536				

TABLE 6.4. (continued)

100|F$_{obs}$|	100|F$_{calc}$|	100|F$_{obs}$|	100|F$_{calc}$|	100|F$_{obs}$|	100|F$_{calc}$|
4 0 L		4 1 L		4 2 L	
-1 408	559	-1 659	476	0 413	729
3 2253	2328	2 772	765	1 1122	1175
-3 910	742	4 1127	1095	-2 556	901
4 1456	1590	-4 1112	1253	3 1506	1679
-5 1225	1206	5 802	872	-3 556	577
-6 1373	1448	-6 467	355	4 507	789
7 950	1015			-5 802	1031
-7 753	813			7 664	603
4 3 L		4 4 L		4 5 L	
0 551	743	0 1397	1411	0 689	671
1 630	478	1 1146	1244	1 413	102
-1 684	838	-1 399	361	-1 1565	1574
2 969	1149	-2 797	722	2 640	476
-2 959	966	3 418	455	-2 1560	1616
4 802	533	-3 1004	972	-4 610	879
-4 1186	1304	4 664	580		
5 989	906	6 600	489		
-5 979	1026				
4 6 L		4 7 L		4 8 L	
0 610	746	1 708	525	2 595	335
1 807	687	-1 1117	1348	-3 600	267
-1 507	359	2 467	467	4 674	518
4 571	757	-2 625	853	-6 526	428
-4 477	128	-5 462	410	-8 497	329
-7 541	146	-6 482	203		
		-8 590	145		
5 0 L		5 1 L		5 2 L	
1 462	474	0 1314	1225	0 492	411
-1 831	988	1 861	826	1 831	825
-4 507	580	-2 448	818	3 526	397
5 546	632	-3 743	717	-3 645	631
-5 531	210	4 699	808	4 699	504
		6 669	481	-4 964	934
		-6 600	498	5 590	678
				-5 787	950
				6 635	649

TABLE 6.4. (continued)

100|F$_{obs}$|	100|F$_{calc.}$|	100|F$_{obs.}$|	100|F$_{calc.}$|	100|F$_{obs.}$|	100|F$_{calc.}$|
5 3 L		5 4 L		5 5 L	
0	1284 1483	1	600 432	1	620 788
1	640 794	-1	615 621	3	733 462
-2	704 780	2	585 540		
4	689 644	-4	1643 1246		
5	571 427	-5	758 660		
-5	551 567	-7	610 282		
-6	585 396				
5 6 L		5 8 L		6 0 L	
0	615 455	4	551 217	0	881 569
1	531 356	6	738 217	-3	959 1175
-1	443 349			-6	620 205
2	576 600				
-3	689 300				
4	748 371				
-4	753 670				
6 1 L		6 2 L		6 3 L	
-1	566 582	0	738 632	0	590 250
-2	699 458	-4	576 181	-5	507 342
6 4 L		6 5 L		6 8 L	
1	708 534	0	600 140	-2	590 384
-4	600 176	1	507 398		
-5	571 296	-7	536 429		

Table 6.12

k=0,l=1		10|F_o|	10|F_c|
0	1		
1		359	358
2		568	622
3		189	193
4		285	345
5		70	48
6		114	36
7		102	94
0	2		
1		144	139
2		119	138
5		158	179
6		95	81
8		71	59
0	3		
0		177	190
2		152	141
3		139	107
4		119	111
5		80	42
6		278	265
7		99	103
0	4		
0		140	141
1		87	85
2		67	45
3		106	95
5		242	224
6		40	22
0	5		
0		140	126
1		81	50
2		166	149
3		85	86
5		41	28
0	6		
0		58	56
1		137	134
2		45	67
3		76	94
0	0		
2		53	73
3		491	456
4		276	286
5		234	216
6		40	43
7		52	65
8		63	61
0	1		
-2		282	249
-4		219	195
-5		145	142
-6		284	258
-8		90	76
-9		148	150
-11		52	88
0	2		
-1		48	54
-2		198	225
-4		254	254
-5		234	238
-6		36	26
-7		351	341
-8		29	37
-9		28	14
-10		91	96
0	3		
-1		33	48
-2		69	57
-3		266	277
-5		140	160
-6		195	195
-7		29	45
-8		113	119
-9		28	50

0 4

-1	57	56
-2	1881	176
-3	61	58
-4	87	115
-5	79	108
-6	29	32

0 5

-2	87	39
-3	69	44
-4	86	85
-5	29	11
-6	90	101
-1	259	254

0 6

-1	41	25
-2	179	156
-3	40	30

1 0

2	410	433
3	208	218
4	365	326
5	28	14
6	98	130

1 1

1	68	61
2	260	248
3	311	289
4	212	186
5	211	199
6	89	64
7	108	69
8	82	82
-1	127	145
-2	249	263
-3	220	173
-4	111	56

1 2

0	55	66
1	240	257
2	239	219
3	161	66
4	232	261
5	121	87
6	109	107
-1	249	274
-2	133	110
-3	252	254
-4	172	152
-6	139	152

1 3

0	157	177
1	177	187
2	161	126
3	157	175
4	179	159
5	217	231
7	107	54
-1	109	79
-2	166	188
-3	141	127
-4	131	134
-5	144	126

1 4

0	77	104
1	139	107
2	95	96
4	98	108
5	59	59
6	107	125
-1	152	176
-2	106	71
-3	181	152
-4	108	112
-5	53	54
-6	83	119

2 6

1	35	50
2	35	34
3	103	67

3 0

-2	119	124
-3	97	79
-4	143	109
-5	42	55
-6	136	132
-8	54	88

3 1

-1	112	167
-2	64	68
-3	59	60
-4	92	97
-5	78	77
-6	81	53
-7	115	99
-8	48	48
1	101	65
2	52	62
3	91	89
4	129	151

3 2

0	46	37
-2	51	29
-3	61	68
-4	90	82
-5	46	55
-6	130	140
-7	34	09
-8	102	83
1	123	110
2	70	91
3	105	100
4	90	81
6	101	116
7	48	49

3 3

0	160	119
-1	39	13
-2	72	78
-3	62	63
-5	75	65
-6	34	40
-7	110	91
1	66	72
2	55	77
3	39	11
4	51	25
5	108	122
6	41	37

3 4

0	36	18
-1	32	84
-2	31	55
-3	81	57
-4	57	12
-5	68	77
-6	76	76
1	52	48
2	53	59
3	45	31
4	90	109
5	48	48
6	84	86

3 5

0	85	101
-1	24	13
-2	96	98
-3	24	31
1	58	51
2	68	89
3	68	61

3 6

0	34	35
-1	63	74

4 0

3	155	163
4	144	156
5	94	89
6	40	39
7	98	103

4 1

0	73	68
1	184	199
2	109	113
3	186	181
4	170	157
5	48	39
6	145	137
-1	171	209
-2	54	20
-3	73	63

4 2

0	101	123
1	23	67
2	141	142
3	157	157
4	59	31
5	85	111
6	77	98
7	66	67
-2	116	142
-3	126	144

4 3

0	81	95
1	74	43
2	138	148
3	53	29
4	135	121
5	42	38
6	61	64
-1	137	168
-2	55	31
-3	111	145
-4	101	133
-5	42	41
-6	111	94

4 4

0	105	79
1	89	69
2	71	61
3	59	51
-1	98	117
-3	64	29
-4	65	64

5 0

-2	78	67
-3	139	140
-4	112	83
-9	82	67

5 1

0	58	54
-1	65	85
-2	147	138
-3	95	88
-4	59	73
-5	121	105
-6	35	27
-7	20	39
-8	51	57
1	71	89
2	112	107
3	140	140
4	85	98
5	108	117
6	40	49
7	81	106
8	78	79

5 2

0	54	64
+1	171	195
-2	86	76
-3	59	66
-4	129	118
-5	44	41
-6	89	79
-7	28	04
1	107	117
2	151	168
4	93	122
5	76	75
6	57	71

5 3

0	125	149
-1	71	77
-2	137	138
-3	94	88
-4	75	67
-5	64	70
-6	45	79
1	142	146
2	66	36
3	101	108
4	44	84
5	41	32
6	73	73

5 4

0	63	69
-1	59	78
-2	45	49
-3	98	99
-4	35	49
-5	80	77
-6	42	50
1	59	75
2	88	103
3	102	66
4	45	66
5	35	29

5 5

0	57	41
-1	76	71
-2	34	33
-3	34	29
-4	92	78

6 0

-2	125	132
-3	36	42
-4	117	73
-5	107	95
-6	57	56
-7	55	75
-8	35	48

6 1

0	97	111
-1	92	92
-2	102	91
-3	141	146
-4	127	121
-5	28	38
-6	69	63
-7	72	69
1	78	49
2	98	74
3	73	51
5	19	20
6	75	105

6 2

0	129	130
-1	69	65
-2	96	108
-3	88	95
-4	34	43
-5	83	88
1	95	101
2	45	18
3	45	51
4	19	12
5	45	44

6 3

0	37	31
-1	119	120
-2	47	24
-3	39	25
-4	49	47
-5	59	51
1	46	45

6 4

-1	40	52
-2	45	43
-3	34	17
-4	51	51
1	49	58

APPENDIX II

NUCLEAR MAGNETIC RESONANCE SPECTRA

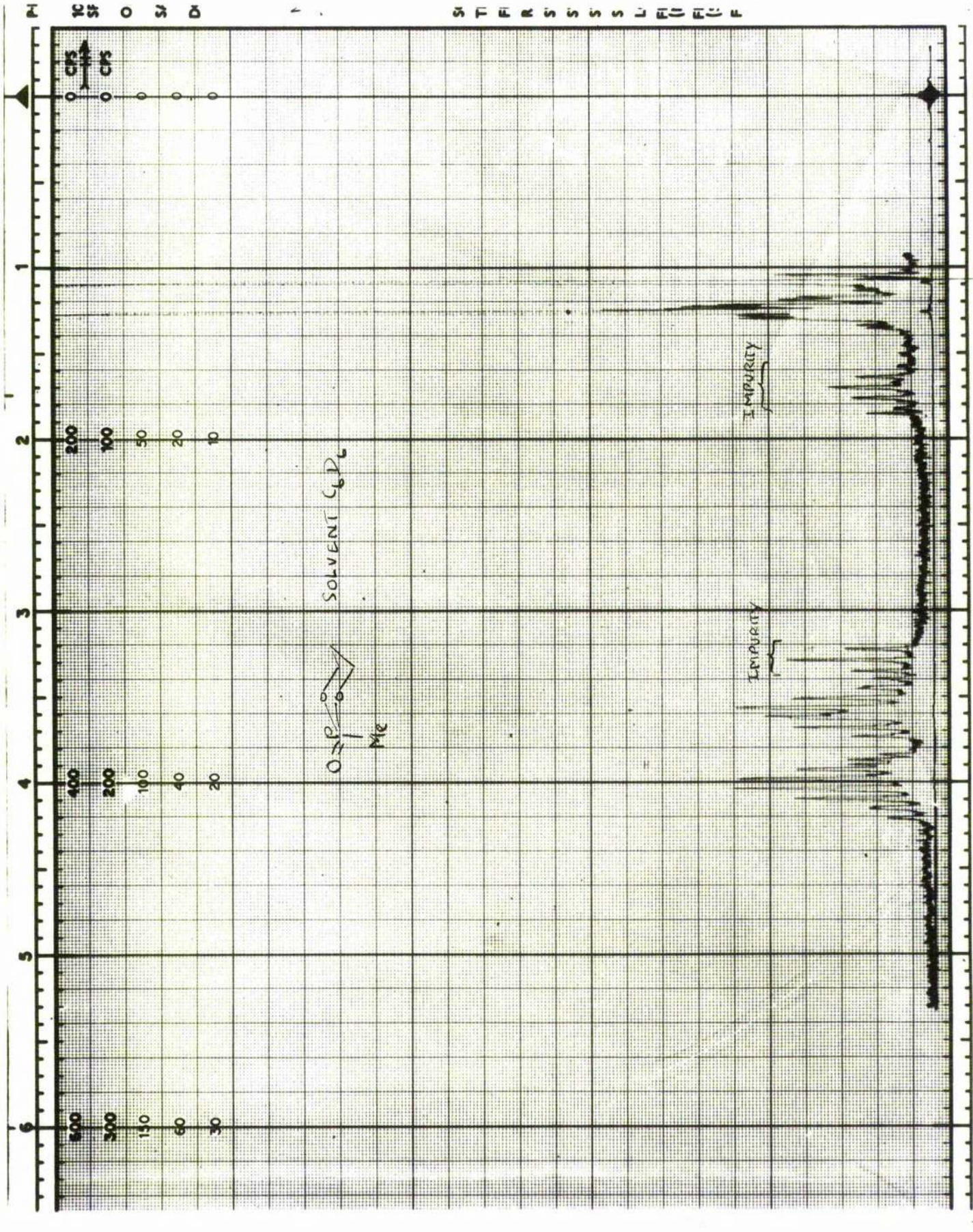
SOLVENT C_6D_6
IMPURITY
IMPURITY
SPECTRUM NO 1

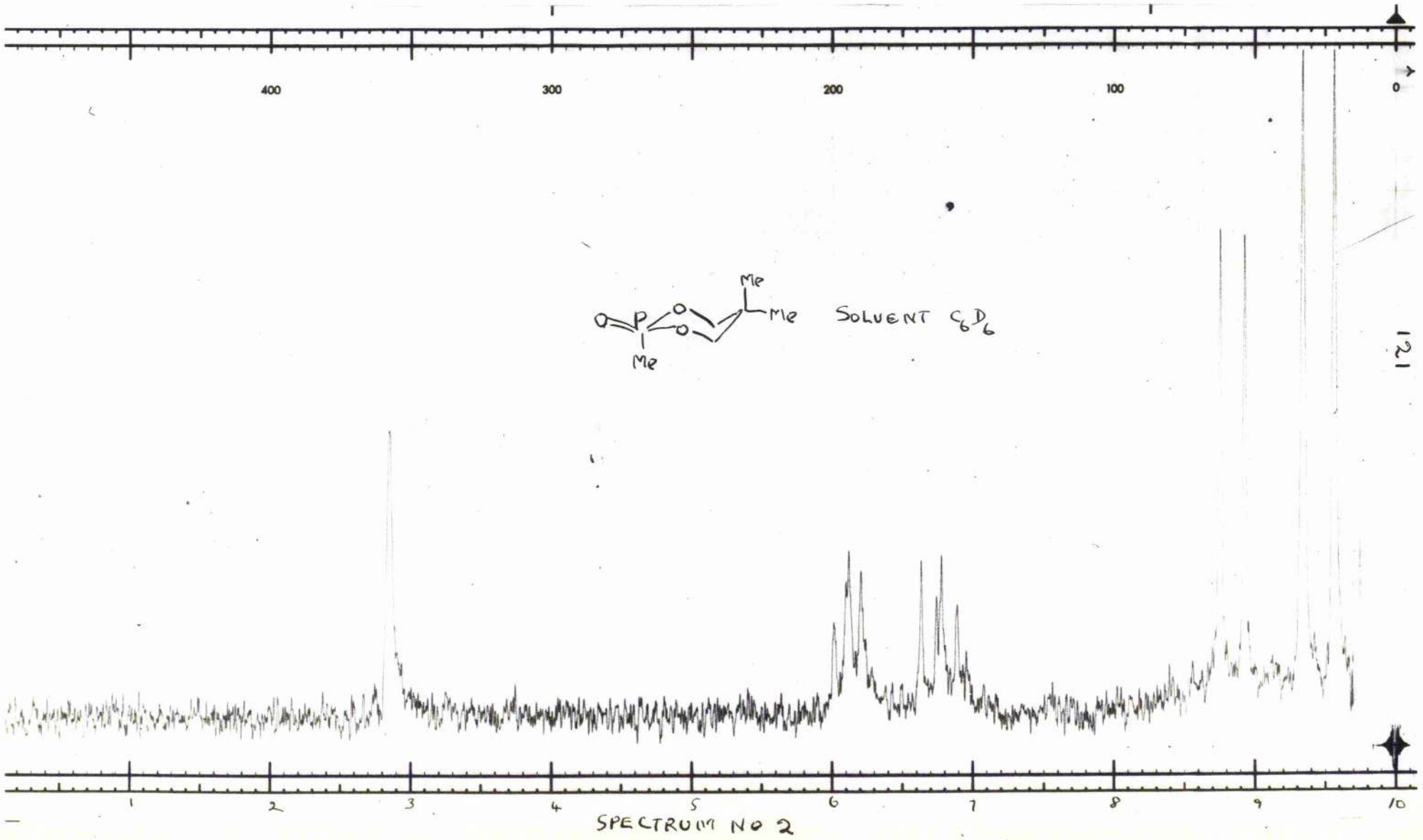

121

SPECTRUM NO 2

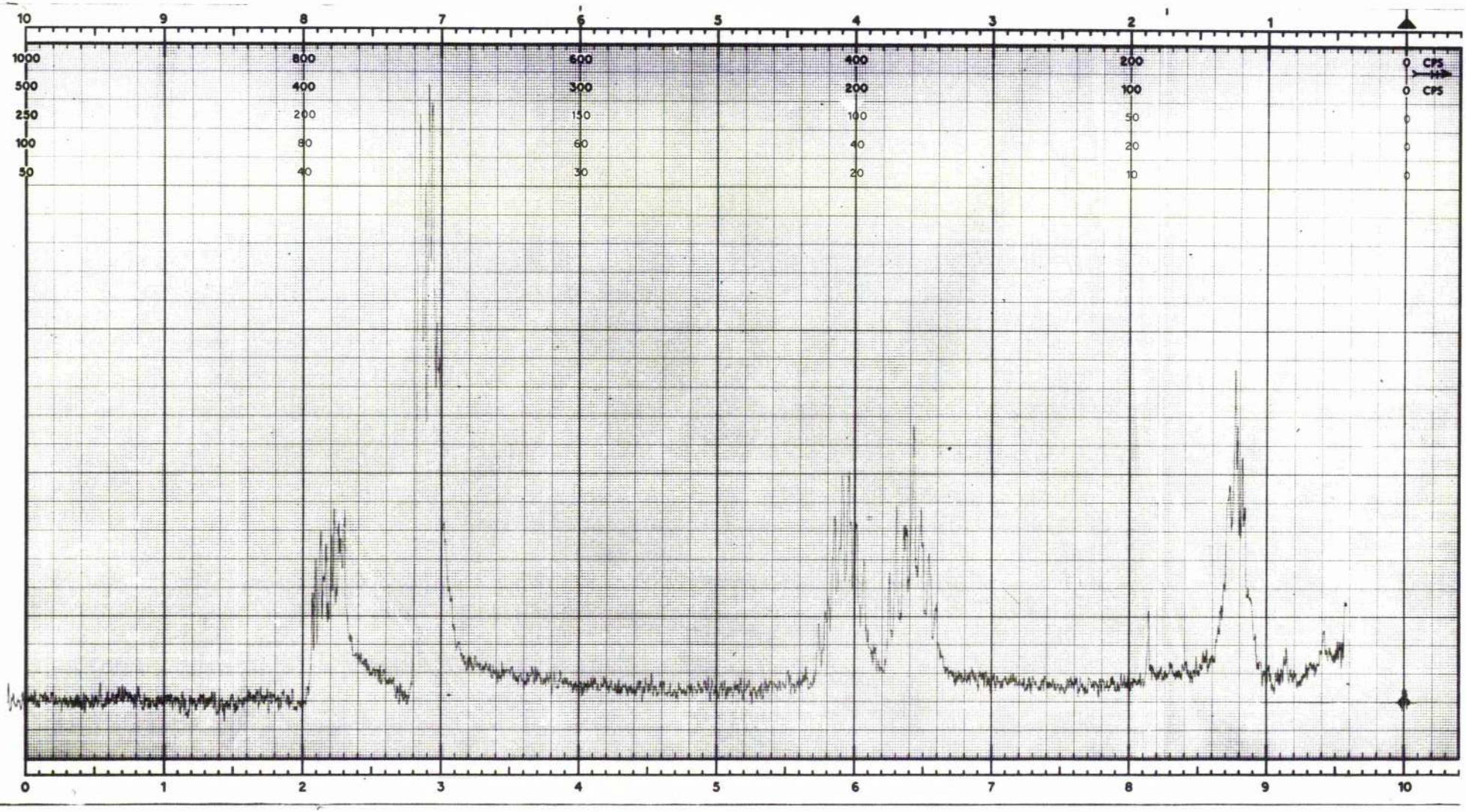

SPECTRUM No 3

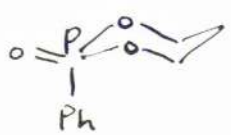

SOLVENT C_6D_6

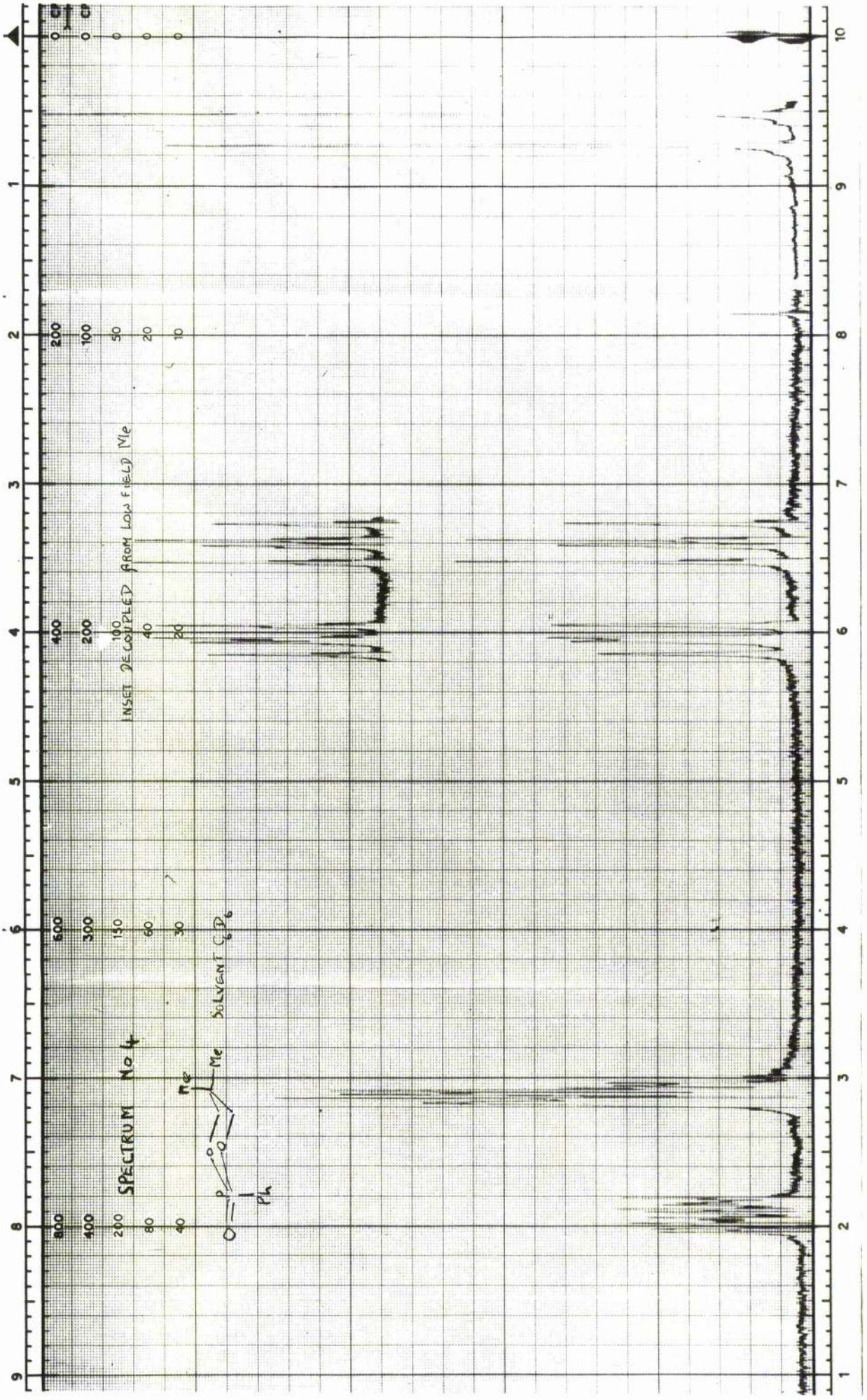
SPECTRUM No 4
INSET DECOUPLED AROM LOW FIELD Me
SOLVENT C6D6
Me
Me
Ph
P
O
O
O
CPS
CPS

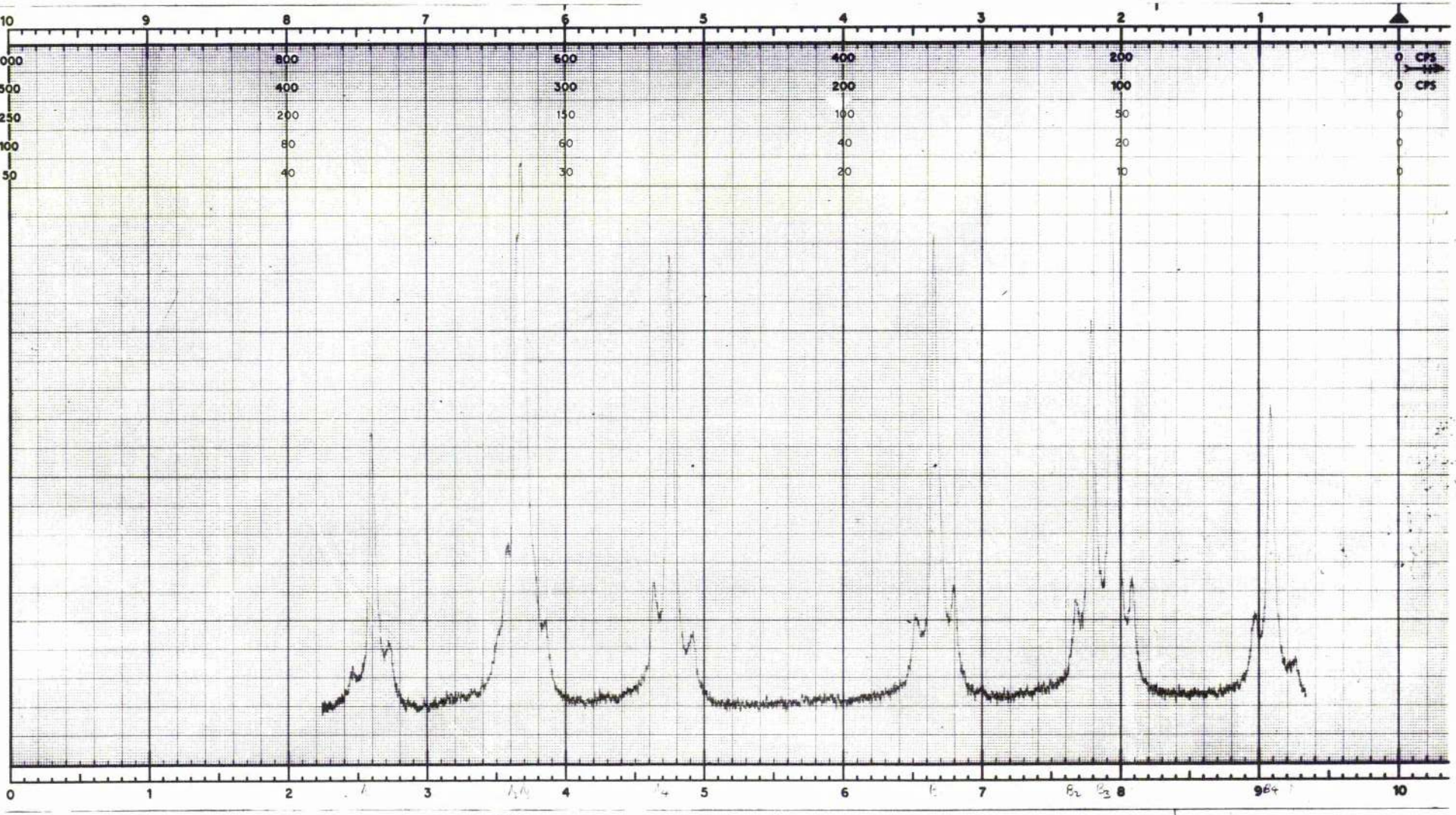

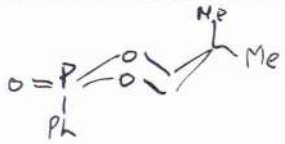

4, 6 protons decoupled from Me, and expanded (100 c/s). SOLVENT $CDCl_3$

SPECTRUM No 5

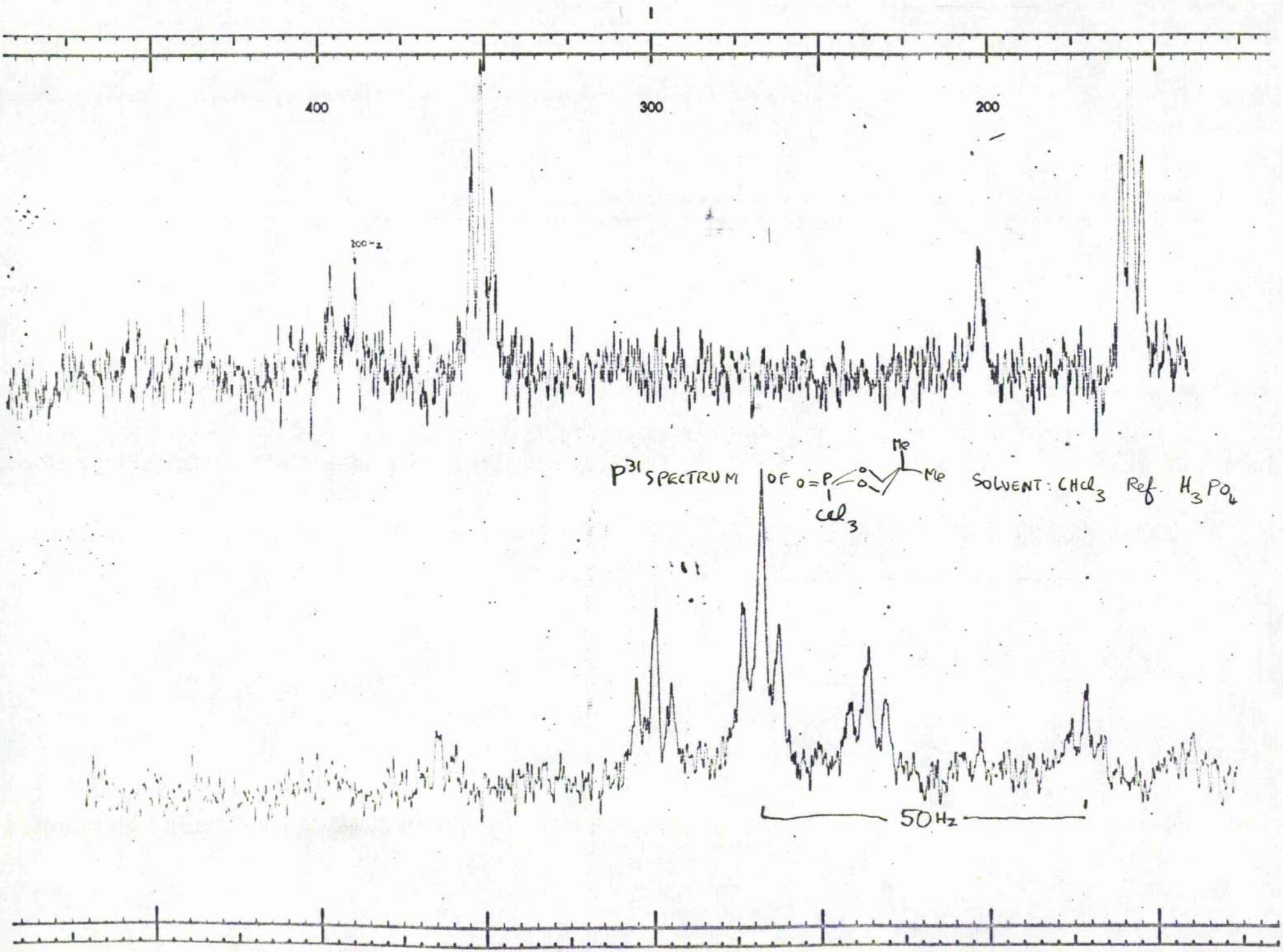

SPECTRUM No 6

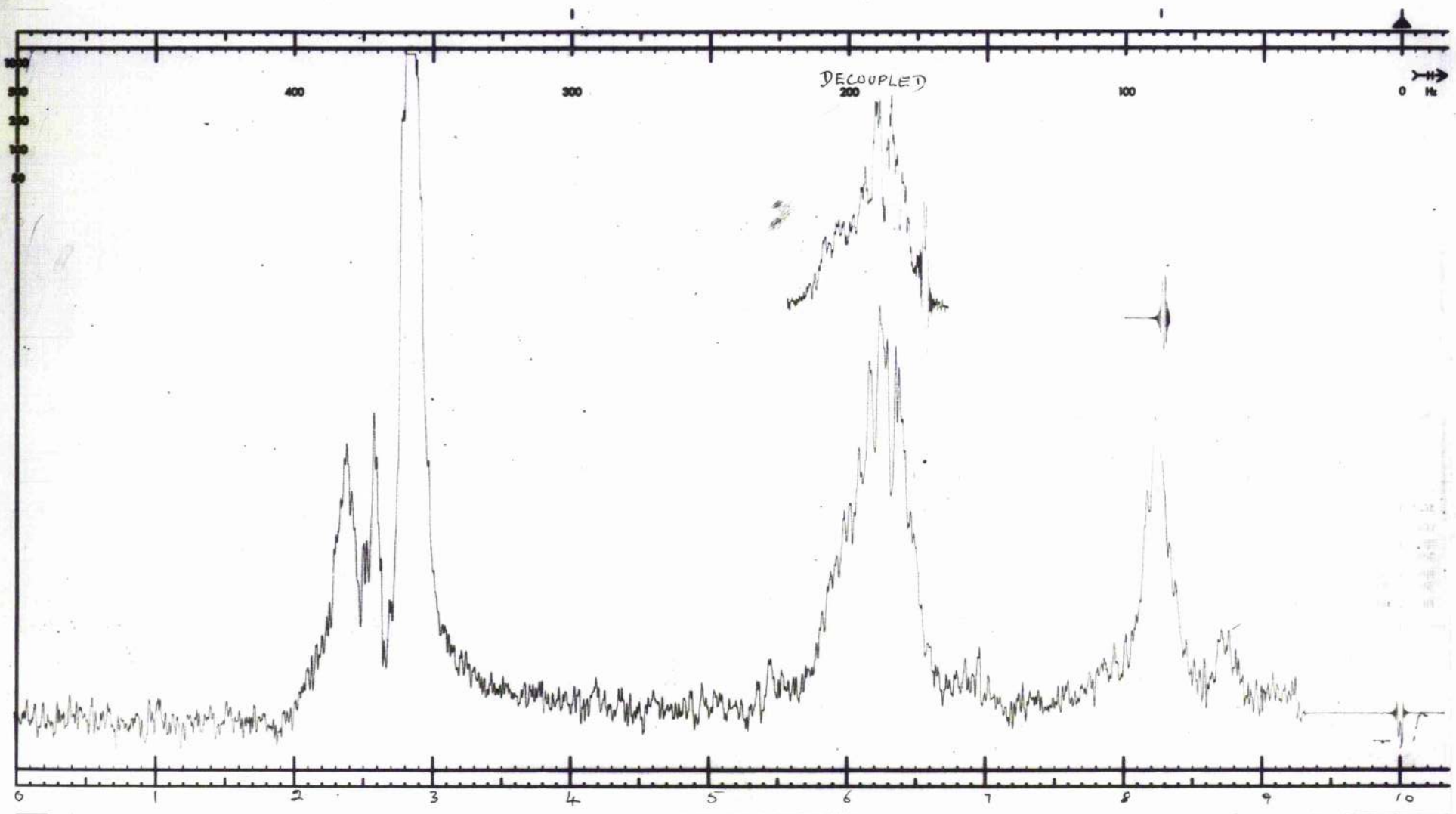

SPECTRUM No 7

SOLVENT C_6D_6

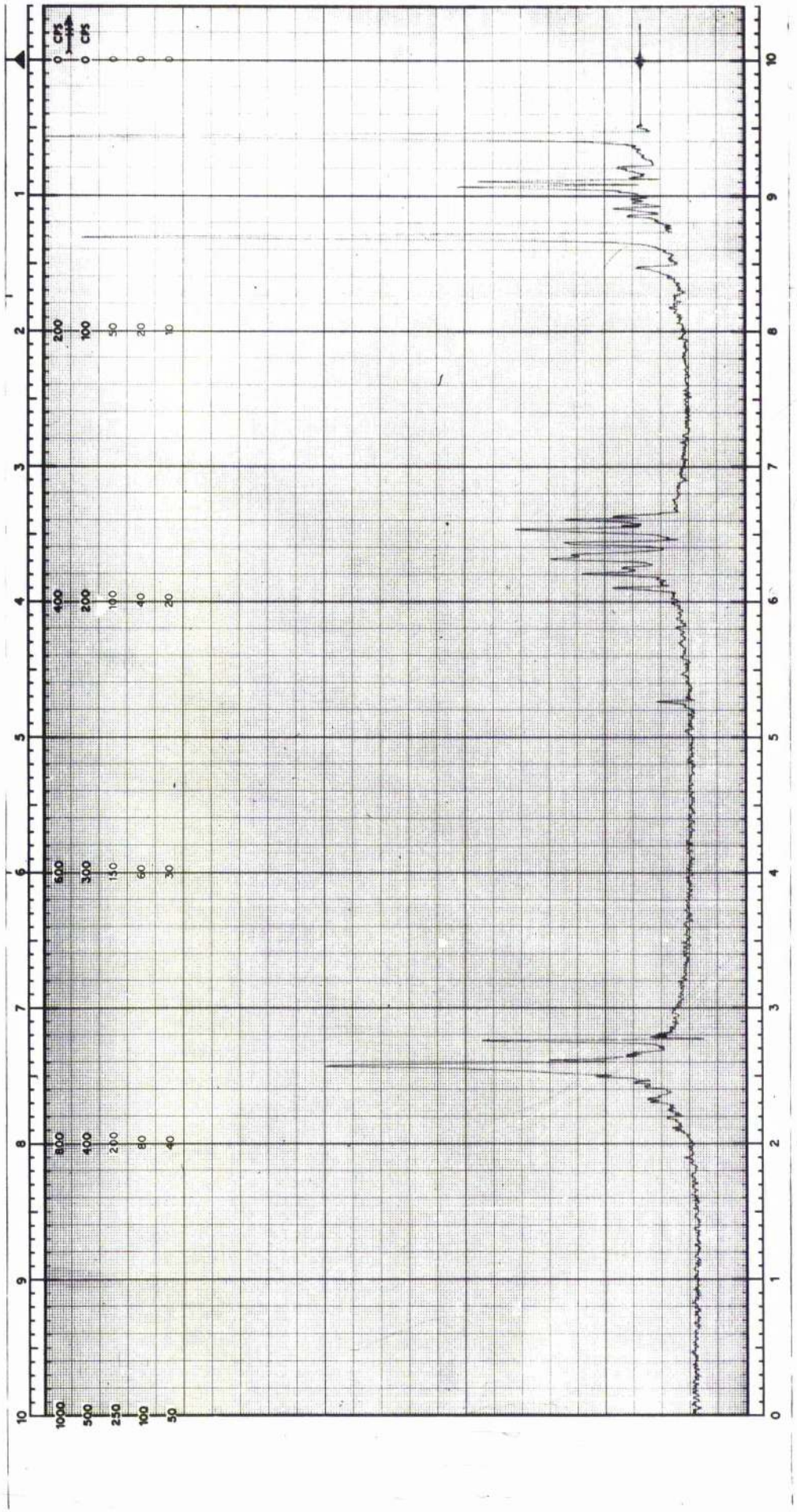

SPECTRUM No 8

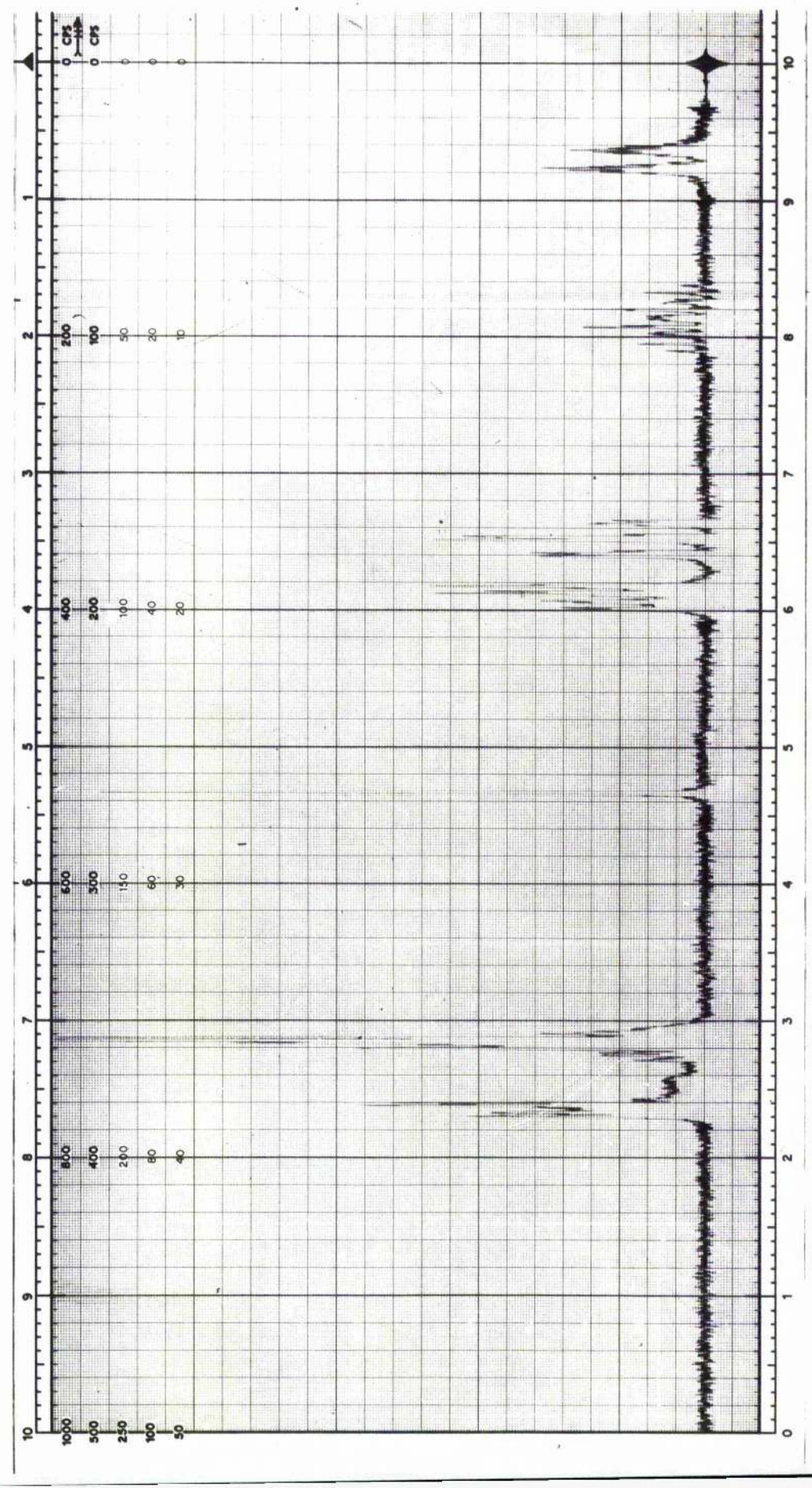

SPECTRUM No 9.0

$Ph-CH<^{O}_{O}>$

SOLUENT C_6D_6

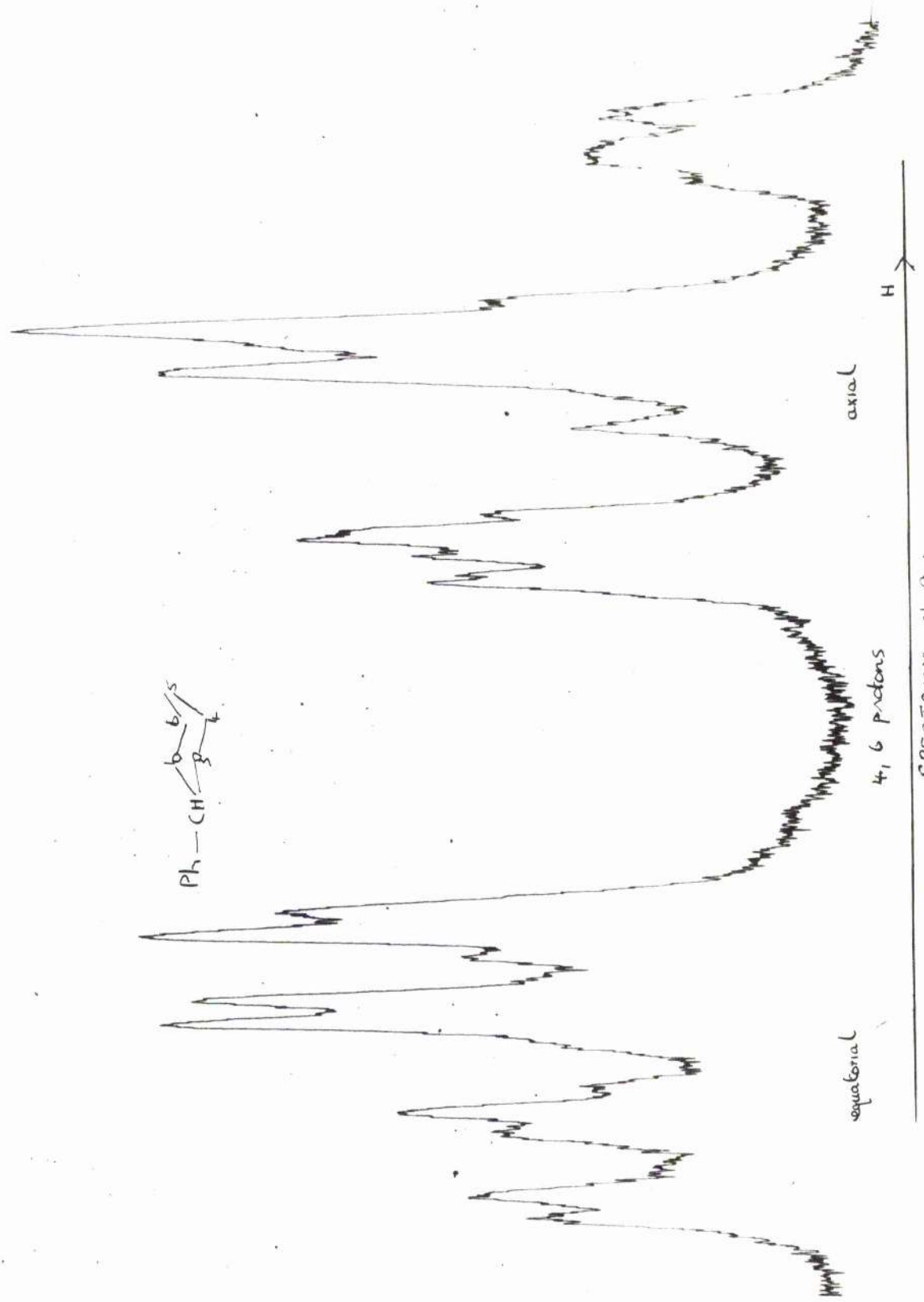

SPECTRUM No 9.1

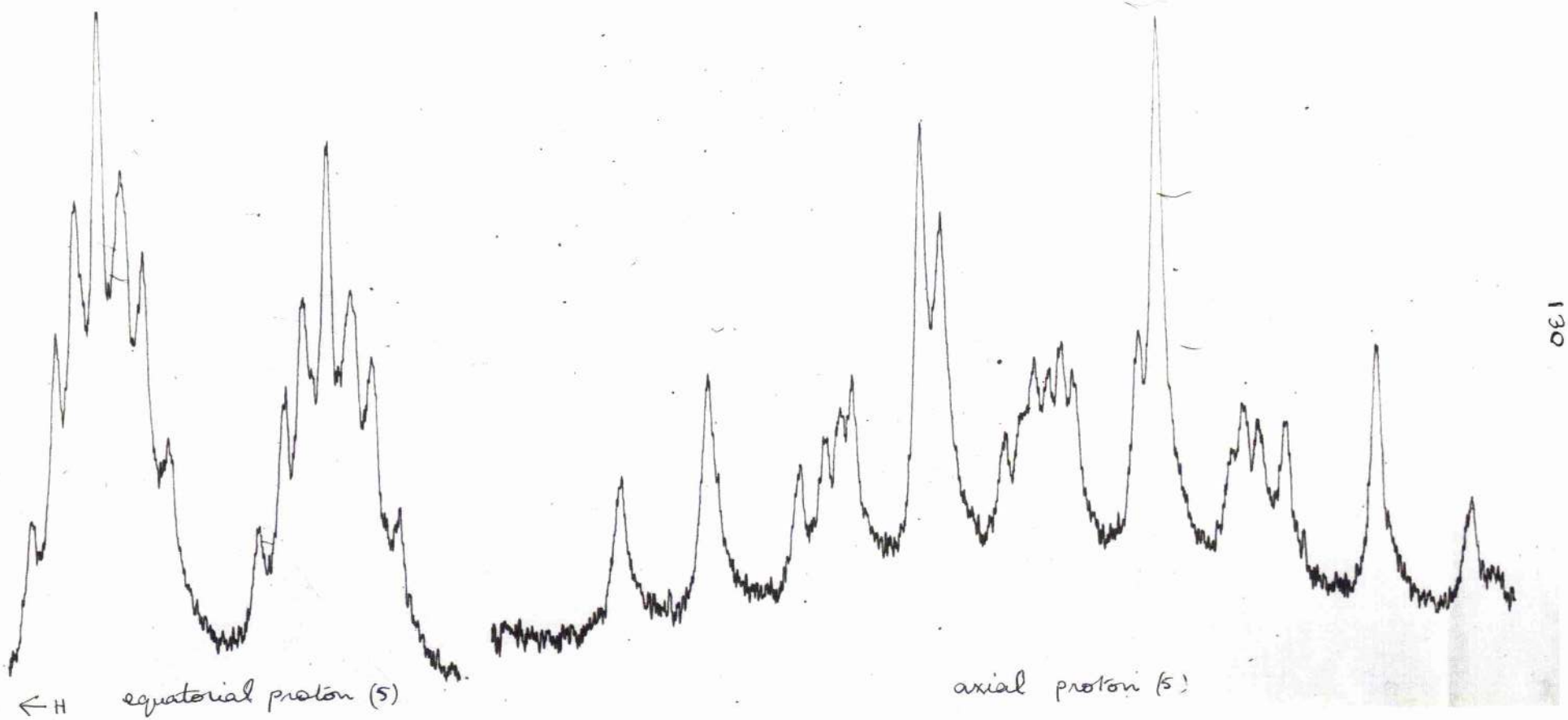

SPECTRUM No 9.2

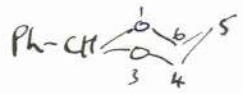

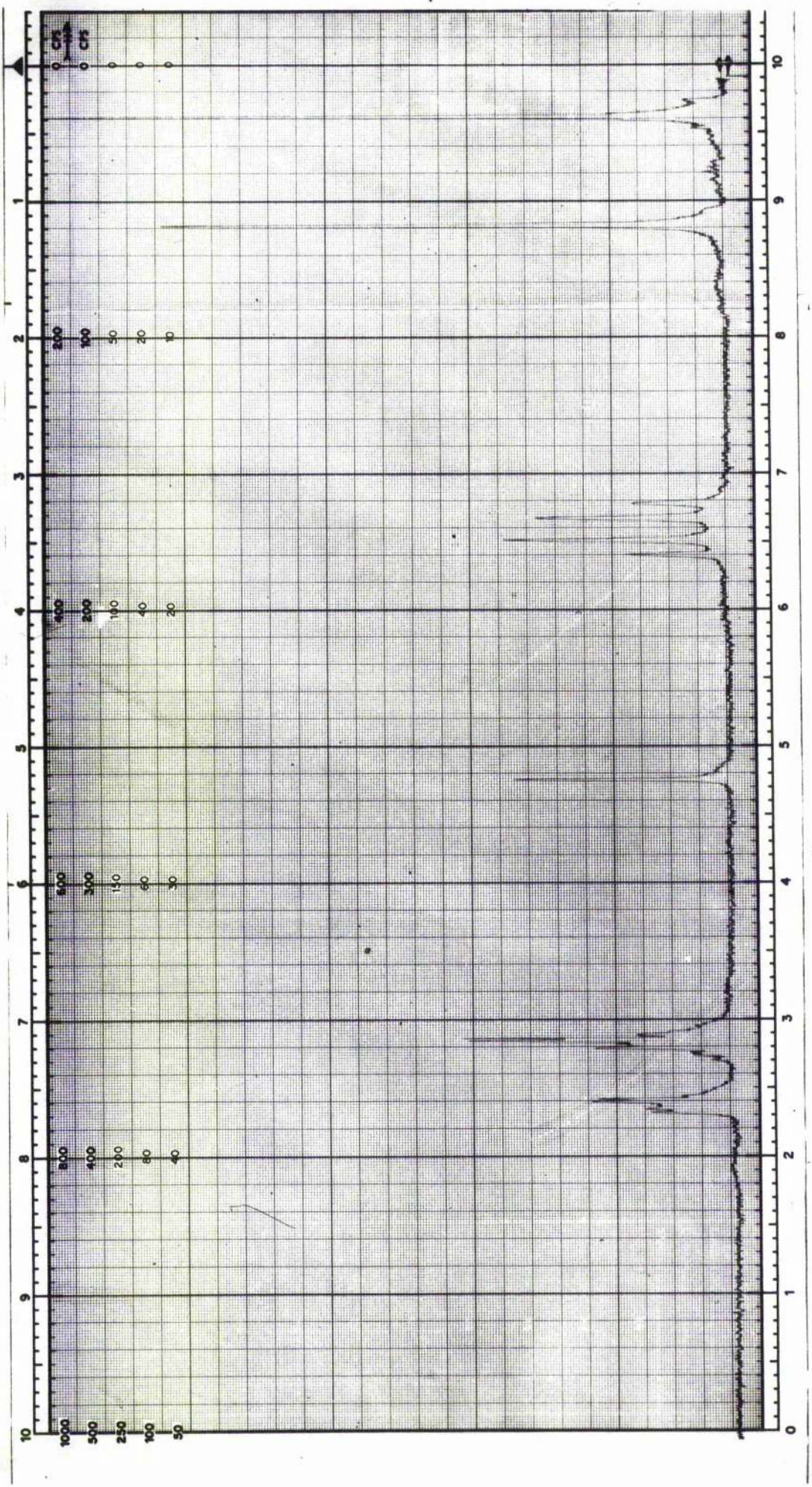

SPECTRUM No 10

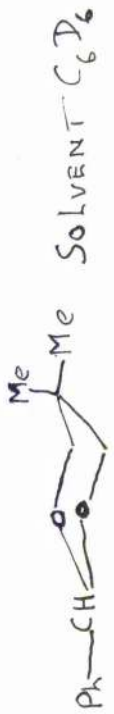

SOLVENT C_6D_6

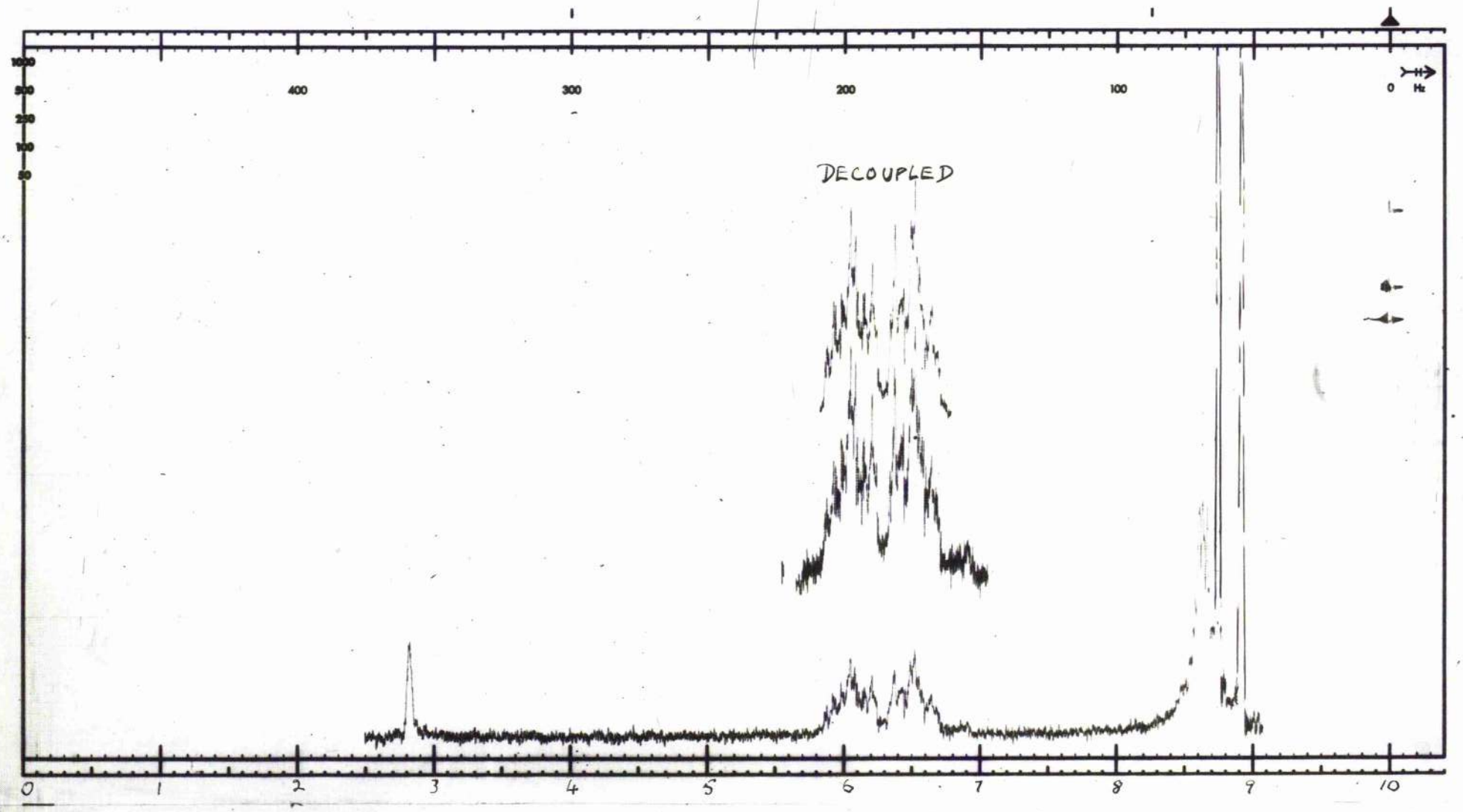

SPECTRUM No. 11

SOLVENT: C_6D_6

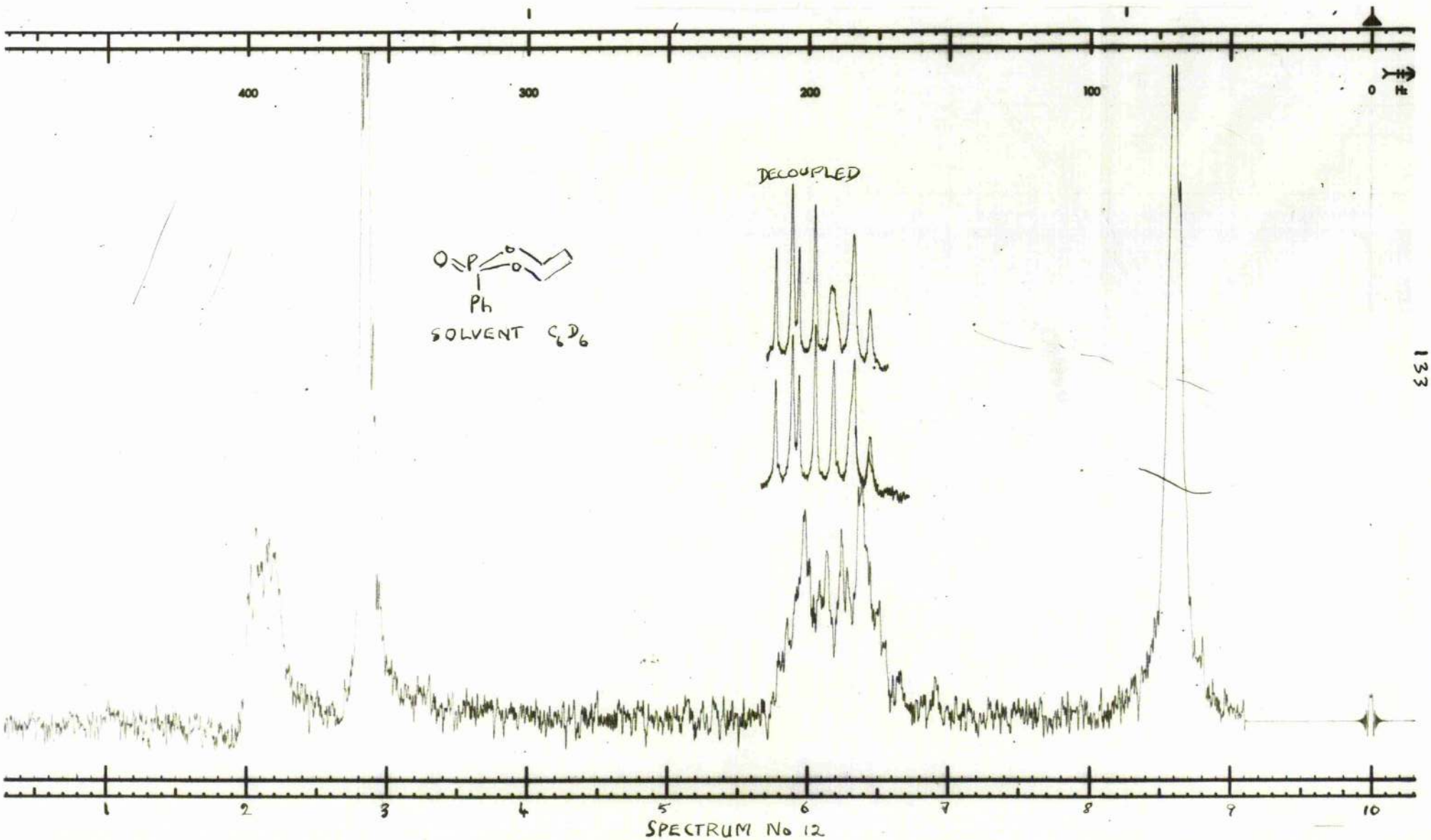

SPECTRUM No 12

REFERENCES

INTRODUCTION

1. Barton, D.H.R., J.Chem.Soc. 340 (1948); 1027 (1953); Experientia 6 316 (1950).

2. Klyne, W., Progr. Stereochem. 1 Chapt.2 (1954).

3. Van't Hoff, J.H., "Dix anneés dans l'histoire d'une théorie" (1887).

4. LeBel, J.A. Bull.Soc.Chim. France [2] 22 337 (1874).

5. Baeyer, A.von, Ber. 18 2277 (1885).

6. Sachse, H., Ber. 23 1363 (1890).

7. Sachse, H., Z.Physik.Chem. (Leipzig) 10 203 (1892).

8. Mohr, E., J.Prakt.Chem. [2] 103 316 (1922).

9. Böeseken, J., Ber. 46 2612 (1913); 55 3758 (1922); 56 2411 (1923).

10. Hassel, O. and Ottar, B., Acta Chem.Scand. 1 929 (1947).

11. Geise, H.J., Rec.Trav.Chim. 86 362 (1967).

12. Tulinskie, A., Gracomo, A.D. and Smythe, C.P., J.Amer.Chem.Soc. 75 3552 (1953).

13. Brande, E.A. and Waight, E.S., Progr. Stereochim. 1 Chapt.4 (1954).

14. Mizushima, S., "The Structure of Molecules and Internal Rotation," Academic Press, New York, Chapt. 1 p.162 ff. (1954).

15. Lide, D.R.Jr., J.Chem.Phys. 30 37 (1959).

16. Le Fèvre, C.G. and R.J.W., J.Chem.Soc. 3549 (1956); 3458 (1957).

17. Djerassi, C., "Optical Rotatory Dispersion, Application to Organic Chemistry," McGraw-Hill, New York (1960).

18. Edmundson, R.S. and Mitchell, E.W., J.Chem.Soc.(C) 2091 (1968).

19. Buys, H.R., Rec.Trav.Chim. 88 1003 (1969).

REFERENCES

INTRODUCTION

20. Fischer, E., Ber. 47 3181 (1914); Ann.Chem. 402 364 (1914).

21. Riddell, F.G., Quart.Rev. 21 367 (1967).

22. Eccleston, G. and Wyn-Jones, E., Chem.Comm. 1511 (1969).

REFERENCES

CHAPTER 1

1. Elmsley, J.W., Feeney, J. and Sutcliffe, L.H., "High Resolution Nuclear Magnetic Resonance Spectroscopy," Vols. I and II, Pergamon Press (1965).

2. Roberts, J.D., "An Introduction to the Analysis of Spin-Spin Splitting in Nuclear Magnetic Resonance," Benjamin (1961).

3. Buckingham, A.D., Schaefer, T. and Schneider, W.G., J.Chem.Phys. 32 1227 (1960).

4. Bothner-By, A.A., J.Mol.Spect. 5 52 (1962); Laszlo, P. and Musher, J.I., J.Chem.Phys. 41 3906 (1964).

5. Schneider, W.G. and Reeves, L.W., Can.J.Chem. 35 251 (1957).

6. Schaefer, T. and Schneider, W.G., J.Chem.Phys. 32 1224 (1960).

7. Chapman, D. and Magnus, P.D., "Introduction to Practical High Resolution N.M.R. Spectroscopy," Academic Press, London and New York (1966).

8. Gutowsky, H.S., McCall, D.W. and Slichter, C.P., J.Chem.Phys. 21 279 (1953).

9. Reference 1 this chapter p.287.

10. Reference 1 this chapter p.309.

11. Rojansky, V., "Introductory Quantum Mechanics," Prentice-Hall, Englewood Cliffs, N.J. (1938).

12. Anderson, W.A., Phys.Rev. 102 151 (1956).

13. Itoh, J. and Sato, S., J.Phys.Soc. Japan 14 851 (1959).

14. Kaiser, R., Rev.Sci. Instruments 31 963 (1960).

15. Bloom, A.L. and Shoolery, J.N., Phys.Rev. 97 1261 (1955).

16. Margenau, H. and Murphy, G.M., "The Mathematics of Physics and Chemistry," Van Nostrand, New York (1956).

REFERENCES

CHAPTER 2

1. Anderson, J.E., Quart.Rev. 19 426 (1965).

2. Riddell, F.G., Quart.Rev. 21 364 (1967).

3. Geise, H.T., Recueil 86 362 (1967).

4. Murayama, W. and Kainosho, M., Bull. Chem.Soc.Japan 42 1819 (1969).

5. Hargis, J.H. and Bentrude, W.G., Tet.Letters 51 5365 (1968).

6. Berneke, T.A., Chem.Comm. 860 (1966).

7. Tsuboi, M. et al., Bull.Chem.Soc.Japan 40 1813 (1967).

8. White, D.W., McEwen, G.K. and Verkade, J.G., Tet.Letters 51 5369 (1968).

9. Lemieux, R.U., Kullnig, R.K., Bernstein, H.J. and Schneider, W.G. J.Amer.Chem.Soc. 80 6078 (1958).

10. Jackmann, L.M., "Applications of Nuclear Magnetic Resonance Spectroscopy in Organic Chemistry," Pergamon Press, London (1959) p.p. 115 - 119.

11. McConnell, H.M., J.Chem.Phys. 27 226 (1957).

12. Shoolery, J.N. and Rogers, M.T., J.Amer.Chem.Soc. 80 5121 (1958).

13. Jackmann, L.M., "Applications of Nuclear Magnetic Resonance Spectroscopy in Organic Chemistry," Pergamon Press, London (1959) p.116.

14. Elmsley, J.W., Feeney, J. and Sutcliffe, L.H., "High Resolution N.M.R. Spectroscopy," Pergamon Press Vol.I. (1965) p.575.

15.a. Kainosho, M. and Shimozawa, T., Tet.Letters 865 (1969).

15.b. Karplus, M., J.Chem.Phys. 30 11 (1959).

16. Jardetzky, C.D., J.Amer.Chem.Soc. 83 2919 (1961).

REFERENCES

CHAPTER 2

17. Lemieux, R.U., Can.J.Chem. 39 116 (1961).

18. Abraham, R.J. and McLauchlan, K.A., Mol.Phys. 5 513 (1962).

19. Karplus, M., J.Amer.Chem.Soc. 85 2870 (1963).

20. Williamson, K.L. and Johnson, W.S., J.Amer.Chem.Soc. 83 4623 (1961).

21. Bhacca, N.S. and Williams, D.H., "Applications of N.M.R. Spectroscopy in Organic Chemistry," Holden-Day Inc. (1964).

22. Banwell, C.N. and Sheppard, N., Discussions Faraday Soc. 34 115 (1962).

23. Gutowsky, H.S. and Porte, A.L., J.Chem.Phys. 35 839 (1961).

24. Jonathan, N., Gordon, S. and Bailey, B.P., J.Chem.Phys. 36 2443 (1963).

25. Benezra, C. and Ourisson, G., Bull.Soc.Chim. France 3161 (1967).

26. Tsuboi, M. et al., Bull.Chem.Soc.Japan 40 1813 (1967).

27. Hargis, J.H. and Bentrude, W.G., Tet. Letters 51 5365 (1968).

28. Kainosho, M., Nakamura, A. and Tsuboi, M., Bull.Chem.Soc. Japan 42 1713 (1969).

29. Malcolm, R.B. and Hall, L.D., Chem.and Ind. 92 (1968).

30. White, D.W., McEwen, G.K. and Verkade, J.G., Tet. Letters 51 5369 (1968).

REFERENCES

CHAPTER 3

1. Korshak, V.V., Gribova, I.A. and Andreeva, M.A., Izvest, Akad, Nauk, S.S.S.R. Otdel Kim Nauk 631 - 7 (1957). (Chem.Abs. 51 14621 g)

2. Edmundson, R.S., Tetrahedron 20 2781 (1964).

3. Kinnear, A.M. and Perrin, E.A., J.Chem.Soc. 3437 (1952).

4. Edmundson, R.S., J.Org.Chem. 29 (9) 2572 (1964).

5. Arkiv. Kemi. 6 523 (1954).

6. Monashefte für Chemie 49 Band (1928).

REFERENCES

CHAPTER 4

1. Jackman, L.M. "Applications of N.M.R. Spectroscopy in Organic Chemistry" Pergamon Press p.117 (1959).

2. Bartle, K.D., Edmundson, R.S. and Jones, D.W., Tetrahedron 23 1701 (1967).

3. Tsuboi et al., Bull.Chem.Soc.Jap., 40 1813 (1967).

4. Kainosho et al., Bull.Chem.Soc.Jap., 42 1713 (1969).

5. Hargis, H.J. and Bentrude, G.W., Tet.Letters, 5365 (1968); Chem.Comm., 1113 (1969).

6. Kainosho, M. and Nakamura, A., Tetrahedron, 25 4071 (1969).

7. Bhacca, N.S. and Williams, D.H. "Applications of N.M.R. Spectroscopy to Organic Chemistry" Holden Day, San Francisco, p.51 (1964).

8. Ref. 2.

9. Shoppee, C.W. et al., Chem.Comm., 347 (1965).

10. Barfield, M.J., Chem.Phys., 41 3825 (1964).

11. Shoppee, C.W. et al., Tet.Letters, 2319 (1964).

12. Bhacca, N.S., Gurst, J.E. and Williams, D.H., J.Amer.Chem.Soc. 87, 302 (1965).

13. Ref. 9.

14. Williamson, K.L., private communication to Shoppee, C.W.

15. Ref. 31.

16. Ref. 2

17. Ref. 10

18. Shoppee, C.W. - see Ref. 9.

19. Delmau, J., Duplan, J.C. and Davidson, M., Tetrahedron 23 4371 (1967).

20. McConnell, H.H., J.Chem.Phys., 27 226 (1957).

21. Marschall, I.W. and Pople, J.A., Mol.Phys., 1 199 (1958).

22. Buckingham, A.D., Canad.J.Chem., 38 300 (1960).

23. Muscher, J.I., J.Chem.Phys., 37 34 (1962).

24. Walker, R. and Davidson, D.W., Canad.J.Chem., 37 492 (1959).

25. White, D.W., McEwen, G.K. and Verkade, J.G., Tet.Letters, 5369 (1968).

26. Kainosho, M. and Shumazawa, T., Tet.Letters, 865 (1969).

27. Chapter 6 (this thesis)

28. Geise, H.J., Recueil, 86 362 (1967).

29. Ref. 26.

30. Edmundson, R.S. and Mitchell, E.W., J.Chem.Soc.(C), 752 (1970).

31. Gagnaire, D., Robert, J.B. and Verner, J., Bull.Soc.Chim., France, 2392 (1968).

32. White, D.W., McEwen, G.K. and Verkade, J.G., Tet.Letters, 5369 (1968).

33. Cameron, J.A., School of Physical Sciences, St. Andrews University, private communication (1970).

34. Schaefer, T. and Schneider, W.G., J.Chem.Phys., 32 1218 (1960).

35. Elmsley, J.W., Feeney, J. and Sutcliffe, L.H., "High Resolution N.M.R. Spectroscopy", Pergamon Press, Vol.I. p.258 (1965).

36. Anderson, J.E., Tet.Letters, 4713 (1965).

37. Ref. 35, Vol.I p.361.

38. McConnell, H.M., J.Chem.Phys. 23 2454 (1955).

39. Ref.2.

40. Ref.31.

41. Karplus, M., J.Amer.Chem.Soc. 85 2870 (1963).

42. Ref.6.

43. Chapter 7 (this thesis).

44. Banwell, C N., Sheppard, N. and Turner, J.J. Spec.Chim.Acta, 16 794 (1960).

45. Schaefer, T. Canad.J.Chem., 40 1 (1962).

46. This thesis.

47. Hall, L.D. and Malcolm, R.B., Chem.and Ind. 92 (1968).

48. Advances in Physical Organic Chemistry, Vol.6

49. Verkade, J.G. and King, R.W., Inorganic Chem., 1 948 (1962).

50. Karplus, see ref.41.

51. Eliel, E.L., J.Amer.Chem.Soc., 92 584 (1970).

52. Eliel, E.L. and Allinger, N.L., "Topics in Stereochemistry", Vol.3.

53. Ihrig, A.M. and Smith, S.L., J.Amer.Chem.Soc., 92 759 (1970).

54. Hanack, M., "Conformation Theory", Academic Press, London, p.160 (1965).

55. Hendrickson, J.B., J.Amer.Chem.Soc., 83 4537 (1961); 84 3355 (1962), Tetrahedron, 19 1387 (1963).

56. Ref.6.

57. Ref.36.

58. Gagnaire, D. and Robert, J.B., Bull.Soc.Chim., France 2240 (1967).

59. Fontal, B. and Goldwhite, H., Tetrahedron, 22 3275 (1966).

60. Gagnaire, D. et al., Bull.Soc.Chim., France, 3719 (1966).

61. Haake, P., McNeal, J.P. and Goldsmith, E.J., J.Amer.Chem.Soc., 90, 715 (1968).

62. Ref.54, p.380.

63. Edmundson, R.S., Tet.Letters, 1905 (1969).

64. Ref.30.

65. Jeffs, M., I.C.I. Runcorn, Cheshire, private communication.

66. Ref.19.

67. Ref.49.

68. Ref.11.

REFERENCES

CHAPTER 5

1. Patterson, A.L., Phys.Rev. 46 372 (1934).

2. Harker, D., J.Chem.Phys. 4 381 (1936).

3. Bragg, W.L., James, R.W. and Bosanquet, C.H., Phil.Mag.42 1 (1921).

4. Debye, P., Annalen Physik. 43 49 (1914).

5. Waller, I., Annalen Physik. 83 153 (1927).

6. Hamilton, W.C., Acta Cryst. 8 199 (1955).

7. Cruickshank, D.W.J., Acta Cryst. 9 747 (1956).

8. Hughes, E.W., J.Amer.Chem.Soc. 63 1737 (1941).

9. Cruickshank, D.W.J. et al., "Computing Methods and the Phase Problem in X-ray Crystal Analysis", Pergamon Press (1961).

10. Killean, R.C.G. and Lawrence, J.L., Acta Cryst.B. 25 1750 (1969).

11. Grant, D.F., Killean, R.C.G. and Lawrence, J.L., Acta Cryst.B. 25 374 (1969).

12. Kitaigorodski, A.I., "Theory of Crystal Structure Analysis", Trans. 1961, p.249, New York, Heywood (1957).

13. Arndt, V.W. and Phillips, D.C., Acta Cryst. 14 807 (1961).

14. Ewald, P.P., Z.Krist., 56 129 (1921).

15. Cochran, W., Acta Cryst. 3 267 (1950).

16. Arndt, V.W., Faulkner, T.H. and Phillips, D.C., J.Sci.Instrum. 37 68 (1960).

17. Ross, P.A., J.Optical Soc.Am. 16 433 (1928).

18. Buerger, M.J. "X-ray Crystallography", Wiley, New York (1942).

REFERENCES

CHAPTER 6

1. Killean, R.C.G. and Lawrence, J.L., Acta.Cryst.B25 1750 (1969).

2. Killean, R.C.G., Acta.Cryst., 23 1109 (1967).

3. Edmundson, R.S., Tetrahedron, 20 2781 (1964).

4. Murayama, W. and Kainosho, M., Bull.Chem.Soc., Japan, 42 1819 (1969

5. Geise, H.J., Recueil, 86 362 (1967).

6. Kraut, J. and Jensen, L.H., Acta.Cryst., 16 79 (1963).

7. Svetich, G.W. and Caughlan, C.N., Acta.Cryst., 19 645 (1965).

8. Davis, M. and Hassel, O., Acta.Chem.Scand., 17 1181 (1963).

9. Mitchell, R., School of Physical Sciences, St.Andrews University (1969) private communication.

10. Cole, A.J. and Adamson, P.G., Acta.Cryst.A., 25 535 (1969).